

Predicting the short-term response to inlet interventions in Lake Bardawil

A study on the initial hydrodynamic and morphological response to inlet dredging interventions in Lake Bardawil, a shallow micro-tidal lagoon in northern Egypt

W. (Wouter) Hoek

Predicting the short-term response to inlet interventions in Lake Bardawil

by

W. (Wouter) Hoek

in partial fulfilment of the requirements to obtain the degree of

Master of Science

in Civil Engineering

at the Delft University of Technology (TU Delft)

Date	09/08/23	
Student Number	4310322	
Programme	MSc Civil Engineering	
Track	Hydraulic Engineering	
Specialisation	Coastal Engineering	
Committee	Prof.dr.ir. Z.B. (Zheng Bing) Wang	Delft University of Technology
	Dr.ir. S.G. (Stuart) Pearson	Delft University of Technology
	Dr.ir. W.M. (Wouter) Kranenburg	Delft University of Technology
	Ir. R. (Rick) van Bentem	The Weather Makers
	Ir. A.C.S. (Arjan) Mol	DEME-group



Preface

First of all, I would like to thank The Weather Makers as a company for allowing me to contribute to this interesting project. I really enjoyed my time working on Lake Bardawil and look forward to hearing about the actual implementation of the project.

I would like to thank my graduation committee for taking the time to guide me through my research. Your feedback has been very valuable and I enjoyed hearing the different views on the project. You have guided me in the right direction and have helped me reach what I think is a nice result.

Special thanks to Rick for the intensive daily contact and collaboration over the last 9 months. I have had a very pleasant experience working together and really appreciate the amount of time you have spent helping me. We have had many fruitful discussions, allowing for valuable progress in my research. In other moments you have helped me overcome the most frustrating modelling issues. You have been a great supervisor, thank you so much.

Abstract

Lake Bardawil is a hypersaline shallow micro-tidal double-inlet lagoon on the northern coast of the Sinai Peninsula in Egypt. The inlets, named Boughaz 1 and Boughaz 2, connect Lake Bardawil to the Mediterranean Sea. The local population relies on the fishing yields from the lagoon, however, in the current situation, the lagoon's inlets are unstable, needing constant maintenance dredging to stay open. Additionally, due to the hypersaline situation (limiting fish attraction) and high fish catch demand, the current fishing situation is unsustainable. The Weather Makers propose a solution to the problem using dredging interventions. Enlarging the inlets of Lake Bardawil is expected to result in increased fish migration, decreased salinity in the lagoon and increased stability of the inlets. This research aims to investigate the short-term response of Lake Bardawil and specifically its inlets to the dredging interventions proposed.

To investigate the response to the interventions, two numerical models are used; a hydrodynamic model in D-flow FM and a coupled morphological model using D-flow FM and D-waves. The model results are analysed in terms of the hydrodynamic tidal response, combined hydrodynamic response to tide and weather and finally the morphological response to tidal and weather effects.

From the hydrodynamic model, it can be concluded that the interventions result in a larger tidal prism for the lagoon by a factor of 1.6. This is expected to result in increased fish migration and reduced salinity in the lagoon. As the tidal prism increases, so does the discharge through the inlets. The increased discharge through the inlets results in inlet velocity amplitudes that exceed the theoretical critical value for convergence to a dynamically stable inlet cross-section for both inlets.

The interventions affect more than just tidal currents in Lake Bardawil. Weather effects in the lagoon are amplified by the interventions. This is demonstrated by increased interaction between the inlets in terms of net import and export of water. During winter storms, the wind-induced flow from Boughaz 1 to Boughaz 2 is greater in magnitude. The wind waves caused by these winter storms result in sediment resuspension. This results in larger sediment transport from the basin to Boughaz 2.

Using the coupled model, the morphological response in both inlets can be predicted. In Boughaz 1, the present sediment-importing character is amplified. Whereas the similar summertime sediment-importing character of Boughaz 2 is reduced substantially. The sediment export of Boughaz 2 during winter is larger in the new situation.

The interventions result in increased sedimentation in the dredged channel of Boughaz 1. This does not hinder the increased tidal discharge at Boughaz 1, which is the main intended function of the interventions. This means the increased sedimentation does not influence the intended functioning of the interventions in the short term. Due to the increased sedimentation in the inner dredged channel, there is no indication of increased stability in Boughaz 1. Boughaz 2 shows less morphological activity in the situation after interventions. As is the case with Boughaz 1, there is no hindrance to the functioning of the interventions during the short simulation period. There is reduced deposition of sediment in the inner flood delta region of the inlet and the updrift side of the inlet channel compared to the known unstable situation during both winter and summer simulations. This indicates improved stability for Boughaz 2.

The short-term response to the interventions in the inlets of the Lake Bardawil system is as intended, the tidal prism is increased and while there is only an indication of increased stability in Boughaz 2, there are no short-term impediments to the intended primary functioning of the interventions in either of the inlets.

Contents

Preface	i
Abstract	ii
Nomenclature	v
Notations	v
Abbreviations	v
1 Introduction	1
1.1 Background Lake Bardawil	1
1.2 Intervention design	2
1.3 Conditions Lake Bardawil	3
1.4 Research objective	7
1.5 Research question	8
1.6 Methodology	8
2 Literature review	10
2.1 Tidal propagation in a shallow micro-tidal lagoon	10
2.2 Morphology of a shallow micro-tidal lagoon system	12
3 Methodology	19
3.1 Hydrodynamic model setup	19
3.2 Hydrodynamic model analysis	21
3.3 Morphological model set-up	22
3.4 Morphological model analysis	24
4 Results	25
4.1 Hydrodynamic response to tidal forcing	25
4.2 Hydrodynamic response to tidal and meteorological forcing	35
4.3 Morphological response to tidal and meteorological forcing	41
5 Discussion	48
5.1 Primary effectiveness of the interventions	48
5.2 Hydrodynamic response to the interventions	48
5.3 Morphological response to the interventions	52
5.4 Considerations interpreting conclusions	57
6 Conclusion	59
7 Recommendations	62
Bibliography	64
A Inlet designs	66
B Model conditions	68
B.1 Weather conditions	68

Contents

B.2 Validation of initial conditions	70
C Additional results	71
C.1 Hydrodynamic response to tidal forcing	71
D Reference figures	77
E Sediment fractions	78

Nomenclature

Notations

\hat{u}_{eq}	equilibrium velocity amplitude
τ_w	wind stress
K	Strickler coefficient
n	Manning's roughness coefficient
u^*_{cw}	bed shear velocity from currents and waves
u^*_c	bed shear velocity from currents
R^2	coefficient of determination

Abbreviations

EW	Early Works
MSL	mean sea level
NE	Northeast
NNW	North Northwest
NW	Northwest
SDB	satellite derived bathymetry
SQ	Status Quo
SSC	suspended sediment concentration
SWAN	Simulating Waves Nearshore
TWM	The Weather Makers
WNW	West Northwest
WSW	West Southwest

1 Introduction

1.1 Background Lake Bardawil

Lake Bardawil is a micro-tidal shallow lagoon in the Mediterranean Sea on the northern coast of the Sinai Peninsula in Egypt. The area of the lagoon is around 550 km², stretching just under 80km at the longest and just over 20 km at the widest. There is no direct fresh water supply for Lake Bardawil. The only source of fresh water are the scarce winter rains. As a result of this low freshwater input and high evaporation, Lake Bardawil is a hypersaline lagoon and is the most saline of the northern Egyptian lakes. In contrast with other deltaic Mediterranean Egyptian lakes, Lake Bardawil is of tectonic origin (El-Bana et al., 2002).

Lake Bardawil is connected to the Mediterranean by three inlets. The most western inlet "Boughaz 1" and the larger of the two eastern inlets "Boughaz 2" are artificial inlets created at the start of the 20th century (Linnarsund and Mårtensson, 2008). The third and easternmost inlet is a small natural inlet, the size of this inlet is considered insignificant compared to Boughaz 1 and Boughaz 2. Lake Bardawil will be considered a two-inlet system for the rest of this thesis. After the artificial opening at the start of the 20th century, the inlets have been naturally closed and artificially opened several times. In the 1950s the two present inlets with concrete jetties on each side were constructed in an attempt to create a permanent connection to the Mediterranean Sea. The jetty on the upstream side of Boughaz 1 was extended in the 1970s. The inlets have been continuously dredged ever since. The dredging efforts were insufficient to keep Boughaz 2 open and it was closed from 1967 to 1972. Using more efficient dredging equipment, Boughaz 2 has been kept open from 1972 until now (Linnarsund and Mårtensson, 2008).



Figure 1.1: Overview of Lake Bardawil with the western inlet "Boughaz 1" in the top left corner and the eastern inlet "Boughaz 2" in the top right corner("Bing Maps", 2023).

1.1.1 Fishing situation

The local population relies on the fishing yields from Lake Bardawil, however the current hypersaline environment and water temperatures of Lake Bardawil result in an unsustainable fishing situation as catch demand exceeds the natural supply of the lagoon.

A report on the marine ecosystem engineering of Lake Bardawil by Wageningen Marine Research (2016) states that the general approach towards a healthy and sustainable fishery situation in Lake Bardawil comprises a combination of improving the environmental conditions and improved management of the fisheries. Wageningen Marine Research (2016) identifies two main mechanisms for improving the environmental conditions: Increasing the depth over the basin to increase plankton primary production and increasing the tidal prism to stimulate migration of fish into the lagoon and reduce hypersalinity.

Increasing the water depth over the lagoon by 0.2 m is expected to result in an increase of harvestable fish of 80 tons annually with total fish production increasing from 830 to 910 ton (Wageningen Marine Research, 2016). As this is only a fraction of the total annual catch WMR concludes that most catches in the lagoon are fish that migrate into the lagoon.

Wageningen Marine Research (2016) states an expectation of an increase in inflow of migrating fish from the Mediterranean Sea to be at least proportional to the increase in tidal prism. With uncertainty around this figure mainly being caused by a lack of data on the availability of fish outside the lagoon. As the current estimated import of fish is in the order of 7200 tons, the potential increase in catch due to increased tidal prism is expected to be much larger than the potential increase in catch due to increased water depth.

While there is no scientifically derived relationship between fish abundance and salinity, literature on Lake Bardawil mention observations of a negative relationship between salinity and fish catch numbers (Wageningen Marine Research, 2016)

1.1.2 The Weather Makers Bardawil Lake development

The Weather Makers (TWM) proposes a plan to restore the local aquatic ecosystem and enrich the adjacent areas by increasing the water exchange between Lake Bardawil and the Mediterranean Sea. To reach this goal, The Weather Makers have proposed dredging interventions in both inlets. In addition to the objective of increasing the fish population, reinforcing biodiversity and contributing to the socio-economic development of the area, the interventions aim to improve inlet stability and decrease dredging maintenance.

1.2 Intervention design

To attract a greater fish population in Lake Bardawil, the interventions work two-fold: Firstly, by increasing the water exchange between the Mediterranean Sea and Lake Bardawil, fish migration into the lake should be increased. Secondly, the water quality should improve by decreasing salinity.

The main function of the intervention design is to increase the water exchange between Lake Bardawil and the Mediterranean Sea by increasing the tidal prism of Lake Bardawil.

The intervention designs are presented in Figure 1.2 and in more detail in Appendix A by TWM is based on a Nature-based Solutions approach. The marked areas in the design are dredged to -9m to mean sea level (MSL) and the narrowest part of Boughaz 1 is dredged to -10m to MSL. Additionally, the dredged sand is used as a nourishment on the downdrift side of each inlet, any analysis of the behaviour of the sand nourishment is outside the scope of this research.

The design aims to mimic the natural configuration of tidal deltas. By mimicking this natural configuration, resistance to flow coming in and out of the lagoon should be as small as possible. The design should reduce the effect of the constraints of the inlets on the tidal prism. Additionally, by increasing the tidal prism of the inlets, their stability should improve.

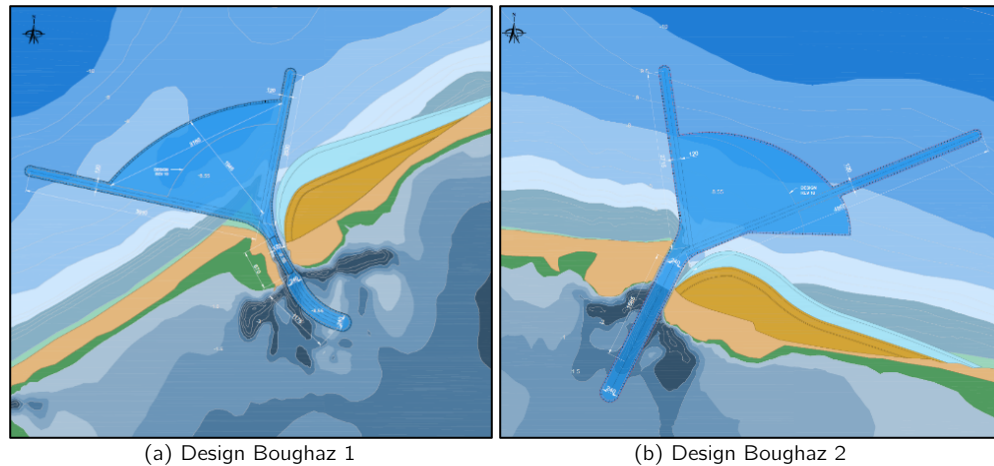


Figure 1.2: Inlet designs by The Weather Makers. Marked areas are dredged to -8.55 m relative to lowest astronomical tide and -9 m to MSL. Complete design drawings can be found in Appendix A.

1.3 Conditions Lake Bardawil

Gaining insight into the coastal system at Lake Bardawil requires a comprehensive understanding of the local conditions. In this section the metocean conditions, sediment characteristics and bathymetry are discussed.

1.3.1 Metocean conditions

The metocean conditions consist of tidal conditions, wind conditions, wave conditions and other climatic conditions.

Tidal conditions

Over the years several studies have been done into the tidal characteristics at Lake Bardawil (Nassar et al., 2018; Linnarsund and Mårtensson, 2008). These studies are based on measurements or numerical models and are located just outside of Lake Bardawil or in Port Said and El Arish (located approximately 50 km west and east of Lake Bardawil). These studies report different values for the maximum tidal range for Lake Bardawil ranging from 0.30 m to 0.55 m. The tidal conditions can be characterised as a semi-diurnal micro tidal. Furthermore, a seasonal variation in mean water level is found in data (Makers, 2022). During spring the mean sea level is lower along the whole northern Egyptian coast. This effect is strongest at Port Said, possibly indicating this effect to be an influence of the Suez Canal that is located at Port Said.

Wave conditions

The wave climate just east of Lake Bardawil can be divided into two seasons: winter and summer (Frihy et al., 2002). The summer season is mainly characterised by low swell waves originating from West Northwest (WNW) and Northeast (NE), rarely exceeding 1 m to 1.5 m. During winter conditions fluctuate between stormy and calm and originate from North Northwest (NNW) to WNW. Winter waves are much higher than summer waves, and are the predominant cause of morphological changes (Frihy et al., 2002). The measurements by Frihy et al. (2002) conclude that the average wave height and period are 0.5 m and 6.3 s. Results from measurements at a different location, Port Said, by Linnarsund and Mårtensson (2008) conclude these same average values, indicating similarity along the coast between these two study locations.

Measurements taken just outside of Boughaz 1 by Nassar et al. (2018) in 2010 confirm the general direction and magnitude of the wave climate. Nassar et al. (2018) mention a maximum wave height of 4 m during the measurement period. The conditions are represented in Figure 1.3.

For analysis in this research, modelled offshore wave data from InfoplazaWaveClimate (2023) will be used.

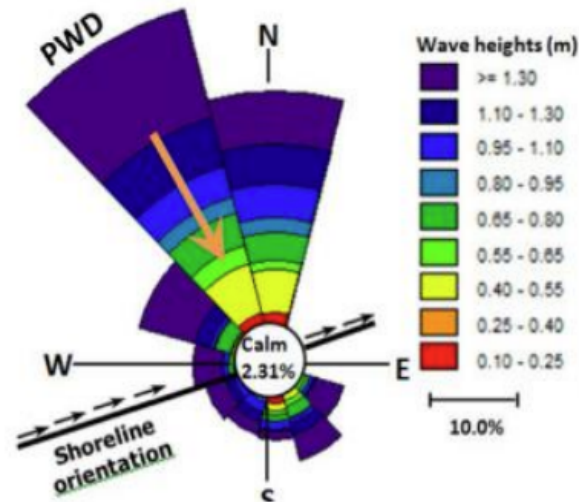


Figure 1.3: Wave rose of conditions measured in 2010 constructed by Nassar et al. (2018)

Wind conditions

The wind conditions for Lake Bardawil are taken from models by Meteoblue (2020). The data is supported by measurements done at Port Said by Linnarsund and Mårtensson (2008). The dataset shows a clear seasonal and daily variation in wind speed and direction. Generally, the largest wind velocities are found in winter in West Southwest (WSW) direction. During spring and through the summer the magnitude of the wind decreases and the dominant wind direction changes to Northwest (NW) to NE. The yearly average wind speed is between 3.7 m/s and 4.9 m/s, with a peak velocity of around 14 m/s. The daily pattern shows that winds are strongest during the afternoon and weakest at night.

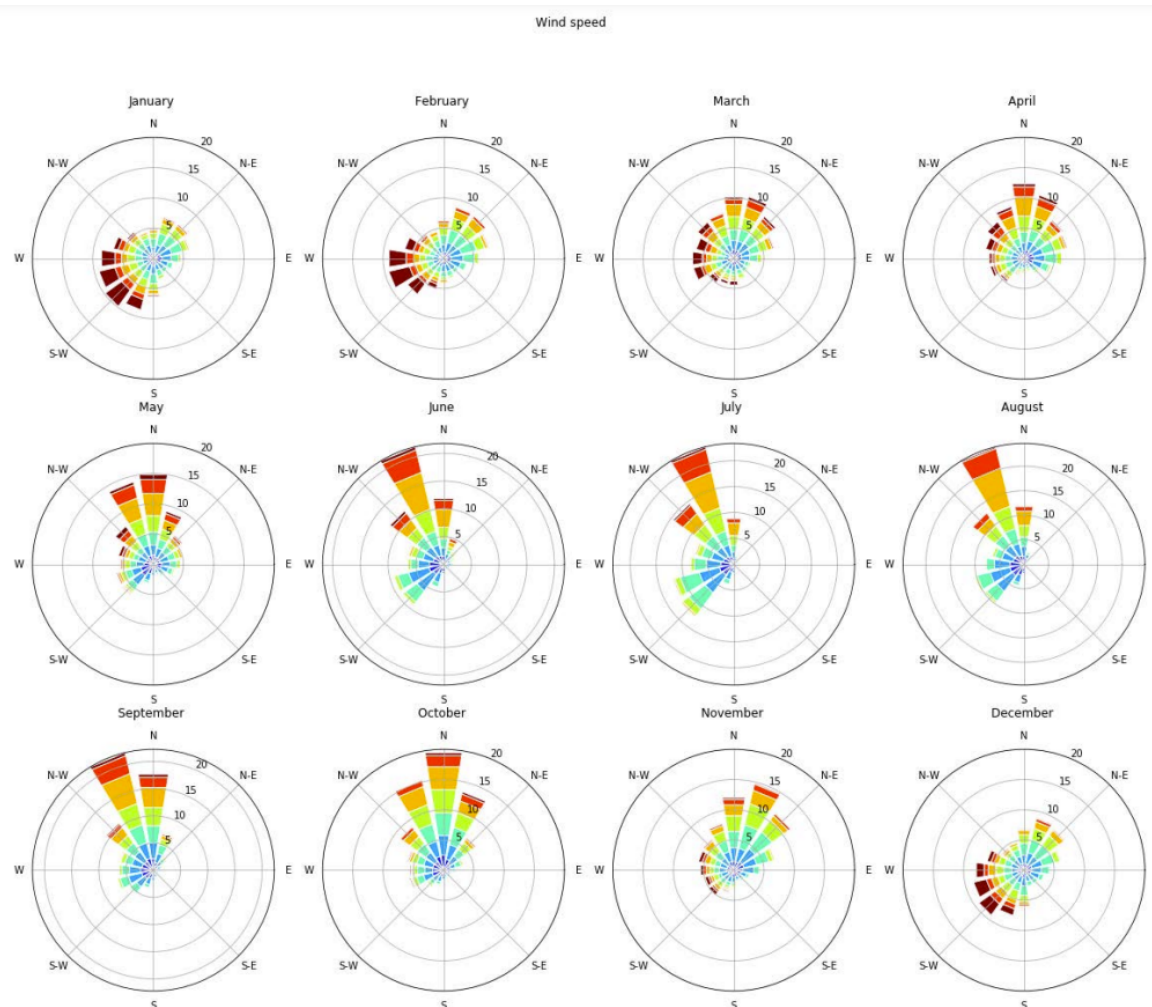


Figure 1.4: Wind roses illustrating monthly wind characteristics over a 26-year period (1992-2018) (van Bentem, 2020)

Rainfall, salinity & evaporation

An overview of climate data at Lake Bardawil can be found in Table 1.1. Low yearly rainfall (80 mm - 100 mm) and high yearly evaporation (1500 mm) results in a hypersaline environment in the lagoon. The salinity in the lagoon ranges from 38.3‰ to 71.1‰, depending on the location (Ellah & Hussein, 2009). Significant climatic seasonal variations result in equally significant seasonal variations in salinity in the lagoon. High evaporation and low rainfall also result in a net water loss in the lagoon. This water loss is compensated by water inflow through the inlets. This means there is a net flow into the lagoon.

	Jan	Feb	Mar	Apr	May	Jun	Jul	Aug	Sep	Oct	Nov	Dec
Mean temperature (°C)	14	15	16	19	22	24	26	27	25	24	21	15
Precipitation (mm)	13	10	9	7	5	0	0	0	0	0	18	20
Evaporation rate (mm)	56	84	96	132	167	189	192	177	153	146	63	50
Net water loss (mm/day)	1.4	2.6	2.8	4.2	5.2	6.3	6.2	5.7	5.1	4.7	1.5	1.0

Table 1.1: Climate at Lake Bardawil (Euroconsult, 1995)

1.3.2 Sediment characteristics

In 2018, grab samples have been taken in several locations in and outside Lake Bardawil. The sample shown in Figure 1.5 has been chosen to represent all of the Lake Bardawil basin. The sample shows that the sediment composition in the basin itself includes, clay, silt, fine sand, medium sand and coarse sand. The sediment composition along the shoreline mainly includes sand fractions, with reduced clay and silt fractions.

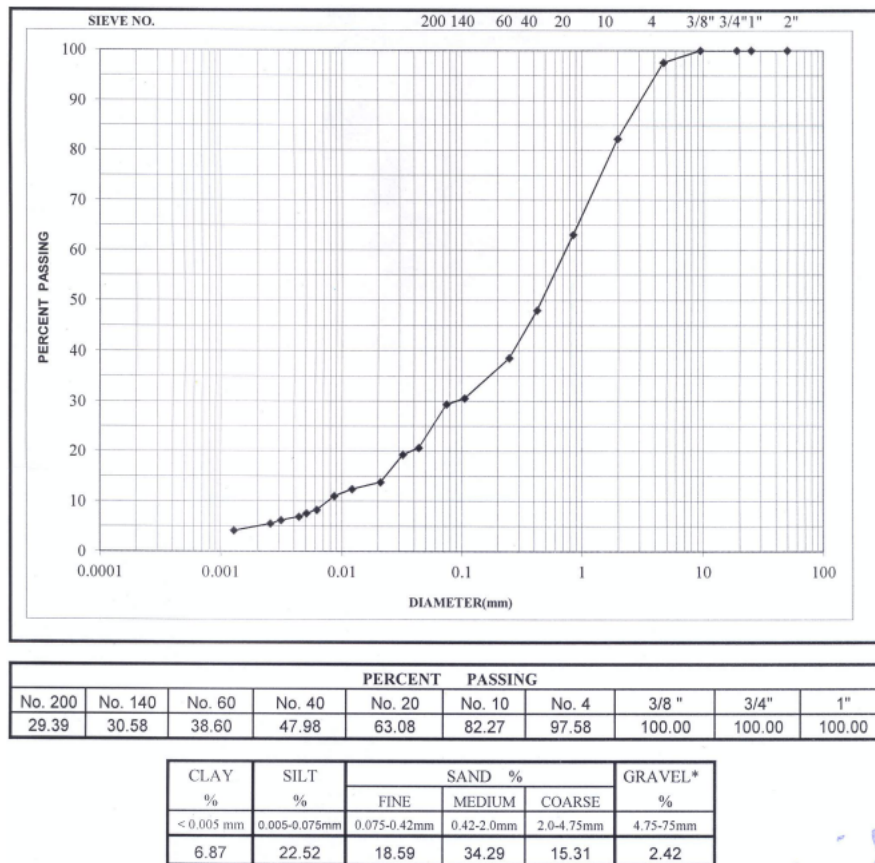


Figure 1.5: Grab sample taken from the eastern basin in 2018.

1.3.3 Bathymetry

The available bathymetry data comes from two sources: A site investigation from 2020 and a satellite derived bathymetry (SDB) using ICESat-2 and Sentinel-2 (OpenAltimetry.org, n.d., Sinergise Ltd., 2023). The data used is a combination of these two sources, taking the SDB and filling in the unavailable data due to turbidity with the on-site measurements.

The combined data is shown in Figure 1.6. In the main channel of the western inlet, depths reach a maximum of approximately 13m. This depth reduces quickly to 3.5m in the flood channels and the main ebb channel. In the eastern inlet, depths range from 9m to 5m in the main channel. The flood channels have a depth of 3.5m to 5m. The depth in the main basins ranges from 1m to 2.5m with an average depth in the lagoon of 1.3m to 1.4m. There is little intertidal area in the basin.

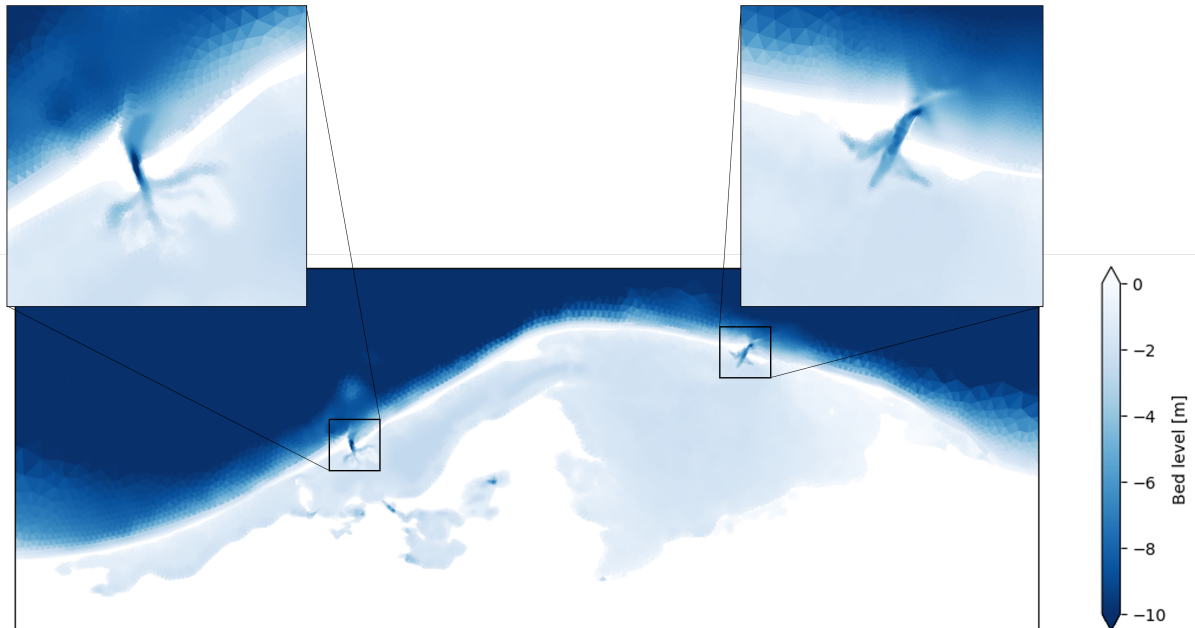


Figure 1.6: Bathymetry gathered from combined data in Lake Bardawil, boxes 1 & 2 highlight the bathymetry of Boughaz 1 & 2.

The offshore bed level as shown in Figure 1.7 ranges from just under -20m on the northwestern side of the domain to under -120m on the northeastern side of the domain.

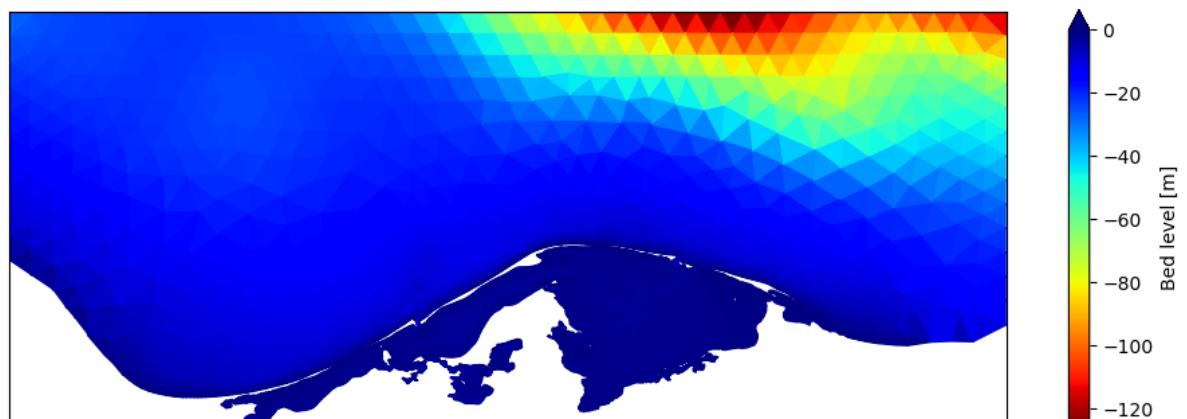


Figure 1.7: Offshore bed levels interpolated onto the D-flow FM unstructured grid in the Lake Bardawil area.

1.4 Research objective

The aim of this study is to assess the short-term response of the Lake Bardawil system to the proposed dredging interventions. The main focus of this study within the response of the system will be on the immediate morphological response of the inlets. The response of the system can be divided into two main parts: the hydrodynamic response to the interventions and the morphological response to the interventions. Research into the hydrodynamic response has three goals: Firstly, gaining more understanding of the general behaviour of the entire basin in the Status Quo situation and its response to the interventions. Secondly, the evaluation of the change in the expected drivers behind increased fish attraction, namely tidal prism and decreased salinity in the lagoon. Lastly and most importantly for this research, looking for indications of

changes to the morphological behaviour in the inlets. The research into the morphological response of the system aims to predict the changes to the morphology of the inlets in the short term. The goal of these predictions is to find any processes impeding the main function of the interventions of increasing the tidal prism.

There is little information available in literature concerning the response to interventions in a multiple tidal inlet system. Combined with the micro-tidal and shallow nature of Lake Bardawil, there is a complete lack of known fitting reference material. Predicting the hydrodynamic and initial morphological response to the interventions at Lake Bardawil should therefore prove valuable for both the project and as an addition to literature and knowledge of micro-tidal systems and multiple-inlet systems.

1.5 Research question

What is the short-term effect of dredging interventions in the tidal inlets on the Lake Bardawil double inlet system?

1. What processes govern tidal propagation in a shallow micro-tidal lagoon?
2. What processes govern morphological response in a shallow micro-tidal lagoon?
3. What methods are most suitable to predict the hydrodynamic and initial morphological response to interventions?
4. What is the predicted hydrodynamic response to the situation before and after interventions?
5. What is the effect of the interventions on the hydrodynamic interaction between the inlets?
6. What is the predicted initial morphological response to the dredging interventions made at the tidal inlets?
7. What can be said about processes impeding the functioning of the tidal inlet interventions?

1.6 Methodology

1.6.1 Literature review

In order to accurately predict the system response, a high level of system understanding is required. The first step towards understanding the system is acquiring the local conditions and information on the history of the lake. The resources from The Weather Makers provide sufficient reading and data for system understanding in this regard. The next step is understanding the processes governing changes to the system. In this literature review, two important categories of processes specifically relevant to Lake Bardawil are distinguished: tidal propagation in a multiple-inlet micro-tidal shallow lagoon and morphological processes in a multiple-inlet micro-tidal shallow lagoon. In the literature review, these processes will be identified and the relevance to Lake Bardawil will be demonstrated.

1.6.2 Hydrodynamic modelling

To make predictions on the hydrodynamic response to the planned interventions, a hydrodynamic numerical model for the lagoon will be made for the lagoon to compute two different scenarios. These scenarios, Status Quo (SQ) and Early Works (EW), represent the situation before interventions are implemented and the situation directly after the implementation of the planned interventions.

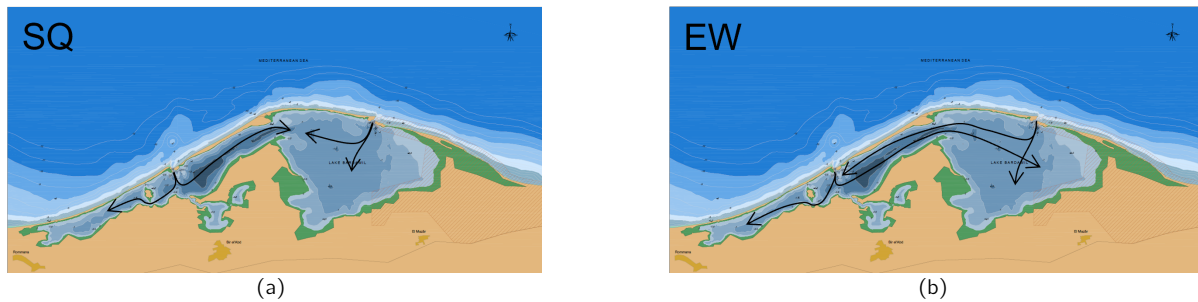


Figure 1.8: Representation of scenarios SQ Figure 1.8a and EW Figure 1.8b, length of arrows indicating the expected change in tidal propagation.

Hydrodynamic simulation of SQ aims to reproduce the current hydrodynamic conditions at Lake Bardawil, creating a baseline for further analysis. Hydrodynamic analysis of EW aims to simulate the hydrodynamic response of the basin to the interventions. The most important results for the hydrodynamic model will be derived from a comparison between EW and SQ. To represent the seasonally varying conditions in Lake Bardawil, the scenarios will be subjected to periods of winter and summer conditions.

The hydrodynamic conditions are analysed in terms of their predicted effect on the morphology of the system and the inlets specifically.

The exact methodology and model setup for the hydrodynamic analysis are described in chapter 3. The hydrodynamic analysis will be used to designate areas of interest and look for important processes for the morphological analysis.

1.6.3 Morphological modelling

For both scenarios and both seasons considered, a morphological model is made to predict the short-term morphological response in the system. The primary objective of this model is to detect potential system responses that may hinder the functioning of the interventions. The primary focus of analysis using the morphological model revolves around examining sedimentation and erosion occurring in and around the inlets. Furthermore, additional analyses are conducted to investigate sediment transport and sediment resuspension.

The same setup for the morphological model will be used for SQ to provide a baseline case to compare the results for EW to. In this way, the morphological response found in EW can be attributed to the dredging interventions.

2 Literature review

To make predictions and understand the context of model results, it is important to explore the hydrodynamic and morphological processes that are specifically relevant to a shallow micro-tidal double inlet lagoon like Lake Bardawil. This chapter studies literature and reference cases to highlight these relevant processes.

2.1 Tidal propagation in a shallow micro-tidal lagoon

Using similar situations and systems all around the world, insight is gained into the processes governing tidal propagation in a shallow micro-tidal double inlet lagoon. Looking at limiting factors on the tidal prism and water exchange and other phenomena observed in these similar systems.

2.1.1 Limitation by inlet

The planned interventions are primarily meant to increase water exchange between the Mediterranean Sea and Lake Bardawil by, among other things, increasing the cross-sectional area of the inlets. The expectation is that the tidal range, and therefore the water exchange, will increase after implementation of the interventions.

This is supported by the empirical A-P relationship between the inlet cross-sectional area A (m^2) and the tidal prism P (m^3) given location specific observed empirical parameters C and q (O'Brien (1969)).

$$A = CP^q \quad (2.1)$$

Several studies into dredging interactions in coastal lagoons along the Mediterranean Sea indicate cross-sectional area limitations on tidal range in sea-lagoon interactions (García-Oliva et al., 2018; Maicu et al., 2021).

In Mar Menor, a micro-tidal hypersaline lagoon located in the Southeast of Spain, dredging interventions on inlets are considered to increase water quality (García-Oliva et al., 2018). The lagoon is connected to the Mediterranean Sea by three inlets. The study by García-Oliva et al. (2018) uses a numerical model to assess the effect of interventions on hydrodynamic conditions and possible ecological consequences. An assessment is made for multiple options for dredging interventions with different cross-sectional areas in different inlets. The total average discharge for all inlets can be compared to the so-called openness parameter, defined as the sum of all inlet cross-sectional areas divided by the total lagoon surface area. The study concludes a high correlation ($R^2 = 0.98$) between the openness parameter and total average discharge through the inlets. As the openness parameter is directly proportional to the inlet cross-section and the total average discharge is directly proportional to the tidal prism, a relation between inlet cross-section and tidal prism can also be concluded for this case.

In a study by Maicu et al. (2021) on the lagoon at Nador, Morocco, the hydrodynamics after interventions to the inlet are modelled. At Nador, the original inlet was closed and a new, much larger, inlet was opened to facilitate navigation, increase water circulation and improve water quality. The cross-sectional area of the new inlet is about five times as large as the cross-sectional area of the original inlet. The hydrodynamic model for the new inlet results in a tidal prism almost four times as large as the tidal prism of the original inlet. Furthermore, the reduction of the tidal amplitude inside the lagoon compared to the tidal amplitude outside of the lagoon was diminished. Originally the amplitude was damped by 21 cm, whereas in the new situation the amplitude is damped by 3 cm.

Based on the increased tidal prism after dredging interventions in these two reference cases, the planned interventions at Lake Bardawil are expected to result in an increased tidal prism and reduced damping of

the tidal amplitude inside the lagoon compared to the tidal amplitude outside of the lagoon.

2.1.2 Limitation by friction

Generally, in tidal basins, two important areas can be distinguished: The tidal channel and the tidal flats. The tidal wave mainly propagates along the deeper tidal channel, while the flats mainly serve as storage. To predict the shape of the tidal propagation in the lagoon, the cross-section of the lagoon is schematised in Figure 2.1. In this schematisation the flow is discharged in A_s and A is just used for storage. A straight basin is assumed.

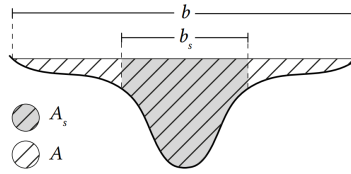


Figure 2.1: Schematisation of the tidal lagoon (Bosboom & Stive, 2021).

Using the mass balance equation (simplified with $b = b_s$ and an assumption of a prismatic channel) and the momentum balance equation (simplified for a small tide by neglecting the advective term) the following expression in Equation 2.2 and further simplified solution in Equation 2.4 and 2.5 can be found (Bosboom & Stive, 2021).

$$\frac{\delta^2 \eta}{\delta t^2} - gh \frac{\delta^2 \eta}{\delta x^2} + \frac{r}{h} \frac{\delta \eta}{\delta t} = 0 \quad (2.2)$$

Simplifying this expression for a shallow basin, where friction dominates inertia results in Equation 2.3 from Equation 2.2 with $D = gh^2/r$.

$$\frac{\delta \eta}{\delta t} = D \frac{\delta^2 \eta}{\delta x^2} \quad (2.3)$$

The solution for this equation can be shown as:

$$\eta(x, t) = ae^{-kx} \cos(\omega t - kx), \text{ with } k = \sqrt{\frac{\omega}{2D}} \quad (2.4)$$

and

$$u(x, t) = \frac{a}{h} \sqrt{\omega D} e^{-kx} \cos(\omega t - kx + \pi/4) \quad (2.5)$$

This shows the tidal wave to be progressively damped in the x direction. Meaning the tidal amplitude will decrease in x direction further into the basin.

2.1.3 Interaction between tidal waves in multiple inlet systems

An interesting case to look at when reviewing interaction between tidal waves in a multiple inlet system is the Santa Maria La Reforma lagoon on the northwestern Mexican coast. This lagoon is similar in size (586 km² to 550 km²) to Lake Bardawil and is quite shallow (minimum of 1.7 m and overall average depth of 3.3 m) (Serrano et al., 2013). The lagoon is connected to the Gulf of California by two large inlets. The tidal climate is micro-tidal like Lake Bardawil, but the tidal range is significantly larger (1.45 m to ± 0.5 m). Interestingly and similarly, there is also a zone of convergence creating a strait like in Lake Bardawil. As the system is so similar, interesting insights can be gained from observing the propagation of the tidal waves.

The study by Serrano et al. (2013) describes the water level variations and tidal currents using a numerical model. The model is calibrated with water level and current measurements. The model shows an 11 min phase lag for the tidal wave between the south and the north inlet. The tidal waves then propagate through the lagoon and meet centrally with a phase lag of roughly 90 min relative to both inlets. Furthermore, ebb duration in the middle is 66 minutes longer than flood duration. This tidal asymmetry is much smaller in

each of the inlets, where ebb duration is only 11 minutes longer. High tide propagates significantly faster than low tide in this lagoon. As the tidal waves interact in the central part of the lagoon, the amplitudes are amplified. This results in a tidal range increase of around 0.3 m in the center, compared to the tidal range in the inlets. The amplification of the tidal range is linked to changes in depth and width of the strait relative to the basins (Serrano et al., 2013).

Analysing the velocity phase in Santa Maria La Reforma, Serrano et al. (2013) concluded the tidal behaviour in the lagoon to be that of a standing or near-standing wave. Initially the tidal behaviour was expected to be of a progressive nature, due to the lengthscale of the lagoon. Serrano et al. (2013) conclude that the lagoon behaves as two short lengthscale lagoons, with the strait and convergence zone functioning as a barrier.

The case at Santa Maria La Reforma can be used to make a prediction on the behaviour of the tidal propagation in Lake Bardawil. Due to the tidal wave propagating from both inlets in Lake Bardawil and meeting in the middle and the similar convergence zone, amplification of the tidal amplitude can be expected in the central area between the inlets. The reference case indicates a spatial variation in tidal asymmetry that could be important to explore in Lake Bardawil. Furthermore, Santa Maria La Reforma could indicate a standing or near-standing nature for the tidal wave velocity phase in Lake Bardawil.

2.2 Morphology of a shallow micro-tidal lagoon system

In this section, the processes governing the morphology and the general behaviour of the inlets and the basin of Lake Bardawil are discussed.

2.2.1 General shape of tidal inlets

When describing the shape of an inlet, two main areas can be distinguished: the flood tidal delta and the ebb tidal delta. The shape of these deltas are influenced by the magnitude of the tidal prism and wave-induced longshore sand transport.

The ebb tidal delta is the body of sand on the seaward side of the inlet. The shape of ebb tidal deltas is well documented in literature and an idealised version can be seen in Figure 2.2. The shape and size of the ebb tidal delta is governed by the relative influence of tidal energy to wave energy (van de Kreeke and Brouwer, 2017). In a tide-dominated system, the ebb-tidal delta would be larger than in a more wave-dominated system.

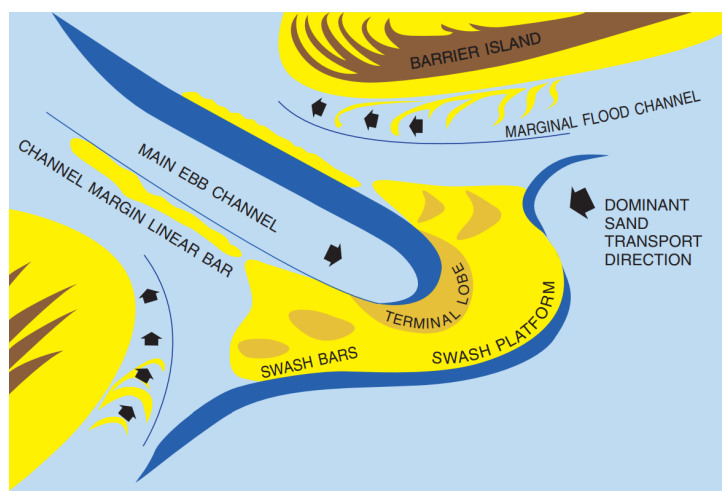


Figure 2.2: Idealised ebb tidal delta (van de Kreeke and Brouwer, 2017).

Similar to Equation 2.1, the empirical relation in Equation 2.6 exists for the volume of the ebb-tidal delta V and the tidal prism P . The coefficients α and b describe the exposure of the coast to wave energy. This relation was established by Walton and Adams (1976) and indicates that the total volume of the ebb-tidal delta will grow after interventions are made to increase the tidal prism.

$$V = \alpha P^b \quad (2.6)$$

Flood-tidal deltas are less well documented (van de Kreeke & Brouwer, 2017). In flood-tidal deltas, the role of waves is much smaller compared to ebb-tidal deltas. Flood-tidal deltas differ widely per case and it is difficult to create a single idealised figure as is given for the ebb-tidal delta Bosboom and Stive (2021). Figure 2.3 by Hayes (1980) does give a roughly accurate description of the most important components of the flood-tidal delta as seen in Lake Bardawil.

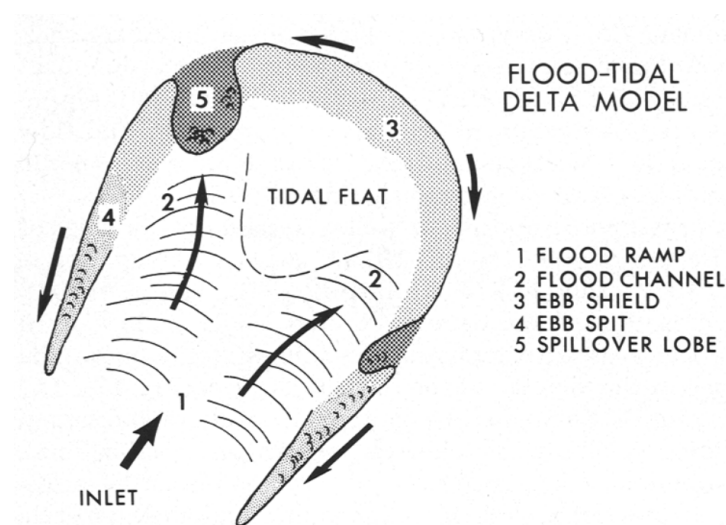


Figure 2.3: Figure of general flood tidal delta (Hayes, 1980).

As there is a lot of information available on the shape of ebb tidal deltas, looking at the shape of the ebb tidal delta in each of the inlets at Lake Bardawil can give an insight into the conditions of the system. The relative tidal or wave dominance can be estimated by identifying the form of sand transport or bypassing over the ebb tidal delta.

2.2.2 Bypassing modes

The transport from the updrift to the downdrift side of tidal inlets is referred to as sand bypassing. van de Kreeke and Brouwer (2017) name four important modes of bypassing: bar bypassing, tidal flow bypassing, spit formation and ebb delta breaching.

The bypassing mode for tidal inlets was related to the P/M ratio for a specific inlet by Bruun et al. (1978), where P is the tidal prism in spring conditions (m^3) and M is the total annual gross longshore sand transport ($m^3/year$).

In bar bypassing, sand is transferred directly onto the ebb tidal delta and subsequently carried to the downdrift side of the inlet. Observations result in a requirement for bar bypassing of a P/M ratio smaller than 50 (Bruun et al., 1978).

In tidal flow bypassing, sand is transported into the inlet during flood. The sand is then transported out of the ebb channel and deposited on the swash platform at the seaward side of the main ebb channel. Under the influence of waves, swash bars are formed that slowly move onshore over the swash platform. The

conclusions from observations by Bruun et al. (1978) require a P/M ratio higher than 150 for tidal flow bypassing to occur.

Spit formation bypassing is when the longshore transported sand is deposited in front of the ebb delta. As more sand is deposited in front of the inlet, a long spit is formed in the downdrift direction. If the spit is breached, the loose end of the spit moves onshore on the downdrift side. Spit breaching could occur due to storm washover and becomes more likely the longer the spit is. Spit formation bypassing is associated with the lowest P/M ratio, van de Kreeke and Brouwer (2017) observe two reference cases where spit formation occurs with P/M ratios of 12 and 17.

In ebb delta breaching sand is transferred over the ebb delta. Sand enters the main ebb channel and is then transported downdrift. This can form a curvature in the channel and eventually causes a new channel to form. The shoal between the old and the new channel moves downdrift to bypass the inlet. A case analysed by van de Kreeke and Brouwer (2017) shows a P/M ratio of 72.

Bypassing at Lake Bardawil

Using open source satellite imagery from Sentinel Playground (Sinergise Ltd., 2023), the inlets of Lake Bardawil are analysed. For Boughaz 1, no clear bypassing mode can be identified from the satellite images. Sand is deposited right next to the main channel, as can be seen in Figure 2.4a. Breaking waves are seen on the sand deposit on a day with rougher wave conditions in Figure 2.4b.



(a) Visible ebb delta formation in Boughaz 1.



(b) Wave breaking over shallow part of ebb delta.

Figure 2.4: Satellite imagery of Boughaz 1 (Sinergise Ltd., 2023).

For Boughaz 2, clear spit formation bypassing can be identified. A long spit is formed in the downdrift direction, as seen in the satellite imagery in Figure 2.5a. Wave breaking on the spit confirms a shallower area in Figure 2.5b. This mode of bypassing indicates that the P/M ratio for Boughaz 2 is low.



Figure 2.5: Satellite imagery of Boughaz 2 (Sinergise Ltd., 2023).

2.2.3 Bypassing mode and stability

The location stability of a tidal inlet is dependent on the mode of bypassing for the specific inlet. Bruun et al. (1978) linked the mode of bypassing and the P/M ratio to a subjective value for stability of: poor, fair and good. Bar bypassing is classified as having poor location stability, spit formation is poorly to fairly stable, ebb delta breaching is fairly stable and tidal flow bypassing is valued as "good" (van de Kreeke and Brouwer, 2017).

Due to the spit formation in Boughaz 2, the inlet should be poorly to fairly stable. The long spit results in the lengthening of the inlet in the shore-parallel direction. This causes the inlet to lose hydraulic efficiency and eventually close (van de Kreeke & Brouwer, 2017).

2.2.4 General stability of tidal inlets

Tidal inlets are in equilibrium when the volume of sand entering the inlet is equal to the volume of sand leaving the inlet. This equilibrium is stable when after a perturbation from the equilibrium, the inlet returns to its equilibrium value.

Escoffier (1940) first described a stability model for tidal inlets. Assuming a sinusoidal inlet velocity, Escoffier reasoned that the inlet is in equilibrium when the cross-sectionally averaged velocity amplitude \hat{u} equals the equilibrium velocity \hat{u}_{eq} . If \hat{u} is larger than \hat{u}_{eq} , the cross-sectional area will increase and vice versa. Both \hat{u} and \hat{u}_{eq} are in principle functions of the cross-sectional area of the inlet. In practice, for \hat{u}_{eq} the relation to the cross-sectional area is weak. Escoffier assumes \hat{u}_{eq} to be ~ 1 m/s.

To visualise inlet stability, Escoffier constructed the Escoffier Diagram. An example of an Escoffier Diagram is shown in Figure 2.6 The Escoffier Diagram consists of the closure curve $\hat{u}(A)$ and the equilibrium curve $\hat{u}_{eq}(A)$. In practice $\hat{u}_{eq}(A) = 1$.

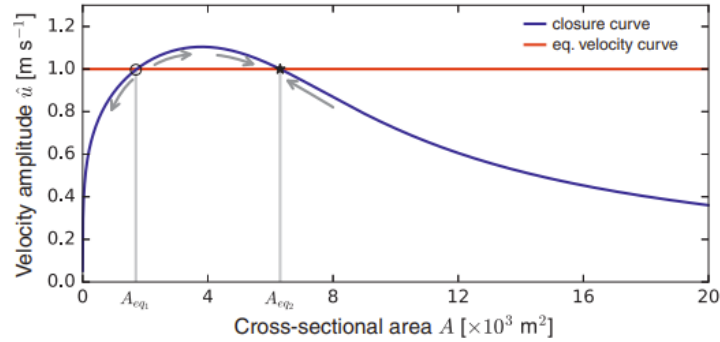


Figure 2.6: Example of Escoffier Diagram relating the cross-sectionally averaged inlet velocity amplitude to the cross-sectional area of the inlet (van de Kreeke and Brouwer, 2017).

In general, for a single inlet system, the Escoffier Diagram looks like Figure 2.6. The functions have two intersections, corresponding to two equilibrium cross-sectional areas: A_{eq1} and A_{eq2} . When $\hat{u} < \hat{u}_{eq}$ the inlet shoals and when $\hat{u} > \hat{u}_{eq}$ the inlet erodes, therefore it can be concluded that the equilibrium corresponding to A_{eq1} is unstable and the equilibrium corresponding to A_{eq2} is stable.

Following this theory, increasing the cross-sectional area of an inlet by a sufficient amount to exceed A_{eq1} , results in a stable inlet. This means the interventions planned for Lake Bardawil could result in a stable situation for the inlets.

Stability of double inlet systems

Applying Escoffier to multiple inlet systems makes it more complex. Analytical computation of simplified basins with two inlets and uniform water levels only results in a stable equilibrium at a cross-sectional area of 0 for both inlets, meaning unconditional closure of the inlets (van de Kreeke & Brouwer, 2017). Adding more detail results in solutions with non-zero stable equilibriums, as supported by the existence of multiple inlet systems in reality. As tidal interaction between the inlets in Lake Bardawil is limited the analysis in this research will be limited to applying Escoffier to the single inlets using their individual tidal prisms.

2.2.5 Tidal asymmetry

To predict changes to morphology in a tidal basin, it is crucial to determine whether it is net importing or net exporting sediment. Net import or export of sediment in tidal basins is highly related to horizontal tidal asymmetry. The relevant type of asymmetry is dependent on the size of sediments, among other things. For this purpose two groups of sediments can be distinguished: Coarse sediment and fine sediment.

Coarse sediment

The basis of the effect of tidal asymmetry on coarse sediment lies in the expression for bed load transport in terms of flow velocity given in Equation 2.7 (Bosboom and Stive, 2021). In which S is the volumetric transport in $m^3/s/m$, c is a coefficient and u is flow velocity. The coefficient n lies between 3 and 5, dependent on mode of transport. For coarse sediment, it is assumed that response to changes in flow velocity is instantaneous (Bosboom and Stive, 2021).

$$S \approx c|u^{n-1}|u \quad (2.7)$$

As the sediment transport rate is related to u^n , higher velocities have a higher impact on total transport rates than lower velocities with a longer duration. In general, for a simple tidal basin with one inlet, a shorter ebb or flood duration (ebb or flood dominance) means higher flow velocities in this direction. These higher velocities result in net sediment transport in the dominant direction.

Generally, a flood dominant system is characterised by shallow channels and limited intertidal storage, while ebb dominant systems are characterised by deep channels and large intertidal storage (Bosboom & Stive, 2021). This points towards flood dominance in Lake Bardawil, as there is little intertidal storage and channels are not abundant throughout the basin.

Fine sediment

In the process of fine sediment transport, due to a lower settling velocity, not only the local instantaneous flow conditions but additionally the flow conditions upstream and in the past need to be considered. As sedimentation happens during slack periods between ebb and flood, the duration of this slack period impacts the initial suspended fine sediment concentration for the ebb or flood period. The suspended fine sediment concentration will only increase due to higher flow velocity. The total transported fine sediment over a tidal cycle is largest for the ebb or flood period following the shortest slack period.

The lack of deep channels and intertidal storage in Lake Bardawil suggests a net import of fine sediments (Bosboom & Stive, 2021).

2.2.6 Wind waves

In the shallow micro-tidal lagoon of Venice, the study by Carniello et al. (2005) notes that over the tidal flats shear stresses caused by tidal currents are insufficient for resuspension of sediment. Tidal currents in the Venice lagoon are only sufficient to resuspend sediments in channels near the inlets. Resuspension of sediment over tidal flats are mainly caused by shear stress induced by wind waves. Suspended sediment is then transported by tidal currents.

Waves can be expected to stir up sediment more effectively for smaller water depths, resulting in a difference in resuspension of sediment between high and low tide (Bosboom & Stive, 2021). The opposite relation is shown however in shallow to intermediate waters Mariotti and Fagherazzi (2013) relate the bottom shear stress due to waves to wind speed, fetch and depth. This shows a positive relation between water level and shear stress in the shallow to intermediate domain as seen in figure Figure 2.7. Depending on the phase lag between the vertical and horizontal tide, wind waves could result in net export or net import of sediment. This effect could be reversed or weakened by high wind speeds in shallow areas.

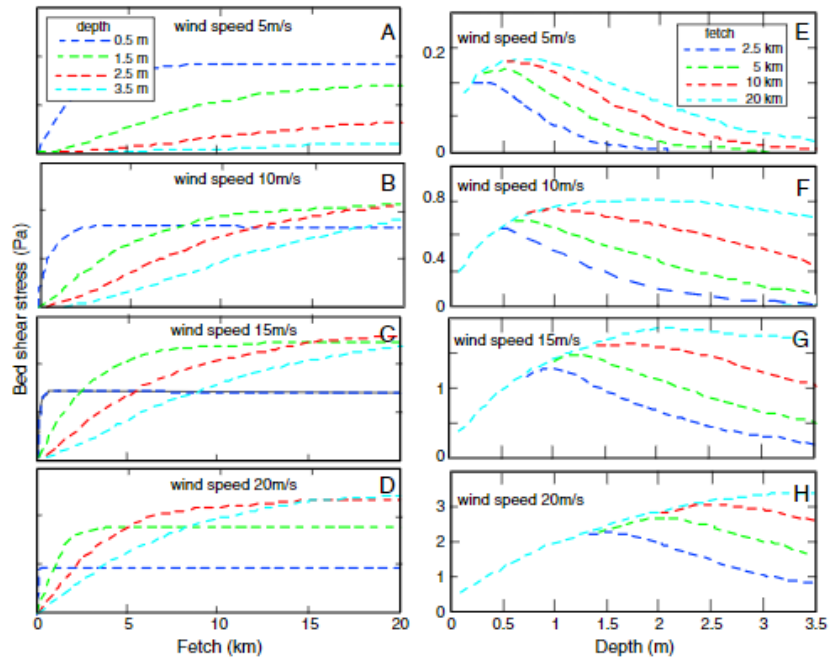


Figure 2.7: Bed shear stresses calculated with the SWAN model as a function of fetch for different wind speeds (A,B,C,D). Bed shear stresses calculated with the SWAN model as a function of depth for different wind speeds (E,F,G,H) (Green and Coco, 2014).

A study by Carlin et al. (2016) based on measurements in Galveston Bay, a shallow micro-tidal lagoon, investigated the effects of a cold front passage on the resuspension of sediments. The study measured currents, waves and used wind measurements from a location nearby. The study relates wind stress (τ_w), bed shear velocity from currents (u_{*c}) and bed shear velocity from currents and waves (u_{*cw}) to suspended sediment concentration (SSC). The relation between u_{*cw} and SSC was found to be the strongest. The data shows that periods of high SSC correspond to the periods with the biggest wave heights, however this relation was not explicitly investigated. The study concludes that the best predictor for SSC is the wave height influenced by wind speed and fetch.

For Lake Bardawil this stresses the importance of both wind speed and wind direction. The lagoon consists mostly of shallow tidal flats with presumably low tidal current velocities where wind waves are expected to be the main cause of sediment suspension. The largest magnitudes of wind speed are found during winter in SW direction. The fetch for this wind condition is large due to the channel in the SW direction. Wind waves are expected to have a significant impact on sediment suspension in the northern part of the lagoon during winter.

3 Methodology

In this chapter, the methodology for analysis of the system and its response to the interventions are discussed. The setup for the hydrodynamic and morphological model and the assumptions used are presented.

3.1 Hydrodynamic model setup

For hydrodynamic analysis, a model is made in D-flow FM. The model applied is a depth-averaged 2D model. In this section, the considerations during the hydrodynamic model setup are explained.

3.1.1 Grid

The grid presented in Figure 3.1 is used for hydrodynamic modelling. For flow computations a flexible mesh is used, using mostly triangular grid cells. The grid is more detailed in locations where more hydrodynamic activity is expected and less detailed in locations where less hydrodynamic activity is expected.

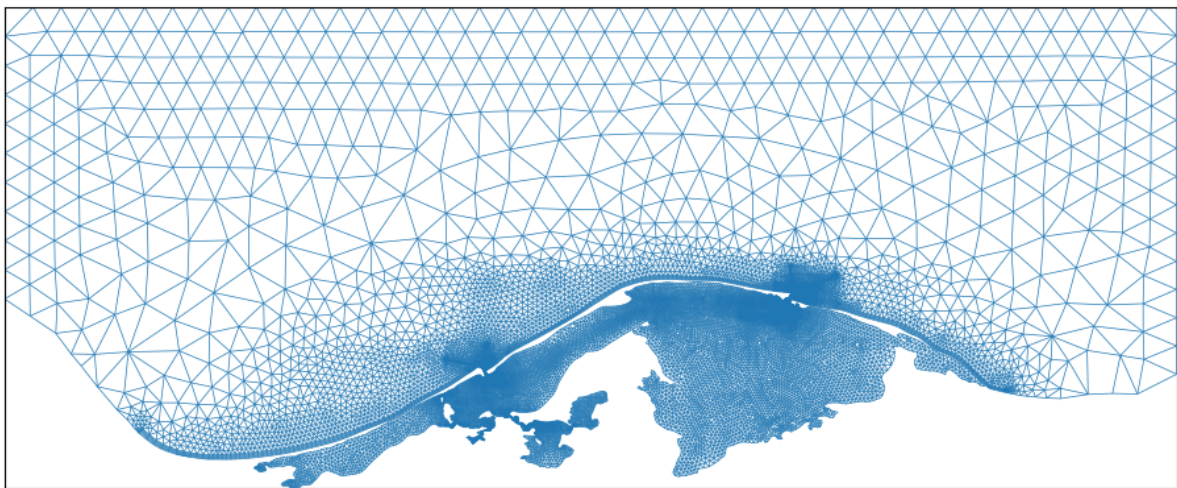


Figure 3.1: Grid used for modelling in D-Flow FM. Grid cell edge length ranges from roughly 15m to 4500m.

3.1.2 Parameters

To set up the hydrodynamic model in D-flow FM, certain parameters are required. In this subsection the decisions for these parameters and the assumptions behind these decisions are described.

Bottom friction parameter

To account for depth dependency on bottom friction, the Manning formula is used. As there is no data available on the friction parameter at Lake Bardawil specifically, data from estuaries by Cai (2014) is used. The Strickler coefficient (K) for a number of estuaries ranges from 31 to 67. The Manning formula uses Manning's roughness coefficient (n), which is defined as $1/K$. A central value for K is chosen from the table by Cai (2014), corresponding to an n of 0.023 this value is applied uniformly. In subsection C.1.4 an insight is given of the sensitivity of the system to bottom friction for a tidal-only situation.

Initial conditions

To reduce spin-up time and to achieve realistic results as quickly as possible, initial conditions are supplied for salinity and temperature. The initial condition for water level is zero over the whole domain.

To achieve somewhat realistic initial conditions in terms of salinity and temperature, a model by TWM was used. This model has been run for a number of years and resulted in realistic values for salinity in most locations. The values for salinity in remote locations are exaggerated in these results. The values for the starting dates have been extracted and modified with a maximum for salinity to take away any unrealistically high salinity values. The validation of these values can be found in section B.2

3.1.3 Tidal conditions

The offshore tidal conditions are taken from Delft Dashboard by Deltares. Delft Dashboard uses tide model TPXO 8.0 to derive tidal constituents for any location globally. The model bases its data on a tidal constituents database, tide gauges and buoys. The tidal constituents are modelled for the boundaries of the hydrodynamic model domain. The components are spacially varying over the edge of the model domain. For the northwestern corner of the domain the values in Table 3.1 are found. These boundary conditions are imposed as water level, normal velocity and tangential velocity in a flow condition in D-flow FM. For any simulation period, the tidal conditions are the same. The resulting tidal signal for water level at a point offshore from Boughaz 1 is found in Figure 3.2.

Component	M2	S2	N2	K2	K1	O1	P1	Q1	MF	MM	M4	MS4	MN4
Water level (m)	0.10659	0.06058	0.01632	0.01829	0.02302	0.01616	0.009	0.00283	0.004	0.00224	0	0.001	0
Normal velocity (m/s)	0.02801	0.01553	0.0042	0.00514	0.00296	0.00195	0.00112	0.00028	4E-05	1E-05	0.00016	0.00047	0.00011
Tangential velocity (m/s)	0.01471	0.00888	0.00218	0.00246	0.00165	0.00111	0.00067	0.00016	2E-05	1E-05	6E-05	0.0002	4E-05

Table 3.1: Tidal constituents at the northwestern corner of the modelling domain.

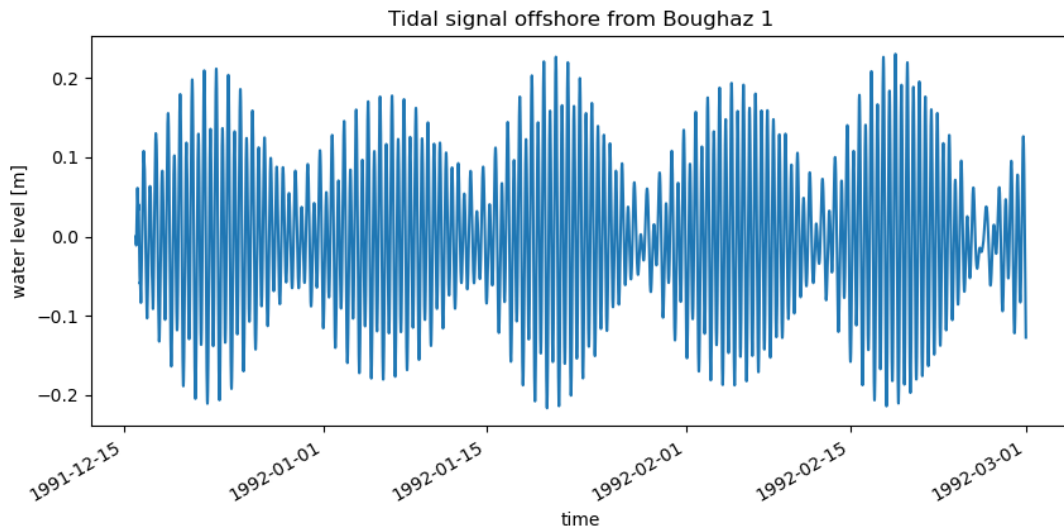


Figure 3.2: Tidal signal (water level) offshore from Boughaz 1, for all simulation periods of 2.5 months.

3.1.4 Weather conditions

Two typical weather time frames can be found at Lake Bardawil. The most important weather conditions represent summer and winter conditions. Analysis of the response to meteorological forcing will therefore be represented by either a summer period or a winter period. For the hydrodynamic simulations, the winter period of 1991/1992 is used. For the hydrodynamic simulations during summer, the summer 2005 is used. The temperature and wind speed for these period are shown in subsection B.1.1

3.2 Hydrodynamic model analysis

As described in section 1.6, the hydrodynamic analysis is conducted using two scenarios. In SQ the current situation is modelled and in EW the situation directly after the implementation of the interventions is modelled. Each of these scenarios is modelled in D-Flow FM as elaborated in section 3.1. To systematically build up understanding of the system, the scenarios are modelled under tidal forcing alone first. Meteorological forcing is added afterwards for winter and summer seasons.

Next to the general understanding of the hydrodynamic response to the interventions, the hydrodynamic analysis is used in combination with the processes identified in section 2.2 to make a prediction on the morphological response and inlet stability.

3.2.1 Hydrodynamic analysis under tidal forcing

To describe the hydrodynamic response to the interventions these scenarios are compared for a number of parameters. First of all, the spatial effect of the interventions is shown by comparing the tidal range over the whole basin. To analyse specific local developments in tidal range, the minimum and maximum water levels for a spring tidal cycle are plotted along the inlets and for other characteristic sections in the basin.

Increasing the tidal prism is the main function of the interventions. To analyse the response of the tidal prism, the tidal prism per inlet per cycle is plotted and compared for SQ and EW. For this analysis, the tidal prism per inlet is defined as the average of cumulative absolute flood and ebb discharge through an inlet during a single cycle. This comparison is done for a full lunar cycle of 28 days.

These two analyses can support the relation of the reference cases given in subsection 2.1.1 on the limitation of the inlet cross-section on the tidal range and prism.

Interaction between inlets in the simplest form is found in import or export of water per inlet. Plotting cumulative discharge shows import and export and allows for comparison and analysis of the interaction between the inlets for SQ and EW.

Analysing flow velocities is important for predicting morphological changes in the basin. Higher flow velocities result in more moving sediment particles and larger areas above certain critical velocity result in a larger morphologically dynamic area. To show the effect of the interventions on the maximum velocities in the whole basin, SQ and EW are spatially compared over a single spring tidal cycle. The change in cross-sectionally averaged velocity amplitude in the inlets is of special interest for morphology of the inlets due to the relation with inlet stability described in subsection 2.2.4. Therefore the cross-sectionally averaged velocities are specifically analysed for the inlets. Local maximum velocities in the inlets could indicate areas of erosion. The maximum velocities are therefore shown spatially per inlet.

For purposes of sediment import and export in the basin, the tidal asymmetry needs to be analysed. The tidal asymmetry is analysed in terms of ebb & flood duration for coarse sediment and slack duration for fine sediments.

For further understanding of the system response and further comparison to the reference case at Santa Maria La Reforma in subsection 2.1.3, the effect of the interventions on the tidal propagation speed is analysed. By comparing the arrival of the peak of the tidal wave at different locations, the effect of the interventions on tidal propagation can be analysed.

To predict the leading direction of sediment transport during resuspension events like a winter storm situation the velocity phase needs to be investigated. As discussed in subsection 2.2.6, resuspension due to wind waves is presumably largest during low tide. The direction and magnitude of tidal currents at this moment are important for understanding transport of this resuspended sediment.

3.2.2 Hydrodynamic analysis under tidal and meteorological forcing

The effect of meteorological forcing is compared to the tidally forced-only situation for water level, interaction between inlets and velocities in the inlet and in the basin.

Meteorological forcing results in some conditions that can not be compared to the tidal-only situation. In addition to the comparisons made, some new analyses are made. As one of the functions of the interventions is decreasing the hypersalinity in the lake, the effect of the interventions on salinity is analysed.

As wind waves are expected to be one of the main drivers of sediment resuspension, the local wave height is analysed for both scenarios in summer and winter. The combined wave height and flow velocities are an indicator for sediment resuspension. As the hydrodynamic model does not include waves, this information is taken from the coupled model discussed in section 3.3.

3.3 Morphological model set-up

The morphological model applies a coupled D-waves and D-flow FM model. The morphological model is a 2D model like the hydrodynamic model. In this section the considerations for model setup of the morphological model are discussed.

3.3.1 Grid

For the morphological model, an adapted version of the same unstructured grid is used to improve sediment transport computations. The rectangular cells along the coast are extended to the lateral boundaries of the flow domain. In addition to the adapted unstructured grid used in D-Flow FM, a structured grid is used for wave computations in D-Waves. The wave grid, and thus the wave domain, extends beyond the flow domain in lateral and seaward directions to ensure wave conditions enter the flow domain along all of its boundaries.

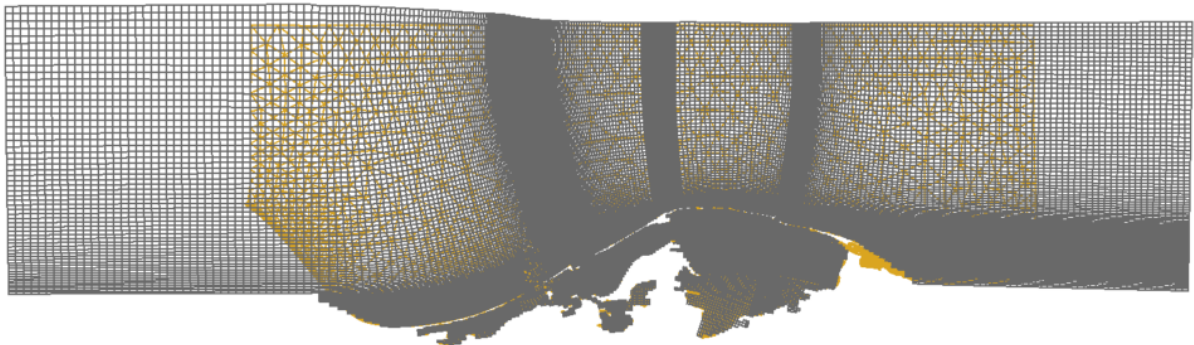


Figure 3.3: Combined structured wave grid (gray) and the adapted unstructured flow grid (yellow) used in the coupled model. The cell edge length for the wave grid varies from roughly 15m to 1300m.

3.3.2 Boundary conditions

In a coupled model, boundary conditions need to be adapted from the boundaries chosen in the hydrodynamic model. The velocity boundary conditions applied in the hydrodynamic model introduce instabilities along the flow boundary due to interactions with incoming wave conditions. To resolve this, all velocity boundaries have been removed from the flow domain's boundary. Additionally, the lateral boundaries of the flow domain have been replaced with a zero water level gradient Neumann boundary condition.

3.3.3 Sediment characteristics

Since the primary objective of the morphological model is to assess the effect of the interventions on the inlets, the sediment fractions used in the model are specifically chosen to suit this purpose. Considering the relatively high velocities and short slack times observed in the inlet and its surroundings, it is expected that the presence of the finest sediments will be limited in this area. To account for this, and to prevent technical issues with modelling, the model incorporates three fractions of sand while disregarding the influence of cohesive sediments. A 5m layer of each of these sediment fractions is spatially distributed uniformly over the flow domain.

These sand fractions have been selected from sample Alx-B-11 discussed in subsection 1.3.2. Clay and silt fractions in the sample are disregarded and the rest of the sample is divided into three equal parts as seen in Figure 3.4, representative D_{50} 's of 0.15mm, 0.7mm and 2 mm are chosen. A representative specific density of 2650 kg/m^3 and dry bed density of 1600 kg/m^3 for sand is chosen (Bosboom and Stive, 2021). Sediment transport for all fractions is calculated using the formulation by Van Rijn (1993) (Deltares, 2022).

Due to unknown (but confirmed by Deltares) technical issues in Delft3D FM, simulations with the chosen coarse sediment run into an error when winter conditions are applied. Therefore the analysis of morphological changes is limited to the fine and medium sediment fractions. A comparison between model results for simulations with all three sediment fractions, only the fine sand sediment fraction, only the medium sand sediment fraction and only the coarse sand sediment fraction is shown in Appendix E.

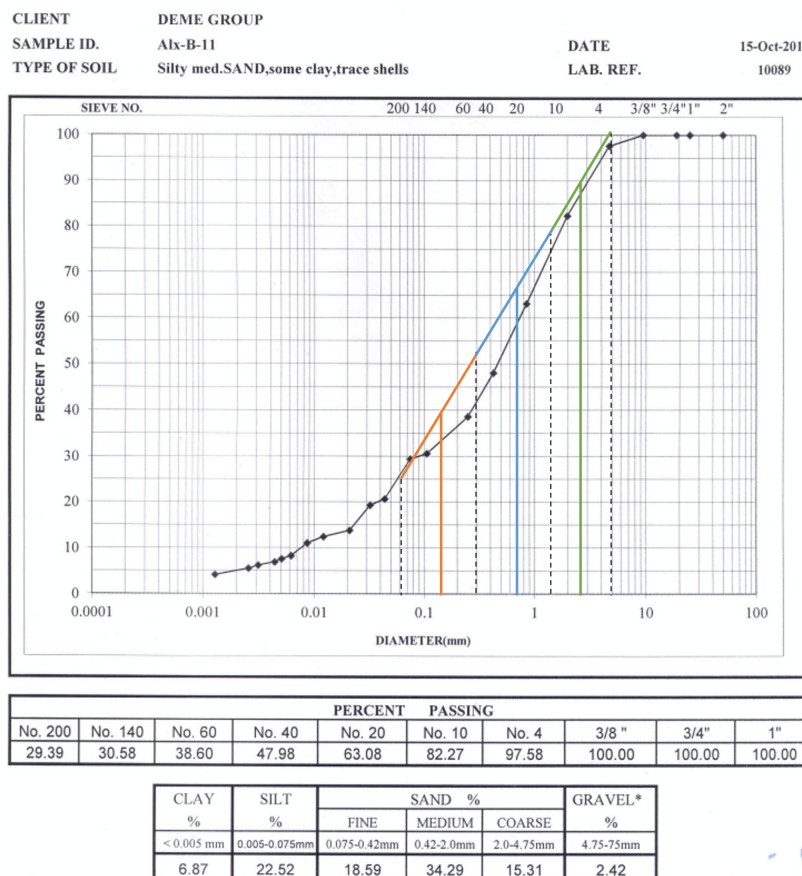


Figure 3.4: Selection of sand fractions from grab sample. Roughly translating to the chosen fractions in the model.

3.3.4 Weather conditions

For morphological modelling, a new dataset for meteorological conditions is used. This dataset is taken from the wave model by waveclimate.com and made available for this research by DEME. This dataset supplies modelled wind and wave data for a location offshore from Bardawil, positioned approximately on the seaward boundary of the flow and wave domain. The wave data is applied uniformly over the boundary of the wave domain while the corresponding wind data is applied uniformly over the entire flow and wave domain. As this data is modelled for this offshore location, the values for wind speeds are generally greater than the values used in the hydrodynamic model. For the morphological model, a winter period from 2014/2015 is used. For the summer period, the summer period of 2005 is used. The wind and temperature input can be found in subsection B.1.1.

3.3.5 Coupling

A new Simulating Waves Nearshore (SWAN) computation is made every three hours by the D-waves model. The SWAN computation computes wave characteristics based on the supplied offshore wave conditions on the seaward boundary, wind characteristics and updated hydrodynamic conditions supplied by the D-flow FM model. These wave characteristics are then used for the next three hours of hydrodynamic computations.

3.4 Morphological model analysis

The morphological model is used to make predictions on sediment transport and the specific locations for sedimentation and erosion. As it is not feasible to predict the exact morphological response to either situation, any meaningful analysis will have to come from a comparison between behaviour in the SQ situation and behaviour in the EW situation.

Morphological behaviour over the whole system is looked at, looking at sediment transport and morphological changes. Changes to transport in the inlet are analysed. Looking at the response of import and export of sediment over the inlets could be interesting for both inlet morphology and basin morphology. Most importantly, erosion and sedimentation in the inlets are compared, looking for processes indicating closure and changes to these processes after implementation of the interventions.

4 Results

In this chapter, the results of the hydrodynamic and morphological model simulations are presented. First, the relevant hydrodynamic response to only tidal forcing is shown, then meteorological forcing is added and lastly the results of the coupled morphological model are presented.

4.1 Hydrodynamic response to tidal forcing

In this section, the relevant results of the hydrodynamic model under tidal forcing only are presented for understanding the system and predictions of morphological changes due to changes in tidal currents.

4.1.1 Tidal range

The easiest way to look at the results of the interventions is to look at the difference in tidal range. After the interventions in the inlets, the maximum tidal range is increased over the entire area of the lake, as can be seen in Figure 4.1.

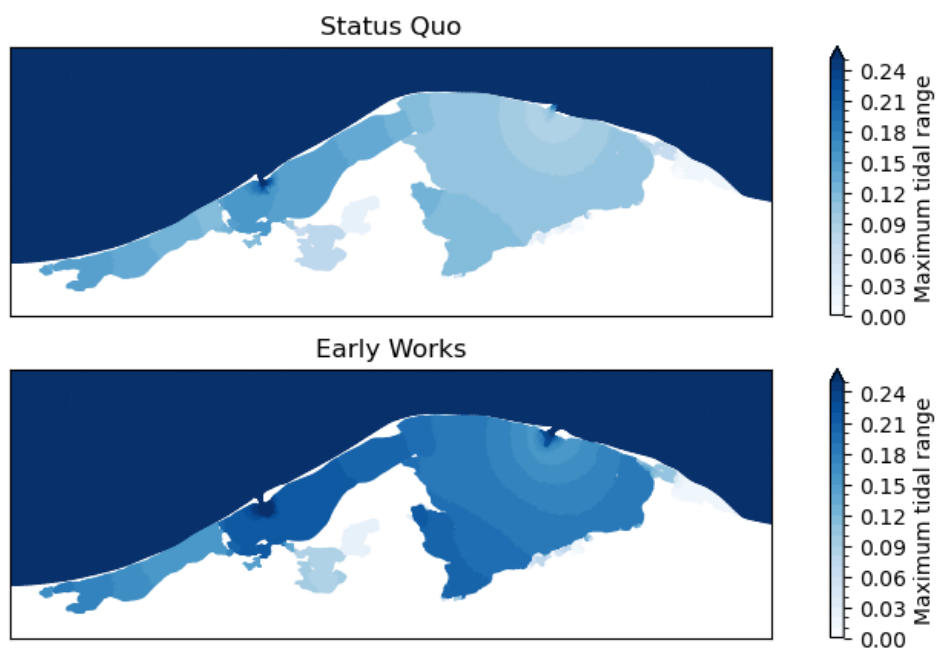


Figure 4.1: Maximum tidal range in spring conditions (20-1-1992 12:00 to 21-1-1992 12:00) comparing SQ to EW.

As seen from Figure 4.1, the largest gradients in the tidal range are found over the length of the inlets. To visualise these gradients the tidal range along the length of Boughaz 1 and Boughaz 2 are shown in figures 4.2 and 4.3.

At Boughaz 1, the tidal range is primarily increased in the areas that were or are shallow relative to the tidal inlet channel. The tidal range in the inlet itself, where the bed level was already low, is relatively unchanged. A larger change is found in the extended inlet channel and the shallow area following the inlet channel.

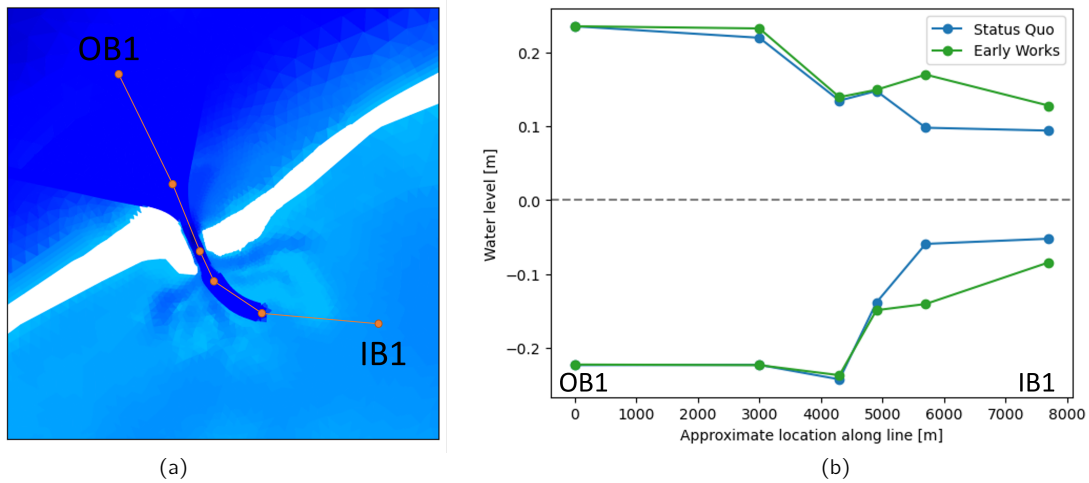


Figure 4.2: (a): Locations of the data points in (b). (b): Maximum and minimum water levels for SQ and EW during a single spring tidal cycle along the length of Boughaz 1. (20-1-1992 12:00 to 21-1-1992 12:00)

Boughaz 2 shows a different response in the inlet. The depth difference between SQ and EW is larger in the inlet at Boughaz 2. This results in a larger increase in tidal range in the inlet itself. The difference in tidal range in the shallow areas behind the inlet channel is similar to the difference found in Boughaz 1.

At the end of both inlet channels locally increased water levels are observed during high tide in EW

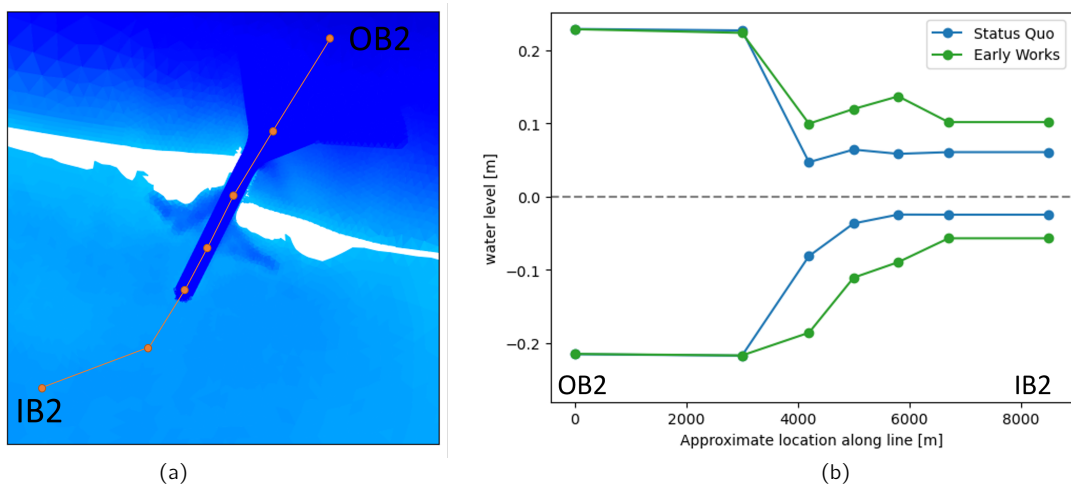


Figure 4.3: (a): Locations of the data points in (b). (b): Maximum and minimum water levels for SQ and EW during a single spring tidal cycle along the length of Boughaz 2. (20-1-1992 12:00 to 21-1-1992 12:00)

The response to the interventions in the rest of the basin is visualised using the locations shown in Figure 4.4. Figures 4.5, 4.6 and 4.7 show the maximum and minimum water levels for scenarios 1 and 4 per location along each of the lines in Figure 4.4.

The section between Boughaz 1 and Boughaz 2 is shown in Figure 4.5 and the orange line in Figure 4.4. The water levels generally decrease in the direction of Boughaz 2. The difference in tidal range along the shallow parts is relatively uniform.

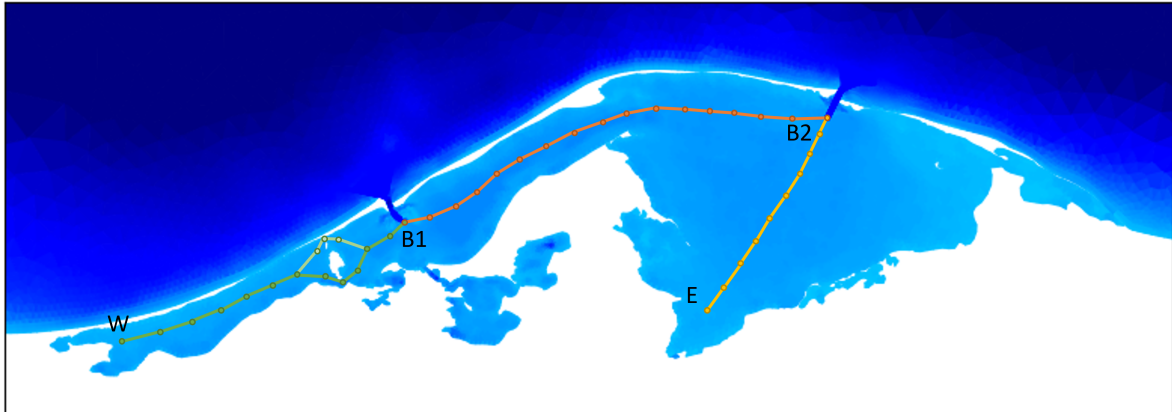


Figure 4.4: Approximate locations of the datapoints used to construct visualisations of the tidal range inside Lake Bardawil. The orange line represents the datapoints found in Figure 4.5 going from Boughaz 1 (B1) to Boughaz 2 (B2). The green line represents the datapoints found in Figure 4.6, going from the westernmost datapoint (W) to Boughaz 1 (B1). The yellow line represents the datapoints found in Figure 4.7 going from Boughaz 2 (B2) to the furthest point in the eastern basin (E).

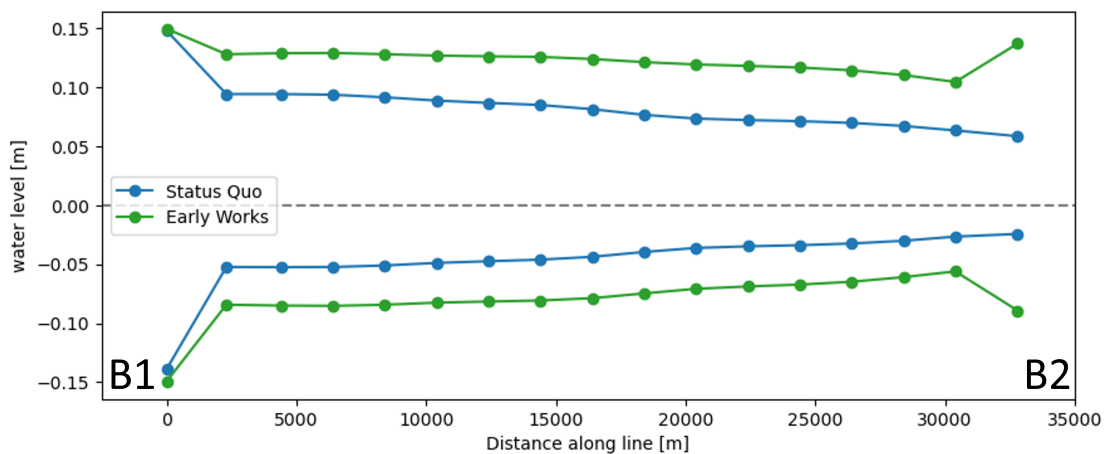


Figure 4.5: Minimum and maximum water levels between Boughaz 1 and 2 (orange line in Figure 4.4) during a single spring tidal cycle for SQ and EW.

The tidal range going westward from Boughaz 1 is steeply decreased over the narrow channels going past the islands. Water levels do not differ significantly between the southern and northern parts of the islands. Behind the islands a sloping effect can be seen in the maximum and minimum water level, increasing the tidal range towards the further ends of the lake.

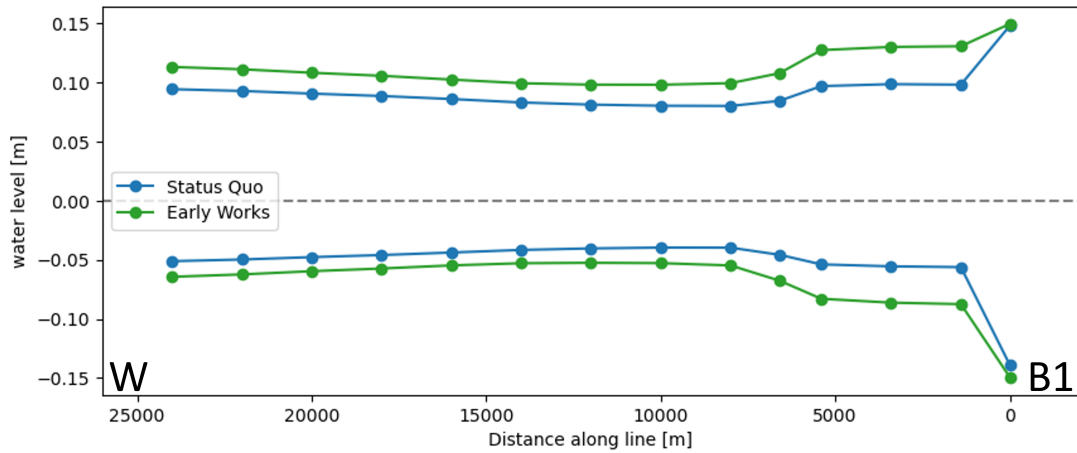


Figure 4.6: Minimum and maximum water levels westwards from Boughaz 1 (green line in Figure 4.4) during a single spring tidal cycle for SQ and EW.

The same sloping effect can be seen going into the main basin southwards from Boughaz 2. The tidal range increases moving away from the inlet.

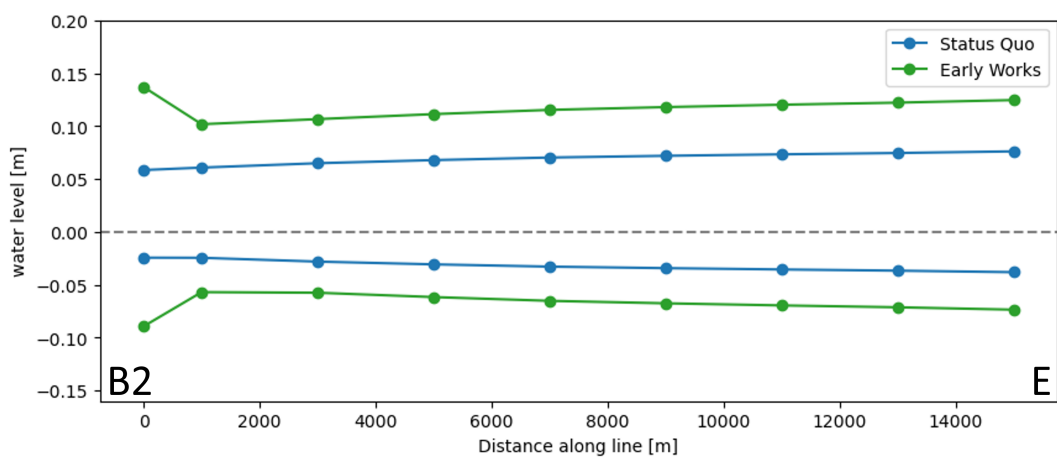


Figure 4.7: Minimum and maximum water levels southwards from Boughaz 2 into the basin (yellow line in Figure 4.4) during a single spring tidal cycle for SQ and EW.

4.1.2 Tidal prism

For analysis of the change in tidal prism after interventions the tidal prism per inlet is defined as the mean between total cumulative ebb discharge and total cumulative flood discharge per cycle. Analysis on the tidal prism is done for a full lunar cycle from 28/1 to 25/2. The mean, maximum and minimum values for the tidal prism are given in Table 4.1. The tidal prism per tidal cycle per inlet is shown in Figure 4.8, with the mean tidal prism over the lunar cycle given by the dashed line.

The tidal prism varies significantly throughout the lunar cycle. The maximum total tidal prism for Lake Bardawil is almost 4.5 times as large as the minimum tidal prism.

The total impact of the interventions on the tidal prism of Lake Bardawil is an increase by a factor of 1.6. The largest impact is found in Boughaz 2. The mean tidal prism of Boughaz 2 is increased by factor 1.84, compared to an increase of factor 1.33 in Boughaz 1.

	Boughaz 1 SQ	Boughaz 1 EW	Boughaz 2 SQ	Boughaz 2 EW	Lake Bardawil SQ	Lake Bardawil EW
Mean tidal prism ($10^6 m^3$)	17.9	23.7	20.9	39.0	38.8	62.7
Maximum tidal prism ($10^6 m^3$)	26.0	34.2	29.4	54.1	54.4	88.3
Minimum tidal prism ($10^6 m^3$)	4.3	7.2	6.1	12.7	10.4	19.8

Table 4.1: Mean, maximum and minimum tidal prism for Boughaz 1, Boughaz 2 and both combined for the characteristics of the whole Lake Bardawil system.

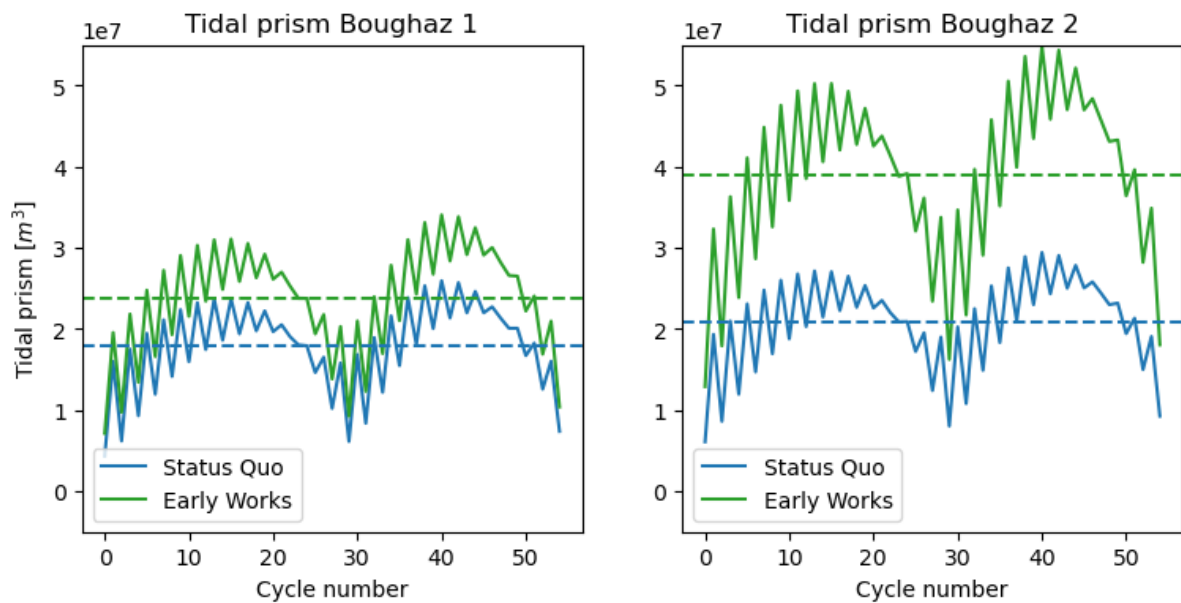


Figure 4.8: The tidal prism for Boughaz 1 and Boughaz 2 in SQ and EW. The mean tidal prism over a full lunar cycle is given for each scenario and inlet by the dashed lines.

4.1.3 Interaction between inlets

To analyse the interaction between the inlets, the rolling daily cumulative discharge for a full lunar cycle for each inlet is shown in Figure 4.9. In this figure discharge directed inward is positive. This means Boughaz 1 is a net importer of water and Boughaz 2 is a net exporter of water. After interventions net import and export due to tidal forcing alone are reduced significantly.

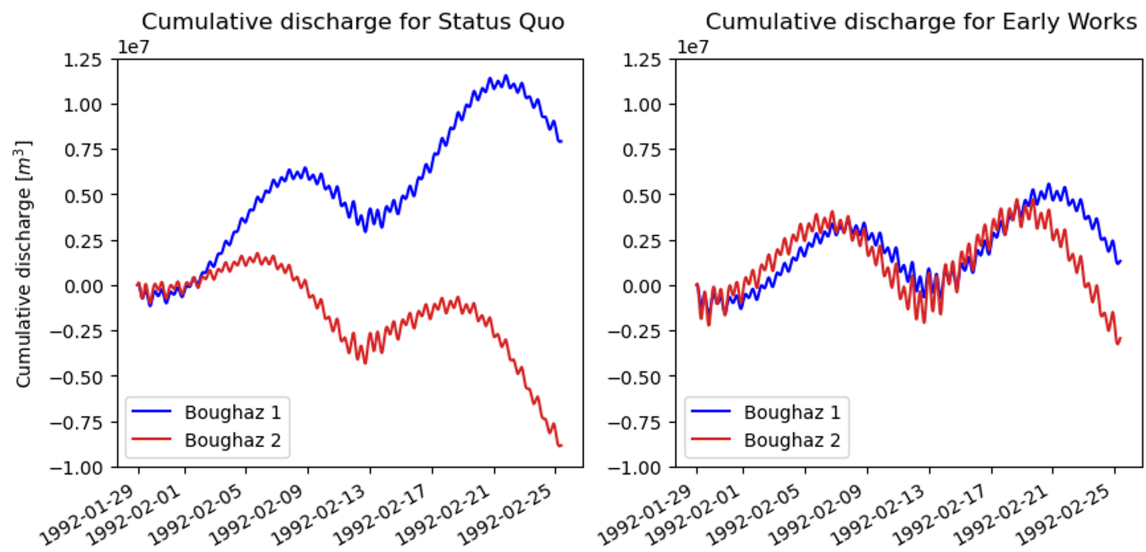


Figure 4.9: Rolling daily average cumulative discharge. Positive discharge is directed into the basin.

The fraction of the total tidal prism that is imported or exported is extremely small. In SQ, the import/export fractions for Boughaz 1 and Boughaz 2 are 0.006 and 0.008 respectively. This reduces to 0.001 for each inlet in EW.

4.1.4 Flow velocities

The effect of the interventions can clearly be seen in the local maximum velocity during a single spring tidal cycle. As seen in the overview of Lake Bardawil in Figure 4.10, the maximum velocities inside the basin are generally larger in EW.

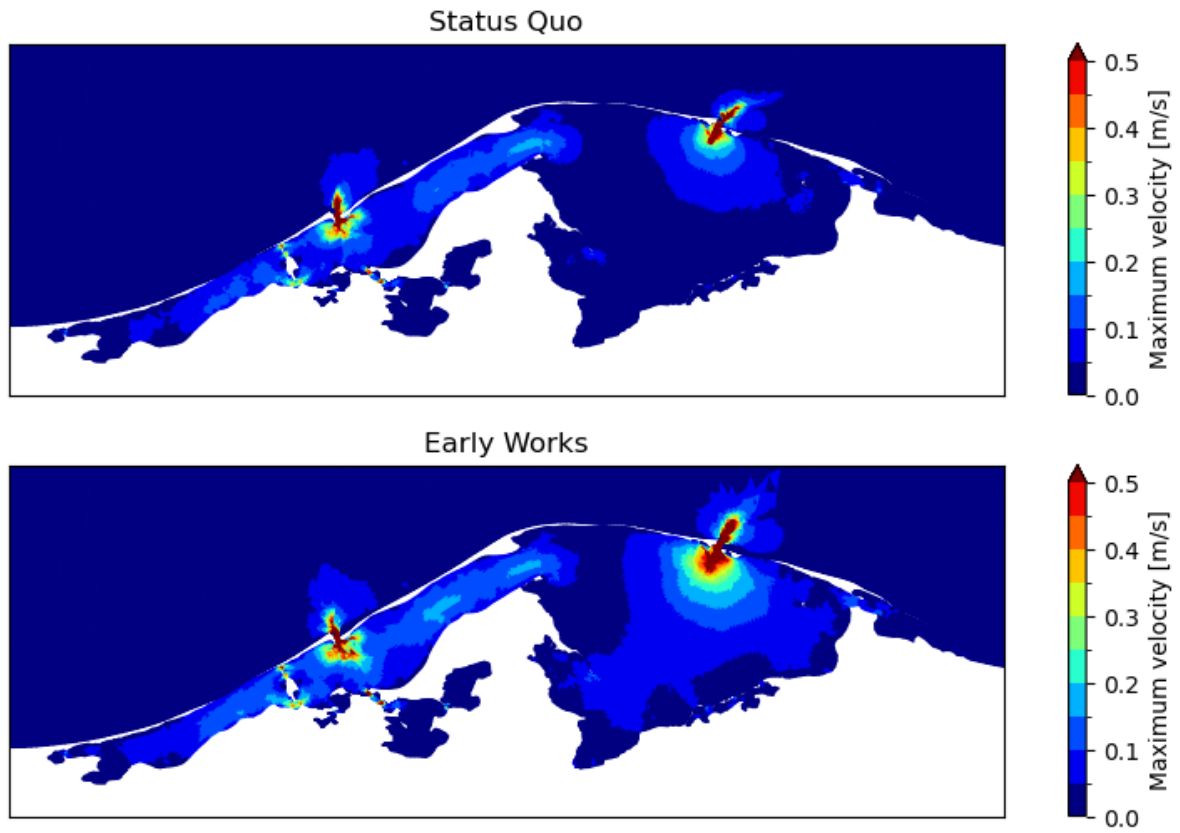


Figure 4.10: Maximum spring flow velocity and percentage of the plotted area exceeding each value for maximum flow velocity.

As shown in Figure 4.11, the maximum velocities in the basin along the orange line in Figure 4.4 are generally increased by 0.02 to 0.03 m/s.

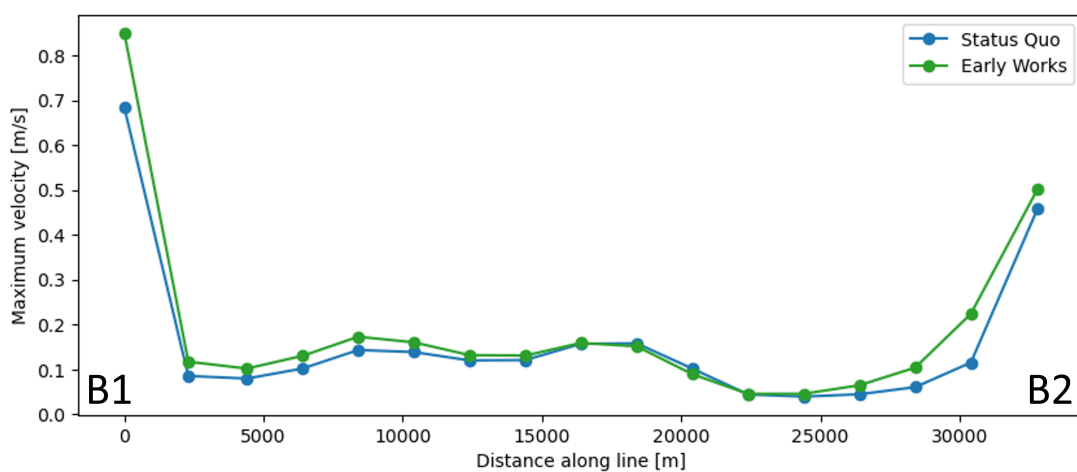


Figure 4.11: Local maximum velocities over a single spring tidal cycle along the orange line in Figure 4.4 between Boughaz 1 and Boughaz 2.

Inlets

The cross-sectionally averaged velocity for Boughaz 1 and Boughaz 2 in SQ and EW is given in Figure 4.12. Both inlets show an increase in velocity amplitude. The maximum cross-sectionally averaged velocity in Boughaz 1 increases by 0.05 m/s from 1.22 m/s in SQ to 1.27 m/s in EW. The increase in maximum velocity in Boughaz 2 is much larger, both in a relative and absolute sense. The maximum cross-sectionally averaged velocity in Boughaz 2 increases by 0.19 m/s from 0.70 m/s in SQ to 0.89 m/s in EW.

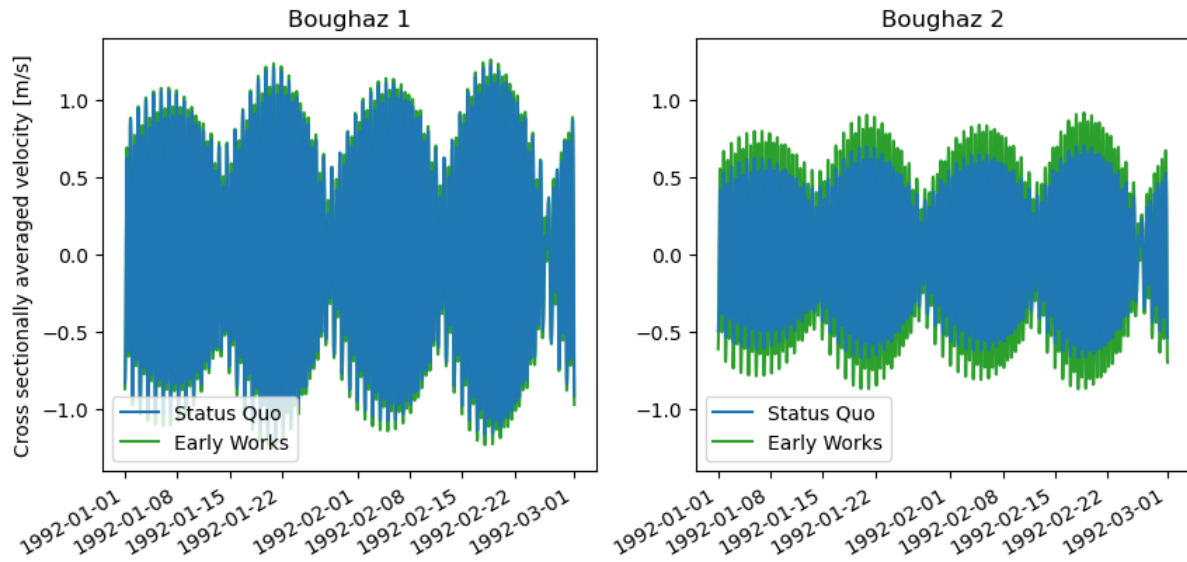


Figure 4.12: cross-sectionally averaged inlet velocities at Boughaz 1 and 2 for scenarios 1 and 4. Positive flow is directed inward.

While the cross-sectionally averaged velocities increase after interventions, the largest local maximum velocities over a single spring tidal cycle in Boughaz 1 and Boughaz 2 are decreased. Figure 4.13 shows the local maximum velocities for Boughaz 1 and Boughaz 2 in SQ and EW. The interventions also have an impact on the flow directions in the inlet.

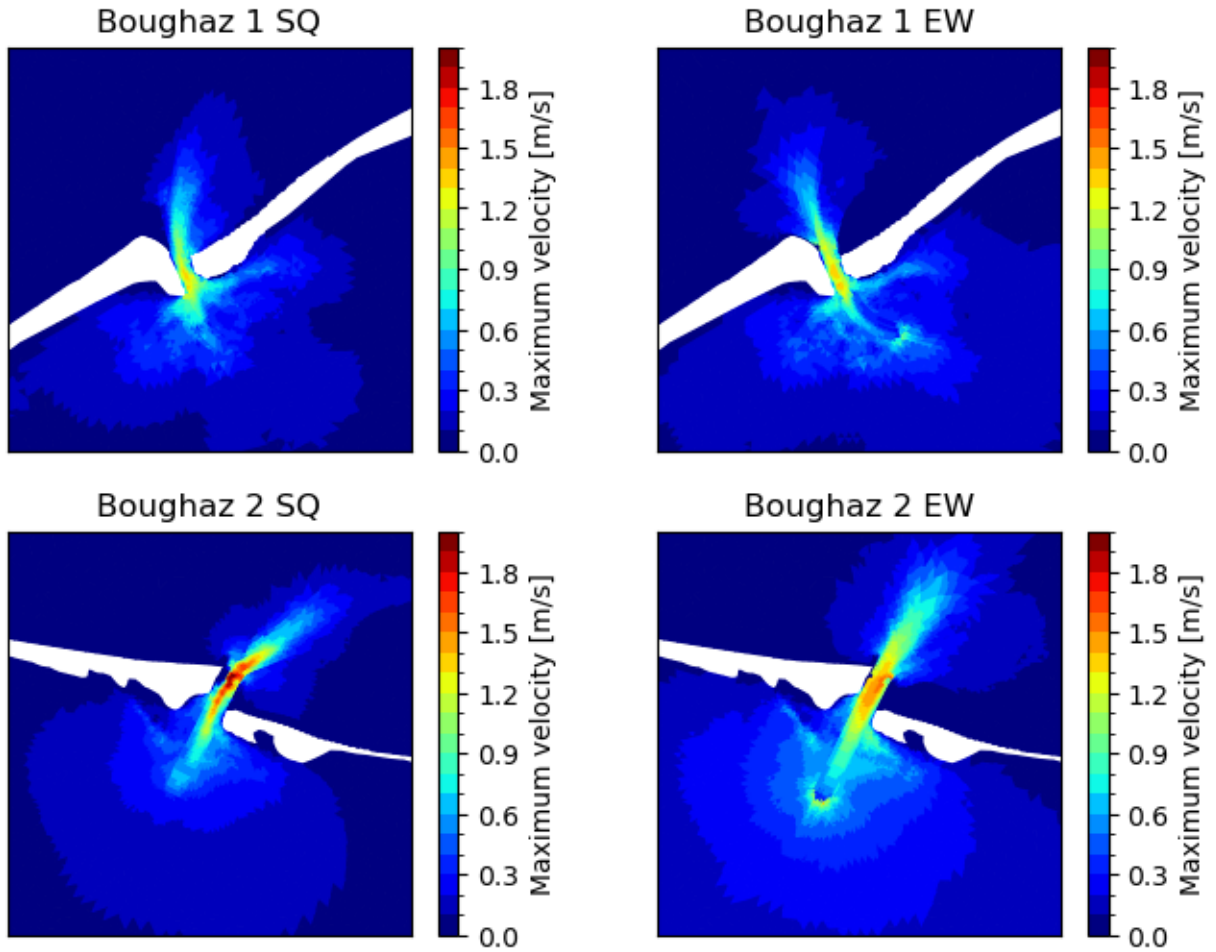


Figure 4.13: Comparison of local maximum velocities in the inlets during a single spring tidal cycle.

4.1.5 Tidal asymmetry

Ebb & flood duration

There is a slight asymmetry between ebb & flood duration, the mean ebb duration is slightly longer. This only changes slightly due to the interventions.

	B1 SQ	B1 EW	B2 SQ	B2 EW
Flood duration (min)	366	365	363	364
Ebb duration (min)	375	377	378	377

Table 4.2: Ebb & flood duration for Boughaz 1 and Boughaz 2 in SQ and EW.

Slack duration

Looking at the orange lines in Figure 4.14, there is no clear difference in slack time between flood and ebb periods. The slack times do not change significantly after interventions.

4.1.6 Tidal propagation

The peaks of the tidal wave arrives at different locations in the basin at different times. The lag between the arrival of the tidal wave at Boughaz 2 and Boughaz 1 is in the order of 5 minutes (Note that 5 minutes

is the time step for the output data in this model).

The tidal wave propagation speed reduces as soon as it enters the inlet. In SQ the total peak lag over the line described in Figure 4.2a is 110 minutes. The peak takes another 70 minutes to reach the tightest part of the basin strait leading to Boughaz 2. In EW the initial lag over the inlet reduces to 105 minutes and the lag over the basin strait reduces to 60 minutes. The total peak lag over the inlet and basin strait is 180 minutes in SQ and 165 minutes in EW.

The peak lag over Boughaz 2 (the line in Figure 4.3a) in SQ is 185 minutes. This reduces to 165 minutes after interventions in EW.

The peak lag over the yellow line in Figure 4.4 in the eastern basin increases by 85 minutes from 70 minutes to 155 minutes in EW. The shape of the vertical tide in Boughaz 2 results in this unexpected increase in peak lag, where a reduction was expected.

The peak lag going westward from Boughaz 1 along the green line in Figure 4.4 is 155 minutes in SQ. This increases to 215 minutes as the moment in time for the maximum water level in the most westward location does not change from SQ to EW.

4.1.7 Velocity phase

As mentioned in subsection 2.2.6, the phase lag between the horizontal and vertical tide could be important for the direction of transport at the moments of largest resuspension of sediments. In the inlets in Figure 4.14, the tidal wave shows a progressive character, with the peaks of the horizontal and vertical tide more or less happening at the same time. The phase lag changes from SQ to EW in the inlets, moving towards a standing wave pattern slightly.

Figure 4.15 shows the horizontal and vertical tide for the strait section in the middle of the basin. In this section, the tidal wave is more of a semi-standing nature. After interventions, the phase lag also moves slightly towards a standing wave pattern.

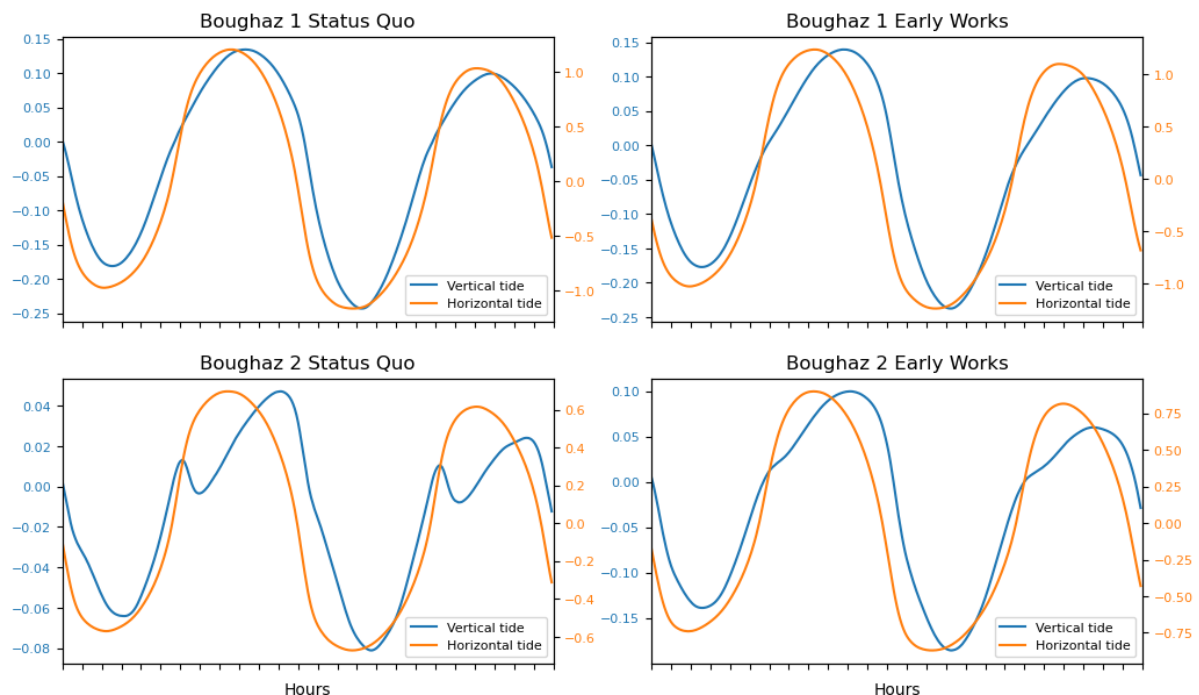


Figure 4.14: Visualisation of the phase difference between the horizontal (orange) and vertical (blue) tide over a spring tidal cycle in Boughaz 1 and Boughaz 2 for SQ and EW.

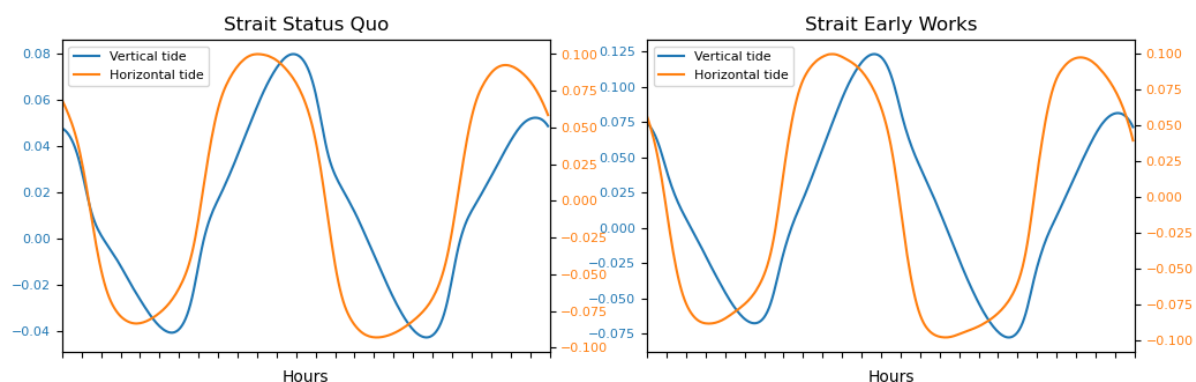


Figure 4.15: Visualisation of the phase difference between the horizontal (orange) and vertical (blue) tide over a spring tidal cycle in the strait section for SQ and EW.

4.2 Hydrodynamic response to tidal and meteorological forcing

In this section, the more complete results of the hydrodynamic model under tidal forcing and meteorological forcing are presented. These results aim to create an understanding of the system's response to winter and summer weather.

4.2.1 Interaction between inlets

Interaction between the inlets is substantially larger when accounting for meteorological forcing. The behaviour of interaction differs significantly seasonally. The cumulative import and export of water through Boughaz 1 and Boughaz 2 are shown in Figure 4.16 for a typical winter and summer period. The storage in the lake and evaporation which is the difference between the total import and export is also shown in Figure 4.16. During the 2.5-month winter period, the amount of interaction in terms of water imported and exported in the inlets is two orders of magnitude larger than the tide-only situation. This interaction is mainly event-based. The southwesterly storms result in a flow pattern with a net import of water in Boughaz 1 and a net export of water in Boughaz 2. The figure shows an increase in interaction from SQ to EW due to the interventions. The evaporation is not significantly affected by the interventions.

During the 2.5-month summer period in 2012, the interaction shows a steady import, export and evaporation pattern on this timescale. The magnitude of interaction is not as event-based as it is during winter. Compared to the situation without any meteorological forcing, the interaction during summer has increased an order of magnitude. Comparing SQ to EW, interaction is increased significantly due to the interventions. Similar to the winter situation, evaporation is not significantly affected by the interventions.

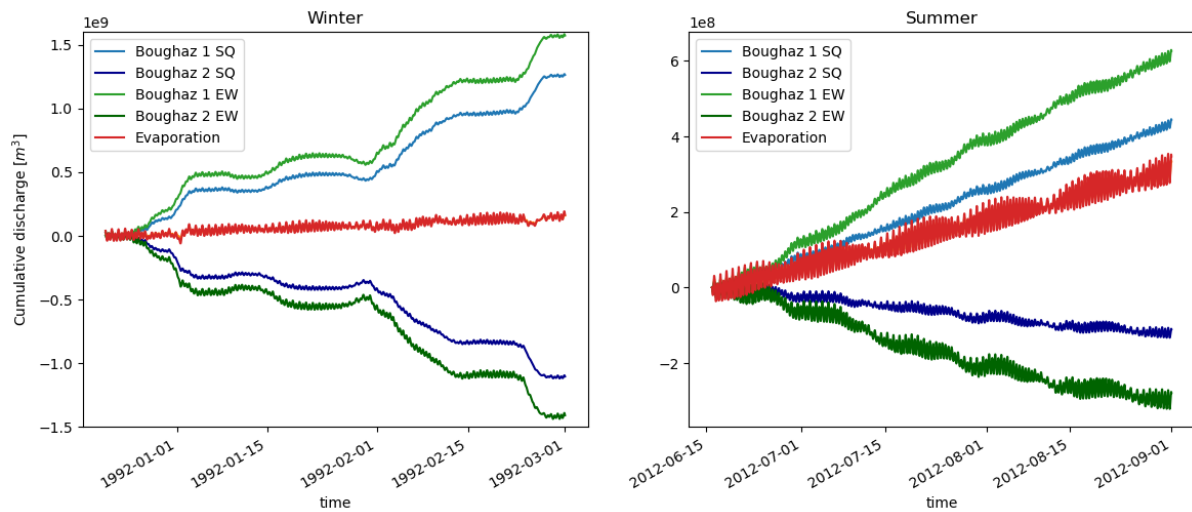


Figure 4.16: Cumulative inward discharge through Boughaz 1 and Boughaz 2 for SQ and EW in the summer of 2012 (right figure) and winter in 1991/1992 (left figure). Storage and evaporation are shown in red and orange for SQ and EW. As there is no meaningful difference in storage and evaporation between the scenarios, only the red line is visible.

4.2.2 Water levels

To find a reason for the event-based increase in interaction during winter, the water levels are analysed. The water levels during a southwesterly storm event show significant differences from those without meteorological forcing. There is a clear effect of wind set-up in the southwestern direction. In the eastern half of the section considered, the water level and set-up are reduced from SQ to EW. During summer these large deviations in the shape of the water level are not found.

4.2.3 Salinity

As mentioned in subsection 1.1.1, the interventions are expected to have an effect on the salinity in the basin. Figure C.10 compares salinity values between the Status Quo and the Early Works situation at a location in the middle of the eastern basin for a summer simulation period of two and a half months. In EW models, the salinity values seem to move towards a lower equilibrium than in the SQ model results. Figures C.11 and C.11 compare the spatial distribution of salinity in the lagoon after a 2-month summer simulation period. The interventions mainly affect the salinity values in the eastern basin, resulting in lower salinity values. A similar comparison for a winter simulation can be found in subsection C.1.5.

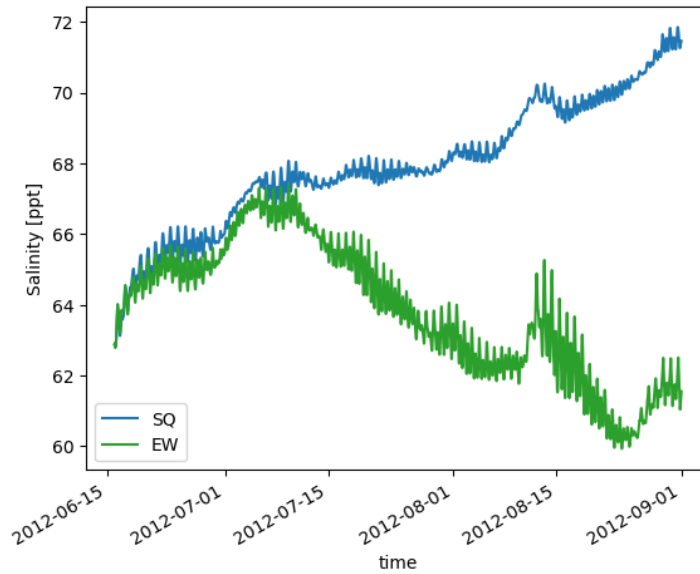


Figure 4.17: Salinity values for SQ and EW in the middle of the eastern basin of Lake Bardawil over a 2.5-month summer period.

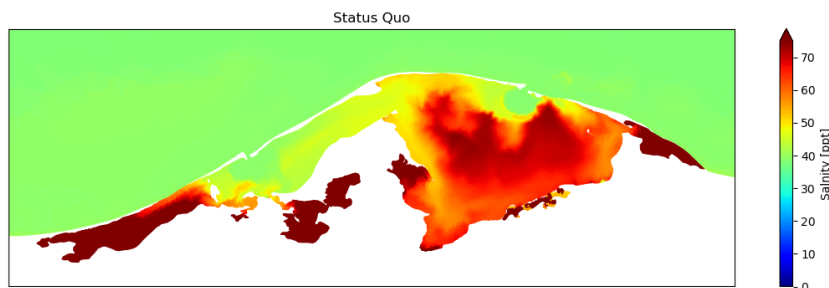


Figure 4.18: Salinity in Lake Bardawil after a 2.5-month summer simulation in the Status Quo scenario.

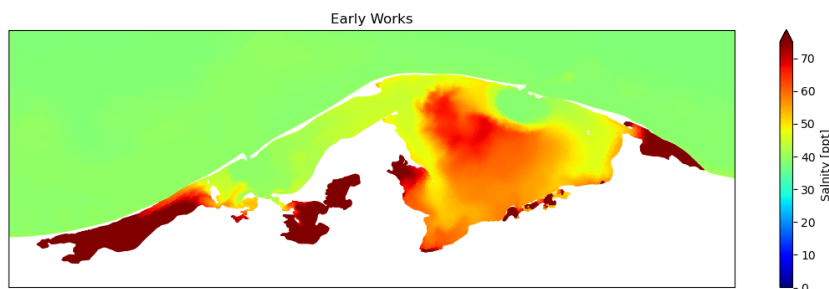


Figure 4.19: Salinity in Lake Bardawil after a 2.5-month summer simulation in the Early Works scenario.

4.2.4 Velocities

Inlet velocities

To analyse the impact of meteorological forcing on velocities within the inlet, a comparative analysis is conducted between the summer, winter, and tidal-only scenarios for each inlet. Figure 4.20 and Figure 4.21 present the results of this comparison in the Status Quo situation. The behaviour of the cross-sectionally averaged velocities in the Early Works situation are similar.

During summer, in Boughaz 1, maximum inward velocities are generally slightly increased and maximum outward velocities are generally slightly decreased. In Boughaz 2, both maximum inward and maximum outward velocities are slightly decreased. This effects the mean tidal prism, which is approximately between 2.5 and 4.2% smaller in the meteorologically forced model compared to the tidal-only model.

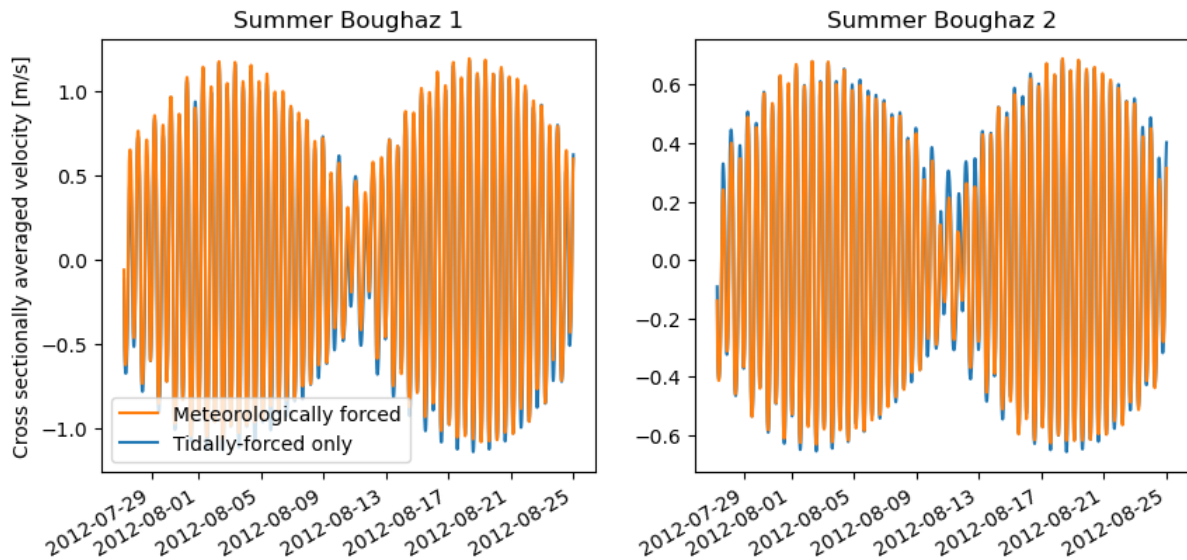


Figure 4.20: Comparison of meteorologically forced inlet velocities to tidally-forced only inlet velocities for a full lunar cycle during summer in the Status Quo situation. Positive flow velocity is directed into the basin.

During winter storms, there are larger differences in inlet velocities. Maximum velocities are considerably larger, especially in neap tidal conditions. During high wind speed storm events, flow is continuously directed inward in Boughaz 1 and outward in Boughaz 2. No sensible conclusions on the mean tidal prism in winter periods can be made due to the effect of storm events.

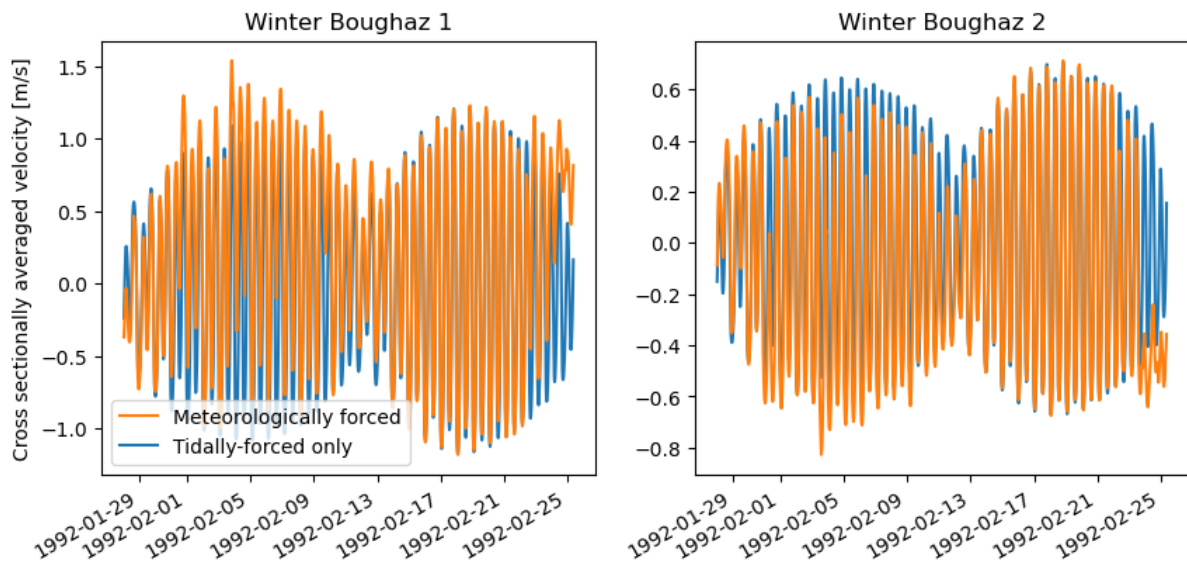


Figure 4.21: Comparison of meteorologically forced inlet velocities to tidally-forced only inlet velocities for a full lunar cycle during winter in the Status Quo situation. Positive flow velocity is directed into the basin.

Basin velocities

To demonstrate the effect of weather on the velocities in the basin, the maximum velocities during an entire 2.5-month summer and winter simulation period for the meteorologically forced situation for the entire basin have been plotted in Figure 4.22. By comparing this figure to Figure 4.10, it becomes evident that the maximum velocities recorded during the entire summer simulation closely resemble those observed during a single spring tidal cycle under tidal forcing alone. The winter months show a notable increase in maximum velocities when compared to the tidally-forced situation.

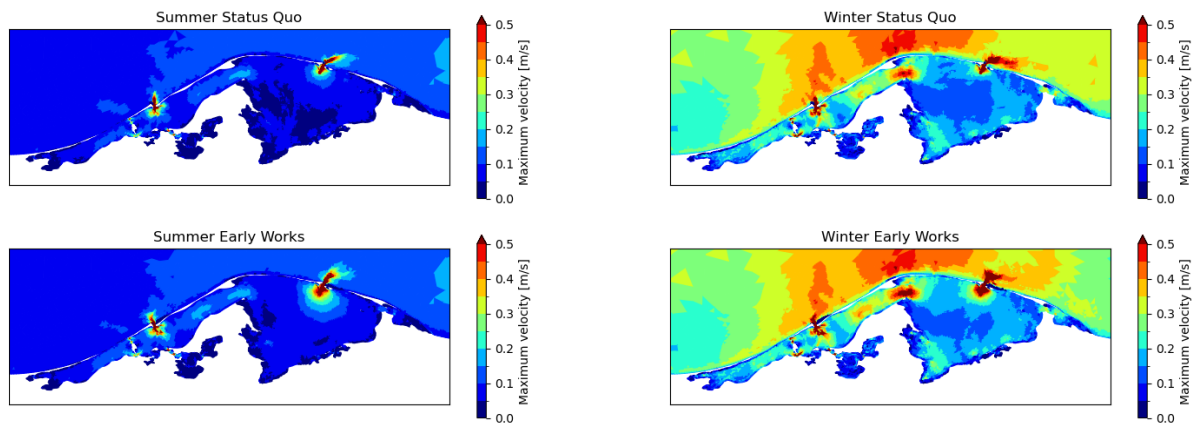


Figure 4.22: Comparison of maximum velocities during a 2.5-month summer and winter period.

During the summer months, the maximum velocities due to weather effects are only slightly larger than the tidally-forced only situation, as seen in the two-dimensional section between Boughaz 1 and Boughaz 2 plotted in Figure 4.23.

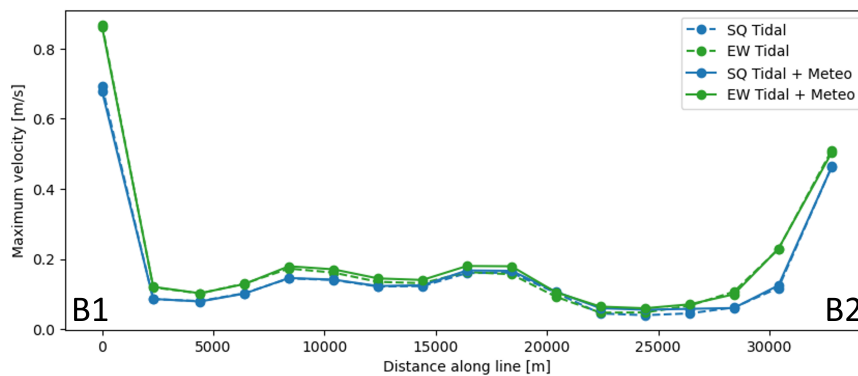


Figure 4.23: Maximum velocities per location during the entire summer simulation period along the orange line in Figure 4.4. Maximum velocities during this period without meteorological forcing are shown by the dashed line.

During winter months, the maximum velocities between Boughaz 1 and Boughaz 2 are increased significantly over the entire two-dimensional section considered. These maximum velocities occur during winter storm events. Figure 4.25 shows the cross-sectionally averaged flow velocity in the tightest part of the strait. During low-velocity winds, the flow velocity is mainly tidally forced, as can be seen by comparing the meteorologically forced result to the only tidally-forced result. When wind velocities increase, the flow velocity through the cross-section follows the shape of the magnitude of the wind velocity. There is no moment during high wind velocity where the cross-sectionally averaged flow is negative, meaning flow is continuously directed towards Boughaz 2 in these situations.

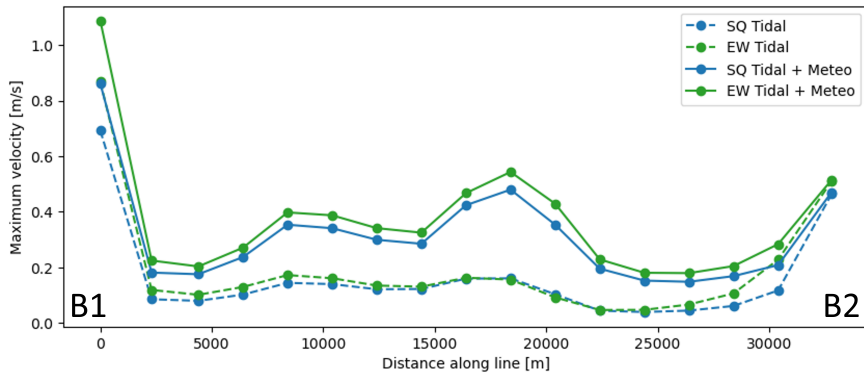


Figure 4.24: Maximum velocities per location during the entire winter simulation period along the orange line in Figure 4.4. Maximum velocities during this period without meteorological forcing are shown by the dashed line.

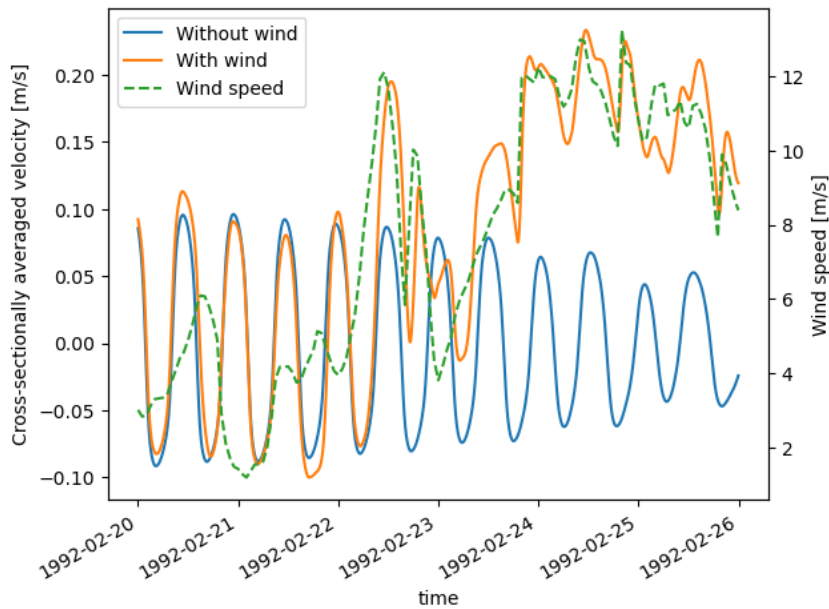


Figure 4.25: Visualisation of the effect of southwesterly wind speed on the cross-sectionally averaged velocity in the tightest part of the strait section and comparison to the situation without meteorological forcing.

4.2.5 Wind waves

Significant wave height over the summer and winter simulation periods are shown in figures 4.26 and 4.27. Similar to the wind-driven currents discussed, the wind waves are much larger during winter. During winter, maximum wind wave height seem to be either fetch or depth limited, depending on the location. During summer, the maximum wind wave height seems to be wind speed limited or fetch limited. There are no significant differences in the maximum significant wave height in the basin between SQ and EW.

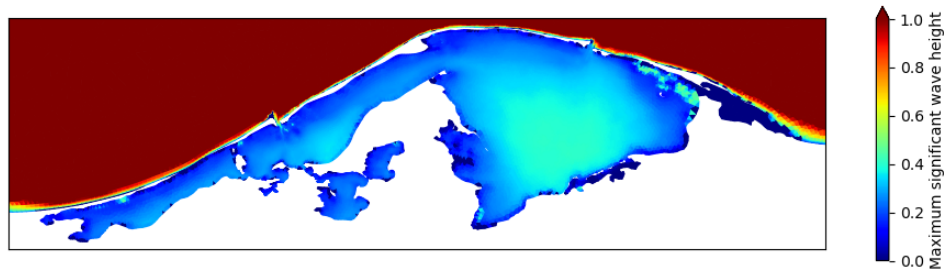


Figure 4.26: Maximum significant wave height modelled during the summer simulation period.

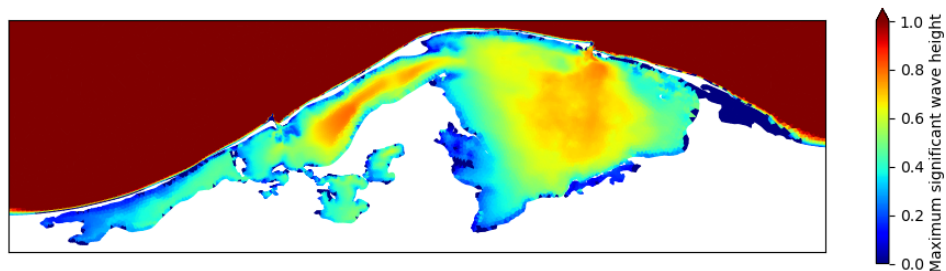


Figure 4.27: Maximum significant wave height modelled during the winter simulation period.

4.3 Morphological response to tidal and meteorological forcing

The general morphological response of Lake Bardawil can be described by Figure 4.28. The response for all sediment fractions is characterised by morphologically dynamic shorelines and inlets. In the basin itself, there is very little change in bed levels for these sediment fractions.

The cross-shore profile changes from a linearly interpolated straight line to a more natural and steeper shoreline profile.

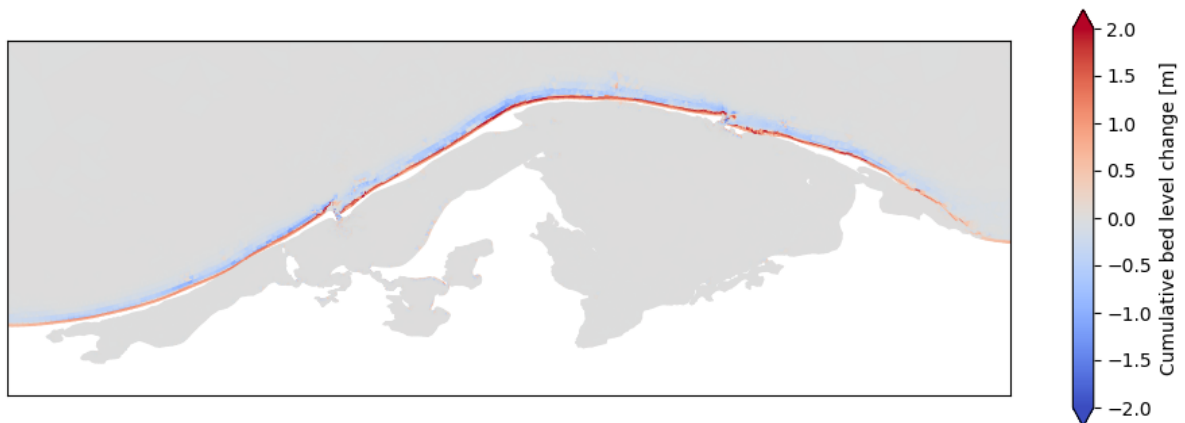


Figure 4.28: Overview of cumulative erosion and sedimentation in Lake Bardawil for Status Quo during a 2-month winter simulation period using the fine sand sediment fraction.

4.3.1 Import & export

The import and export of fine sand sediment over each of the inlets for both seasons and scenarios are shown in figures 4.29 and 4.30. The corresponding figures for the medium sand and coarse sand fractions can be

found in Appendix C.1.3. For the SQ scenario, the inlets primarily exhibit an importing nature under normal conditions. However, during storm events, Boughaz 1 experiences an increased import while Boughaz 2 demonstrates sediment export. In the EW scenario the regular importing character is increased in Boughaz 1, while it is decreased in Boughaz 2. For the medium sand sediment fraction, the import reduces to a roughly balanced import and export in the EW scenario. The importing and exporting effects of storm events are greater in EW than in SQ.

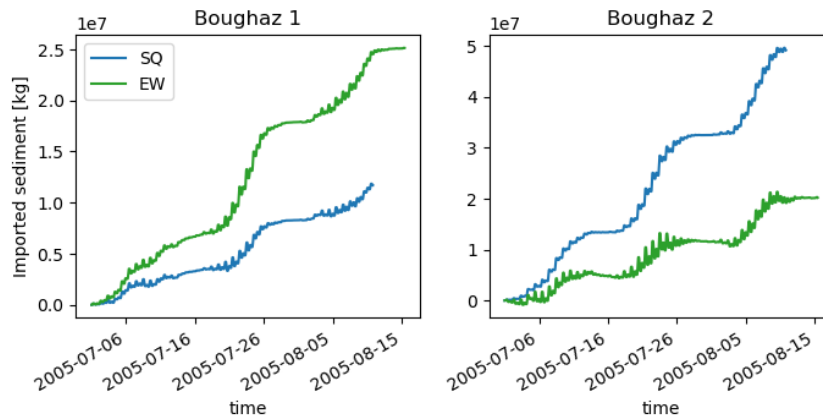


Figure 4.29: Sediment import (positive) and export (negative) for SQ and EW over Boughaz 1 and Boughaz 2 during summer for the fine sand sediment fraction with $D_{50} = 0.015$ mm.

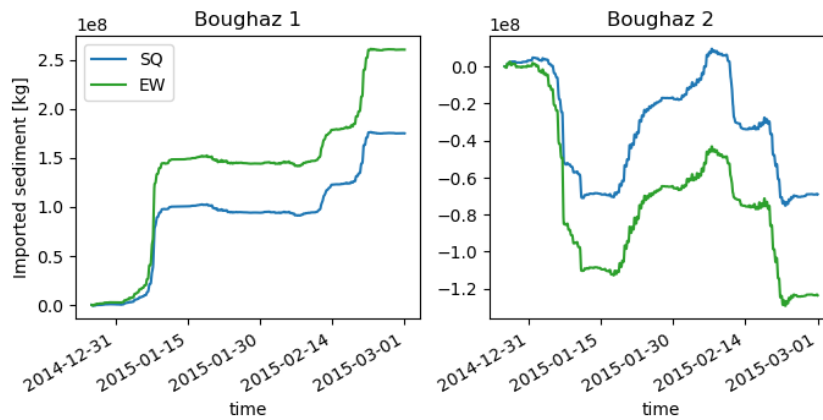


Figure 4.30: Sediment import (positive) and export (negative) for SQ and EW over Boughaz 1 and Boughaz 2 during winter for the fine sand sediment fraction with $D_{50} = 0.015$ mm.

4.3.2 Erosion & sedimentation of inlets: Sections

To allow for quantification of erosion and sedimentation in the inlets and comparison between SQ and EW the inlets have been divided into several sections. These sections are shown in Figure 4.31 and the total cumulative erosion and sedimentation over the simulation period per inlet is presented in tables 4.3 & 4.4. The large scale of these sections results in the loss of some nuance required for standalone analysis. These results can however be used to support analysis.

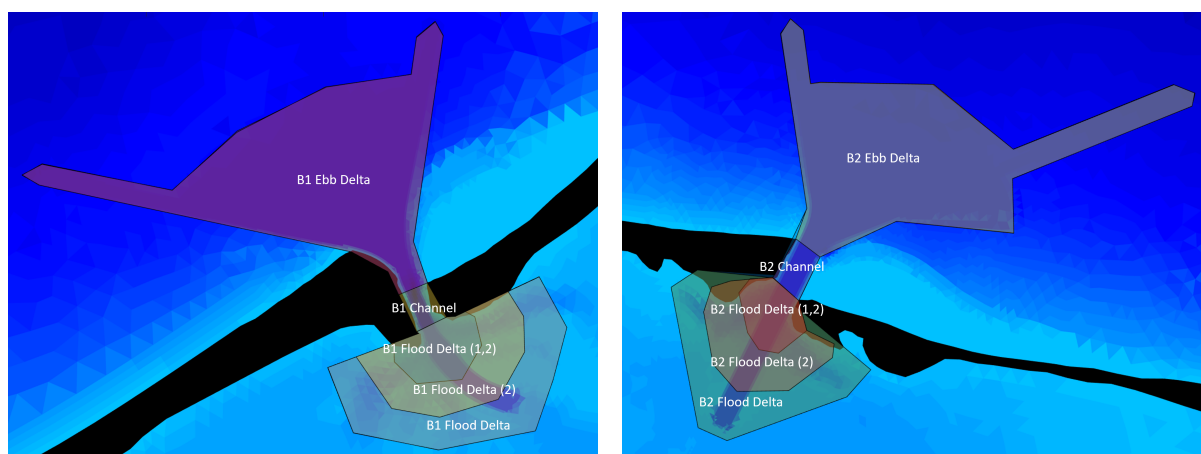


Figure 4.31: Sections used for quantification of erosion and sedimentation. The sections in the flood delta overlap, with the total Flood Delta section encompassing both Flood Delta 1 and Flood Delta 2. Likewise, Flood Delta 2 encompasses Flood Delta 1

Section	SQ Summer (10^3 m^3)	EW Summer (10^3 m^3)	Change	SQ Winter (10^3 m^3)	EW Winter (10^3 m^3)	Change
B1 Flood Delta	185	225	+22%	55.7	8.57	-85%
B1 Channel	-2.51	-8.58	-240%	-32.7	-48.0	-47%
B1 Ebb Delta	472	481	+2%	-8.54	21.7	+354%
B1 Total	654	698	+6%	11.1	-11.1	-200%
B1 Flood Delta 1	48.5	64.8	+33%	-21.4	132	+717%
B1 Flood Delta 2	111	132	+19%	74.5	129	+42%

Table 4.3: Cumulative sedimentation and erosion of fine sand sediment for Boughaz 1 in Status Quo and Early Works during both summer and winter.

Section	SQ Summer (10^3 m^3)	EW Summer (10^3 m^3)	Change	SQ Winter (10^3 m^3)	EW Winter (10^3 m^3)	Change
B2 Flood Delta	108	133	+23%	187	207	+11%
B2 Channel	-93.0	-65.2	+30%	-248	-164	+34%
B2 Ebb Delta	655	669	+2%	55.7	517	+828%
B2 Total	667	735	+10%	-0.679	557	+82100%
B2 Flood Delta 1	67.6	56.1	-17%	18.9	-8.73	-146%
B2 Flood Delta 2	92.8	110	+19%	145	123	-15%

Table 4.4: Cumulative sedimentation and erosion of fine sand sediment for Boughaz 2 in Status Quo and Early Works during both summer and winter.

4.3.3 Erosion & sedimentation of inlets: Status Quo

Before analysing the morphological response to the interventions, first, the morphological response of the Status Quo needs to be documented as a baseline scenario. The observations for the Status Quo scenario are split up into summer observations and winter observations. The morphological changes for fine sand and medium sand sediments are shown.

Summer

The cumulative changes in bed level in the inlets over this two-month simulation are shown in figures 4.32 and 4.37.

During the summer months, there are a few observations to be made in Boughaz 1. The main observation is that Boughaz 1 is relatively morphologically static during the summer. The morphodynamic behaviour that is occurring during this period can be described as slight erosion of fine sand sediments in the main

channel and slight sedimentation of fine sand sediments in the area of the flood tidal delta. The medium sand sediment remains very static.

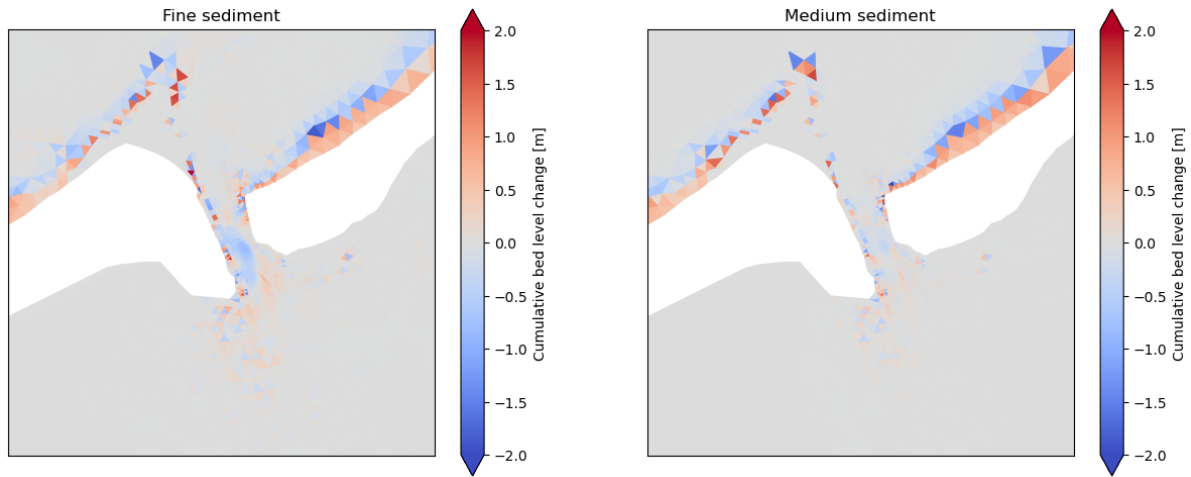


Figure 4.32: Cumulative bed level change in the Status Quo scenario for Boughaz 1 for a 2-month summer simulation period for fine sand and medium sand sediment.

Compared to Boughaz 1, Boughaz 2 is much more dynamic. Bed level changes in the inlet are significantly larger. The spit that is already present in the original bathymetry grows in size substantially. The main channel erodes more than in Boughaz 1 and there is larger sediment deposition in the inner flood tidal delta region, mainly occurring in the main channel of the delta. Furthermore, heavy deposition occurs on the inward western side of the channel, seemingly narrowing the channel. The changes are comparable for both fine and medium sediment fractions, although the changes are generally more pronounced for fine sand sediments. The area of erosion is slightly smaller for medium sand sediments, while sediment deposition extends further into the main channel for medium sand sediments.

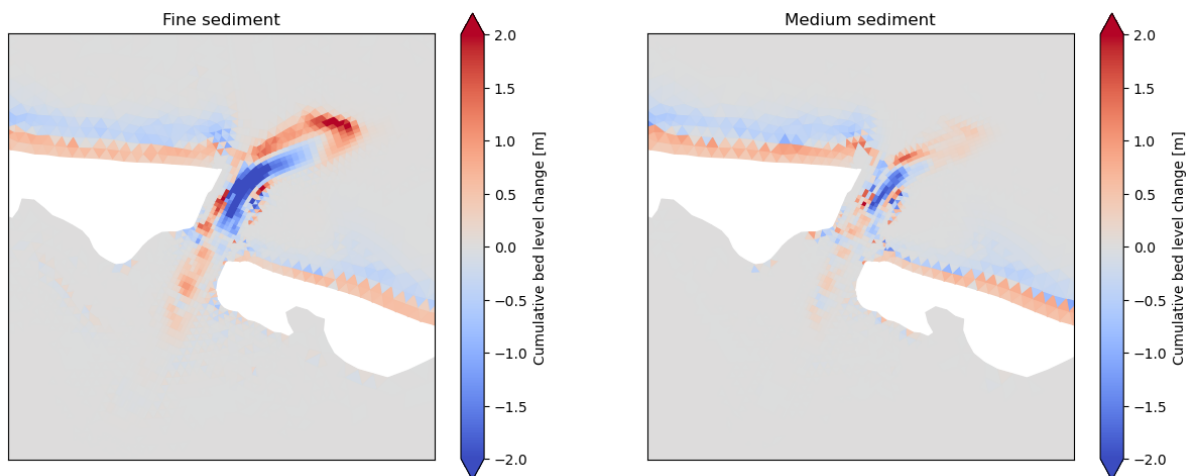


Figure 4.33: Cumulative bed level change in the Status Quo scenario for Boughaz 2 for a 2-month summer simulation period for fine sand and medium sand sediment.

Winter

During winter, sedimentation occurs on both the seaward and inward sides of Boughaz 1. A spit-like shape forms on the seaward side of the inlet. Similar to summer conditions, the flood-tidal delta generally decreases

in depth. The erosion occurring in the channel is more outspoken during the winter season. While the overall patterns are similar in the fine sand and medium sand sediment simulations, the fine sand sediment appears to shape a narrower and deeper channel within the main channel.

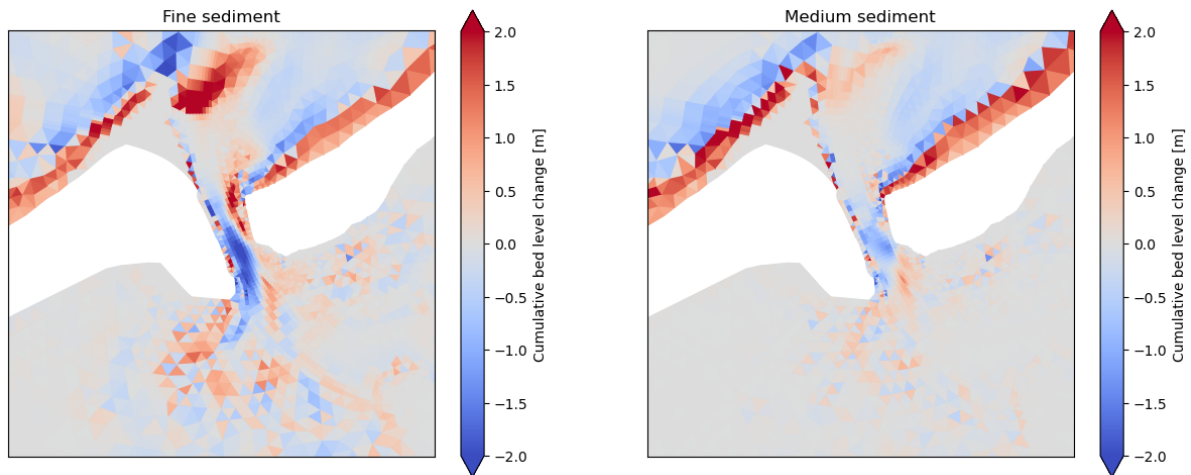


Figure 4.34: Cumulative bed level change in the Status Quo scenario for Boughaz 1 for a 2-month winter simulation period for fine sand and medium sand sediment.

The bed level changes in Boughaz 2 during winter are completely different from the summer behaviour. Instead of growing, the spit migrates due to the storm events. The direction of migration varies for different sediment fractions, with an eastward movement observed for fine sand sediment and a more southern movement observed for medium sand sediments. Additionally, slight deposition occurs at the point of connection between the updrift shoreline and the old spit. The erosion pattern is influenced by the direction of spit migration, as the relocated spit blocks the original channel in the scenario with a medium sand fraction.

The winter storms also result in substantial deposition of fine sand sediments in the channels of the flood-tidal delta.

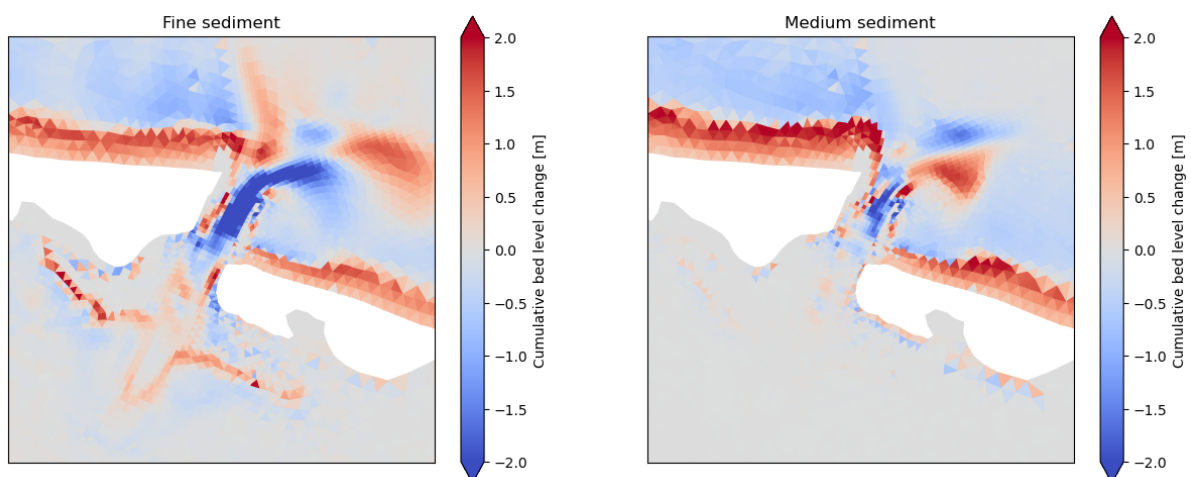


Figure 4.35: Cumulative bed level change in the Status Quo scenario for Boughaz 2 for a 2-month winter simulation period for fine sand and medium sand sediment.

4.3.4 Erosion & sedimentation in inlets: Early Works

The cumulative erosion and sedimentation in EW are presented for comparison to SQ.

Summer

In the situation after interventions, Boughaz 1 stays quite static in the morphological sense. The bottom of the channel evens itself out a little for both the fine sand sediments and the medium sand sediments. There is a noteworthy increase in deposition occurring in the dredged channel right after the transition from the narrowest part of the inlet to the more open basin.

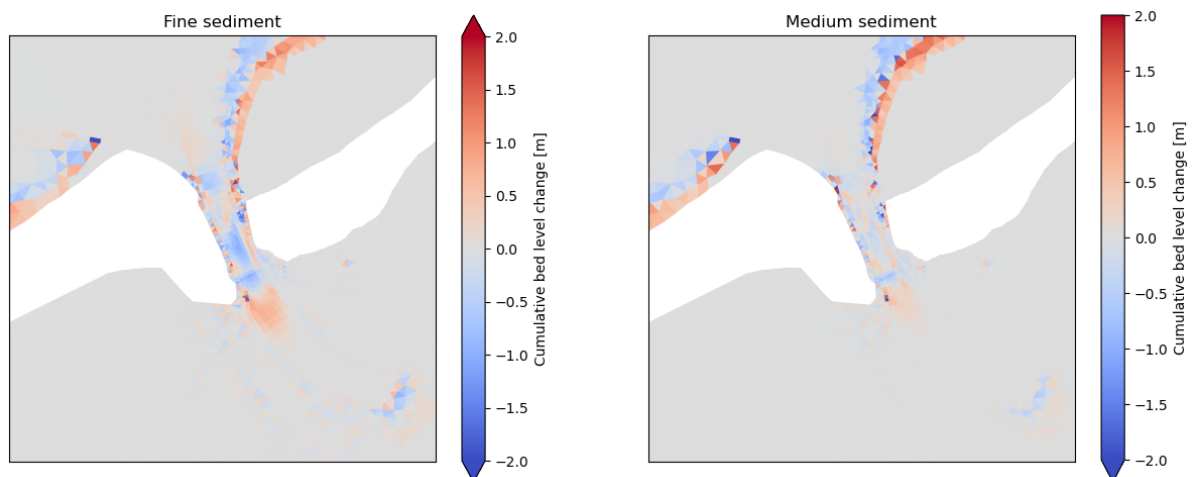


Figure 4.36: Cumulative bed level change in the Early Works scenario for Boughaz 1 for a 2-month summer simulation period for fine sand and medium sand sediment.

Boughaz 2 is a lot more morphologically static in the EW situation compared to the SQ situation, the changes in bed level are much smaller. For medium sand sediments, there is no notable pattern of erosion or sedimentation. Fine sand sediments do show the beginning of a new spit forming and an erosion pattern in a northeastern trajectory.

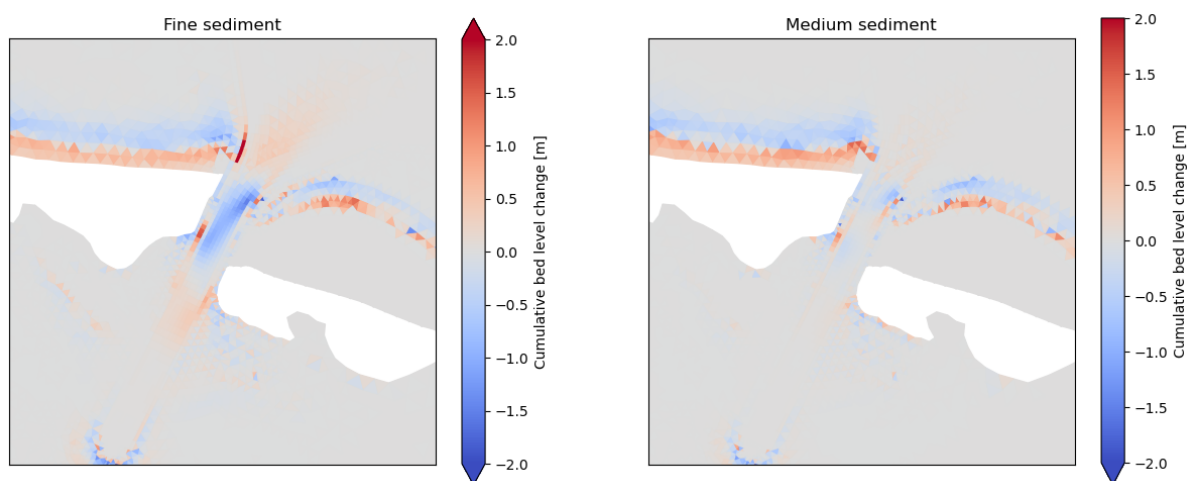


Figure 4.37: Cumulative bed level change in the Early Works scenario for Boughaz 2 for a 2-month summer simulation period for fine and medium sediment.

Winter

In Boughaz 1, in the winter season, there is some difference in behaviour between medium sediment and fine sand sediment. The fine sediments start settling in the dredged areas and seemingly start forming a spit-like shape. There is also substantially more erosion of fine sand sediment in the main channel compared to medium sand sediments. Both medium sand and fine sand sediments settle in the channel right after leaving the narrowest part of the inlet.

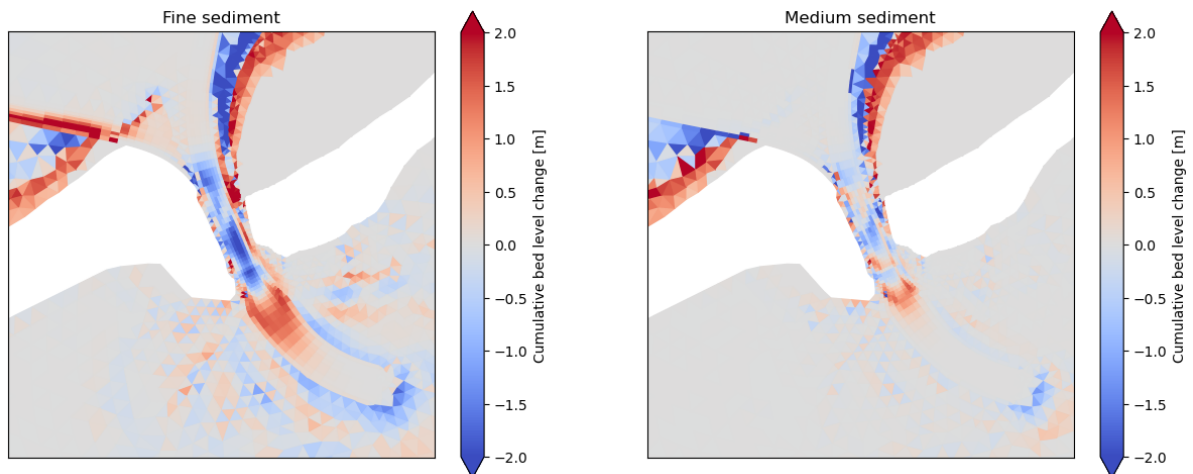


Figure 4.38: Cumulative bed level change in the Early Works scenario for Boughaz 1 for a 2-month winter simulation period for fine sand and medium sand sediment.

The behaviour outside of Boughaz 2 for the winter situation is similar to Boughaz 1. The area remains relatively morphologically static for medium sediment fractions. For the fine sand sediments, sediment deposition occurs on the updrift side of the dredged area. Similar to the summer situation, the channel erodes in a northeastern direction. Furthermore, comparable to the winter situation in SQ, there is substantial deposition happening in the flood-tidal delta and the dredged channel.

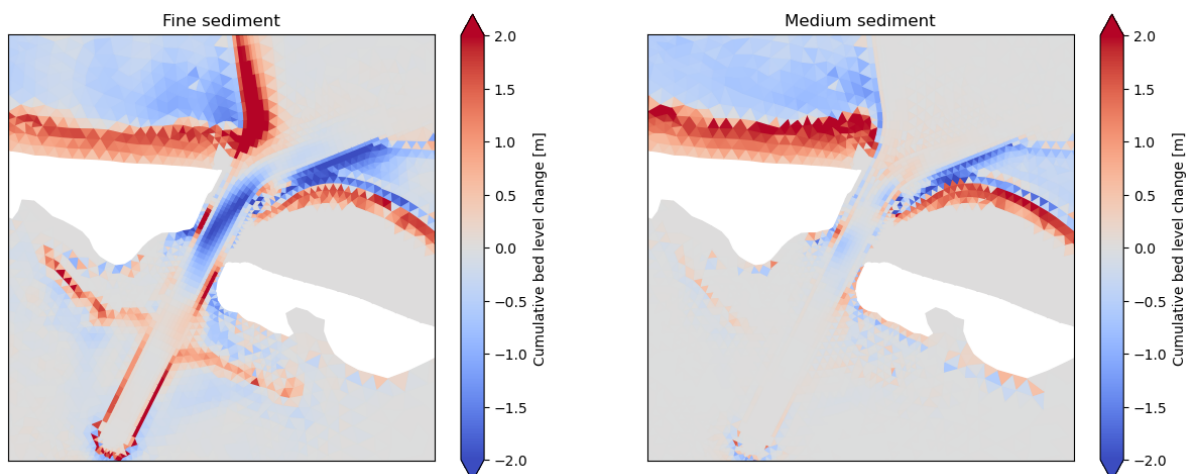


Figure 4.39: Cumulative bed level change in the Early Works scenario for Boughaz 2 for a 2-month winter simulation period for fine sand and medium sand sediment.

5 Discussion

5.1 Primary effectiveness of the interventions

The first step in assessing the response of the Lake Bardawil system to the interventions involves investigating the primary drivers for the intended result, which is the enhancement of the environmental conditions and fishery potential. Based on the assumptions that an increase in total tidal prism will result in greater fish migration and decreased salinity will result in an increased fish population, these factors will be used to evaluate the immediate impact of the interventions.

The results show that the mean tidal prism increases from 38.8 Mm³ to 62.3 Mm³. While both inlets benefit from the interventions in terms of increased tidal prism, the impact is largest in Boughaz 2. The mean tidal prism of Boughaz 2 increases by a factor 1.84, compared to a factor 1.33 in Boughaz 1. As seen in Table 4.1 the interventions are expected to result in a total increase of the tidal prism by a factor of 1.60. Based on the expectations by Wageningen Marine Research (2016), the fish import into Lake Bardawil increases by at least factor 1.60.

Part of the aim of the interventions is to increase water quality in terms of salinity. The interventions result in a larger exchange with the Mediterranean Sea and increased interaction between the two inlets. The combination of these effects results in a reduction of salinity throughout the eastern basin. As per Wageningen Marine Research (2016), this should result in higher fish catch. The 2DH model results in terms of salinity in this research should be handled with care. The difference in water density due to the difference in salinity between Lake Bardawil and the Mediterranean Sea is expected to result in stratification in Boughaz 2 in the SQ scenario (Bangen, 2021). Increasing the depth of the inlets could enhance this effect of stratification in both inlets. A stratified inlet is expected to increase the net export of salt due to circulation currents when compared to the 2DH model used. Therefore the result presented for the effectiveness of salinity reduction is deemed to be conservative due to the modelling approach used.

5.2 Hydrodynamic response to the interventions

As the goal of the interventions is not only to be effective but equally to stay effective over multiple years, the results of the hydrodynamic model are analysed for any factors that could influence morphology in the basin and specifically the short-term morphology of the inlets.

5.2.1 Response of tidal currents

The response of the tidal currents at different locations going from SQ to EW has an impact on morphological changes in the Lake Bardawil system.

Inlet velocities

The primary response to the interventions in the inlets is the increase in tidal prism and tidal discharge per inlet. The increase in tidal discharge is a combination of both an increase in cross-sectional area and an increase in cross-sectionally averaged velocity. The maximum cross-sectionally averaged velocity and cross-sectional area are identified in subsection 2.2.4 to be the most important factors for stability of tidal inlets following the theory by Escoffier (1940).

To approximate the shape of the closure curve in each inlet in SQ and EW, at least two new tidal-only model situations per scenario are computed, using both increased and decreased cross-sections for both inlets. Using Equation 5.1, the equivalent inlet velocity amplitude (\hat{u}) for non-sinusoidal tidal velocity, the

locations on their respective closure curves for both inlets in SQ, EW are computed in Table 5.1. Using small changes to the cross-sectional area of the inlets the slope and rough shape of the closure curve in SQ and EW can be estimated. Assuming a general shape for the closure curve similar to Figure 2.6 and equilibrium velocity amplitude (\hat{u}_{eq}) of 1 m/s, the Escoffier curves found in figures 5.2 and 5.3 can be approximated van de Kreeke and Brouwer, 2017. From a direct comparison found in Figure 5.1 of the values of the inlet velocity amplitude and the corresponding cross-sectional area of both inlets between SQ and EW, it can be concluded that the interventions do not move along the original closure curve. The interventions result in a completely new situation, with new corresponding closure curves for each inlet.

$$\hat{u} = \frac{\pi P}{AT} \quad (5.1)$$

	$A_{SQ} (m^2)$	$P_{SQ} (10^6 m^3)$	$\hat{u}_{SQ} (m/s)$	$A_{EW} (m^2)$	$P_{EW} (10^6 m^3)$	$\hat{u}_{EW} (m/s)$
B1	1320	17.9	0.95	1676	23.7	0.99
B2	1918	20.9	0.77	2578	39.0	1.06

Table 5.1: Cross-sectional area, tidal prism and equivalent velocity amplitude for B1 and B2 in SQ and EW.

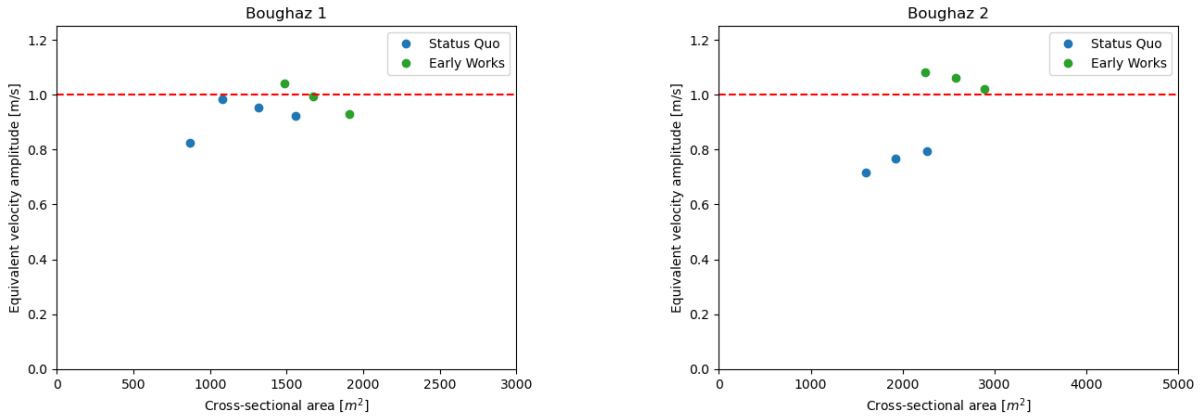


Figure 5.1: Comparison of the points used to approximate closure curves for Boughaz 1 and Boughaz 2 in SQ and EW.

The approximations for the closure curve of both inlets in the Status Quo situation shown in Figure 5.2 do not intersect with \hat{u}_{eq} . This means the only equilibrium situation along the curve is located at $A = 0$. This implies that both inlets are always on a closing trajectory. This corresponds with closure documented by Klein (1986) and explains the constant need for maintenance dredging. It is known that Boughaz 2 closes more quickly than Boughaz 1. This could be explained by how much closer the equivalent velocity amplitude for Boughaz 1 is to equilibrium velocity amplitude compared to Boughaz 2. Boughaz 1 is very close to a theoretically stable situation.

The value for \hat{u}_{eq} is a rough approximation and is location dependent (estimated to be 1.03 m/s for the Dutch Wadden Sea inlets)(van de Kreeke and Brouwer, 2017). \hat{u}_{eq} introduces uncertainty for the theoretical stability of Boughaz 1 as the approximation of the top of the closure curve comes close to $\hat{u}_{eq} = 1$ m/s. As it is known the inlet is constantly closing, it can be assumed the curve is completely below the threshold value of $\hat{u} = 1$ m/s, as the location of the inlet on the curve in SQ would result in convergence to a stable root if the closure curve would intersect with \hat{u}_{eq} .

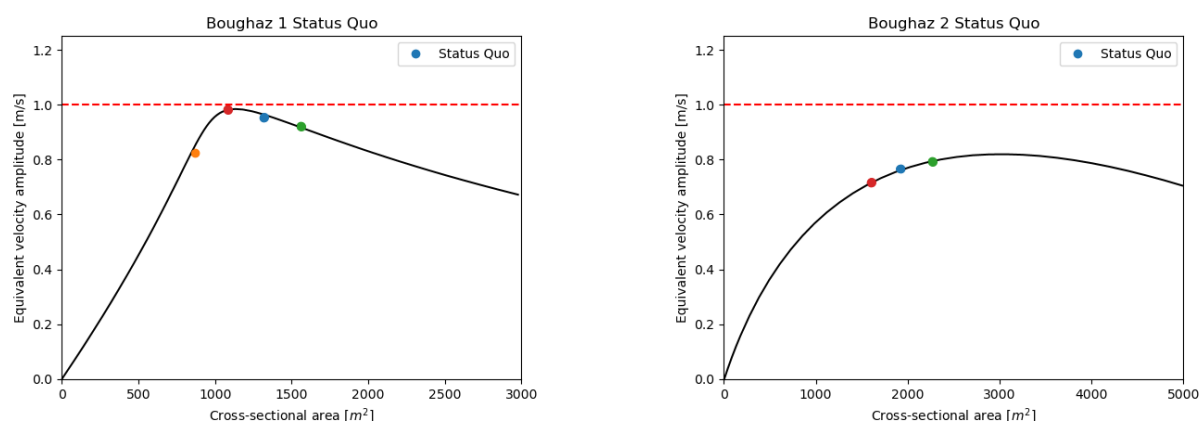


Figure 5.2: Approximation of Escoffier curves for Boughaz 1 and Boughaz 2 in the Status Quo scenario. The blue points represent the Status Quo situation, the orange and red points represent situations with slightly reduced cross-sections and the green point represents the situation with a slightly increased cross-section.

The interventions result in a new closure curve for both inlets. The approximations for each of these curves are presented in Figure 5.3. Both new situations result in a location on the right side of the Escoffier curve, implying future convergence towards the stable equilibrium. As \hat{u} for Boughaz 1 in EW is below 1 m/s, the cross-section of Boughaz 1 is expected to reduce slightly by means of sedimentation to move towards the stable equilibrium. \hat{u} for Boughaz 2 in EW is larger than 1 m/s, this means the cross-section is expected to erode, moving towards a larger cross-section to reach the stable equilibrium cross-section.

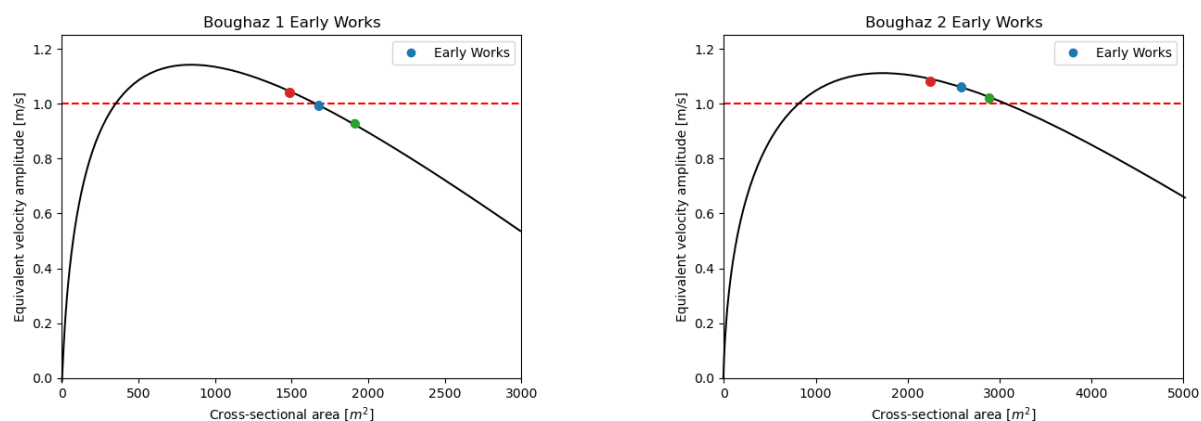


Figure 5.3: Approximation of Escoffier curves for Boughaz 1 and Boughaz 2 in the Early Works scenario. The blue points represent the Early Works situation, red point represents the situation with a slightly reduced cross-section and the green point represents the situation with a slightly increased cross-section.

Local maximum velocities

By analysing the local maximum tidal current velocities, expectations for morphological changes in different locations can be made. From Figure 4.10 it can be seen that in both SQ and EW, velocities reduced dramatically moving away from the inlets. To analyse the potential effect on morphological changes, a critical depth-averaged velocity for initiation of motion needs to be assumed. This critical value is taken from Figure D.1 for the smallest sediment fraction used ($D_{50} = 0.00015$ m) and an assumed lower bound value for the water depth of 1 m, and is estimated as 0.3 m/s (Van Rijn, n.d.). As seen in Figure 4.10, while the total area of occurrence of maximum velocities exceeding the critical velocity is almost twice as

big in EW as it is in SQ, it still does not occur outside the immediate vicinity of the inlets. This indicates no expected notable morphological changes for the sand particles due to increased tidal currents in EW for the majority of the basin.

Tidal asymmetry

Changes in tidal currents in the basin are not the only option for morphological change with regard to sand. It is important to look for changes in tidal asymmetry over the inlets to identify changes in import or export of sediment.

Table 4.2 shows little asymmetry in the duration of ebb and flood over both inlets. Flood is a little shorter over both inlets, indicating slight flood dominance and thus import of sand. The interventions do not have a large impact on ebb and flood duration. It is expected that there is slight import over both inlets due to tidal currents in both SQ and EW

5.2.2 Response of meteorologically forced currents

Just analysing the response of tidal currents does not give the complete image of current-based effects on morphology in Lake Bardawil. Meteorological forcing mainly affects the flow in the system in two ways: evaporation and wind forcing. Evaporation results in net import of water over the whole system and high wind speeds result in wind set-up and wind-driven currents.

Summer

During summer months, the meteorologically forced situation strongly resembles the tidal-only situation in terms of velocities. As mentioned in section 4.2, the wind and evaporation during summer result in interaction between the inlets and a net import of water over the whole system. Weather effects result in net import of water in Boughaz 1 and net export of water in Boughaz 2. A logical explanation for the slight changes in maximum inlet velocities noted in subsection 4.2.4 in both inlets can be found in these meteorologically forced phenomena. A reduction of maximum outward inlet velocities in both inlets can be logically explained as a result of evaporation in the basin. The reduction of outward flow coincides with high water during daylight, pointing towards a relation to evaporation. Furthermore, the slight increase of maximum inward inlet velocities in Boughaz 1 and the corresponding decrease of maximum inward inlet velocities can be attributed to the interaction between the inlets.

The relative difference between the tidal prism for Boughaz 2 in the tidal-only situation and the meteorologically forced situation in EW is of approximately 2.5%. This is smaller yet comparable to the relative margin of around 6% between the equivalent velocity amplitude and equilibrium velocity amplitude calculated in subsection 5.2.1. Depending on the new location on the Escoffier curve for Boughaz 2, exceeding this margin could be critical for the behaviour and stability of the inlet. The location of Boughaz 2 on the Escoffier curve is however expected to be close to the stable equilibrium cross-section, and this margin is therefore expected to be insignificant for the stability of the inlet.

The examination of meteorological forcing's effects on morphology should extend beyond the confines of the inlets themselves. By comparing Figure 4.22 with Figure 4.10 and employing a similar line of reasoning concerning critical depth-averaged velocity as applied to tidal currents in subsection 5.2.1, it can be deduced that sand-related morphological activity solely driven by currents will not be significant in the areas that are not in the direct vicinity of the inlets.

Winter

In the winter months, two distinct situations can be distinguished: calm periods and storm events. During calm situations, the flows in Lake Bardawil closely resemble those observed during the summer and under

tidal-only conditions. However, during storm events, the impact of wind on flow becomes substantial, leading to significant deviations in flow velocities compared to the tidal-only scenario.

As these storm events have strong effects on inlet velocities, there will also be an influence on the inlet stability discussed in subsection 5.2.1. Due to the irregular velocities through the inlets, predicting the morphological response during storm events is not straightforward. While maximum velocities in the inlets are larger than under tidal-only conditions, there are some other factors that influence erosion and sedimentation in the inlet. In cases where meteorological forcing opposes tidal forcing, the cross-sectionally averaged inlet velocity can decrease compared to the tidal-only scenario. Consequently, using only the observed cross-sectionally averaged velocities does not yield a clear prediction of the response of the inlet's cross-section. Additionally, when comparing cross-sectionally averaged velocities through the inlets, it is important to note that the total duration of these storm events is very short compared to the duration of inlet velocities under regular conditions.

As flow velocities increase over the entire basin during storm events, some kind of increased sediment transport is expected during this time. Most of the local maximum flow velocities still do not exceed the critical value for initiation of motion for depth-averaged flow velocity determined in subsection 5.2.1. In the strait section of the basin, there are some locations where this value is exceeded. Maximum flow velocities of just under 0.6 m/s are found, which, based on Figure D.1, would result in the suspension of fine sands. Some erosion of fine sediment is expected in the strait section of the basin.

Interestingly, the results show substantially higher values for these wind-driven velocities in the strait section in the Early Works situation. As mentioned in subsection 2.2.5, sediment transport has an exponential relation with flow velocity. An increase in flow velocity after the interventions results in a larger increase in sediment transport. This means erosion in these areas is expected to be larger in the Early Works situation than in the Status Quo situation based on currents only. This could result in relatively large sediment transport towards Boughaz 2 during the first storms after execution of the interventions.

The phase lag between the horizontal and vertical tide was expected to be important for the direction of sediment transport during high sediment resuspension due to wind waves. Through an analysis of the storm events, it can be deduced that the currents during these periods are predominantly driven by meteorological factors rather than tidal influences.

5.2.3 Wind waves

Due to the large differences in maximum wave height in the basin between the summer and winter seasons, and knowing that in reference lagoons sediment resuspension is mainly driven by wind waves, the winter season is expected to be more morphologically dynamic in terms of sediment transport in the basin itself. As the maximum wave heights are not significantly influenced by the interventions, there is no higher amount of sediment resuspension expected due to wind waves after the interventions. However, as these wave heights occur during winter storms, and there is a higher known flow towards Boughaz 2 during heavy storms after interventions, this leads to an increase of sediment transport to Boughaz 2 in the Early Works situation.

5.3 Morphological response to the interventions

The morphological response of the system is analysed in this section. First, the behaviour of the system in the model is compared to the known behaviour of the system in reality. Then the behaviour of the inlets in the Status Quo is compared to the behaviour of the system in the Early Works scenario.

5.3.1 Validation

The possibility of validation of the morphological behaviour of the model is very limited as there is very little knowledge of the morphological behaviour in reality. There are however a few things that can be used: Firstly, due to observations we know both inlets are closing and additionally, Boughaz 2 closes quicker than

Boughaz 1. And secondly, satellite data can be used to track the behaviour of the spit at Boughaz 2. If the behaviour observed is found in the morphological results for SQ, it would be an indication that the model results somewhat represent real-world dynamics.

Based on aerial photography described by Klein (1986), it is known both inlets have had sediment accumulating on the updrift (western) side of the channel. This process can be found in the results for cumulative bed level change for Boughaz 2 in Status Quo, where heavy sedimentation occurs on the updrift side of the channel. There is however no definitive evidence of this process in Boughaz 1. Both inlets show sedimentation on the inner side of the inlet in the flood-tidal delta. Whether this results in the closure of the inlets can not be concluded from the limited time simulated. Closure of the inlets would not logically start from the locations with the highest flow velocities. The deposition in the flood-tidal deltas could increase resistance to inward and outward flow, decreasing the capacity for sediment transport in the inlet, possibly leading to closure.

As mentioned in subsection 4.3.3, Boughaz 2 is much more morphologically dynamic than Boughaz 1. Again, the length of the simulation periods is too short to conclusively say anything about closure of the inlets. If sedimentation in the flood-tidal delta is an indication of closure, then the larger sedimentation in Boughaz 2 is an indication of quicker closure compared to Boughaz 1.

Another interesting way to attempt to validate the results of the morphological model is by making a comparison between reality and the model results for the behaviour of the spit at Boughaz 2.

Combining the approximate date of measurements used for the bathymetry with Sentinel satellite data, it can be deduced that the bathymetry used represents the condition of Boughaz 2 after recently undergoing maintenance dredging. The assumption is that the spit formation has also been partially dredged, meaning it is lower than it would be in a natural equilibrium condition. In the model result, sediment accumulates on top of the spit quickly, becoming higher. The equilibrium height of the spit in the model is larger than the bathymetry input. If the assumption that the spit has been dredged is correct, this would be realistic behaviour for the model.

Next to growth during summer simulations, the spit also exhibits interesting behaviour during winter season simulations. From satellite imagery, it can be seen that the spit as it is in SQ is shorter than it is in reality. Due to winter storms, the spit migrates in a southern and eastern direction depending on the sediment size considered. The resulting depth profile after a two-month winter simulation is compared to the input bathymetry for SQ in Figure 5.4. Comparison to the satellite imagery in Figure 5.5 shows similar a similar shape in reality.

The model successfully mimics these natural processes around the inlets, this allows for some confidence in the behaviour of the model.

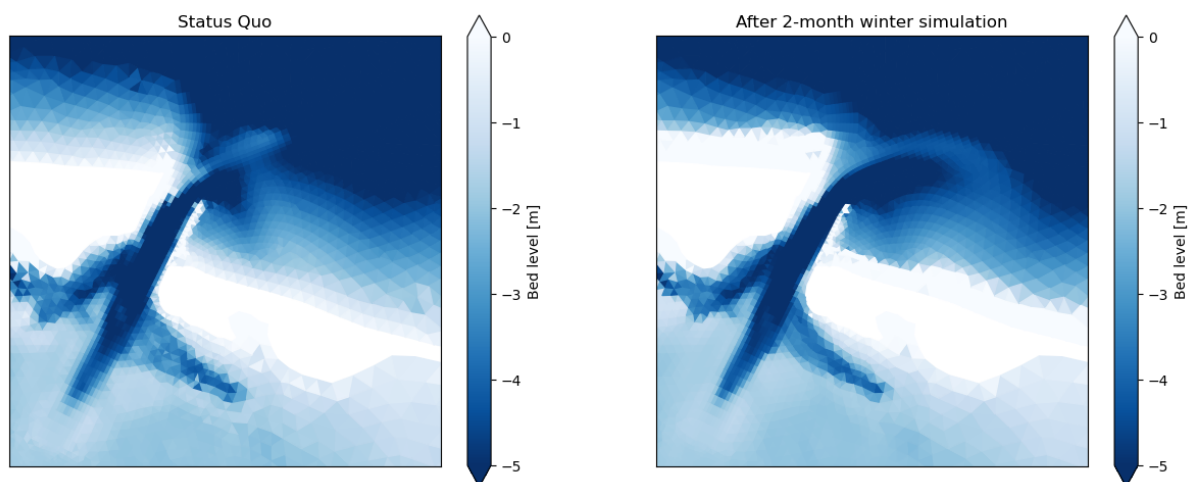


Figure 5.4: Comparison of the spit at Boughaz 2 between initial bathymetry in SQ to bathymetry after 2-month winter simulation for fine sand sediment.

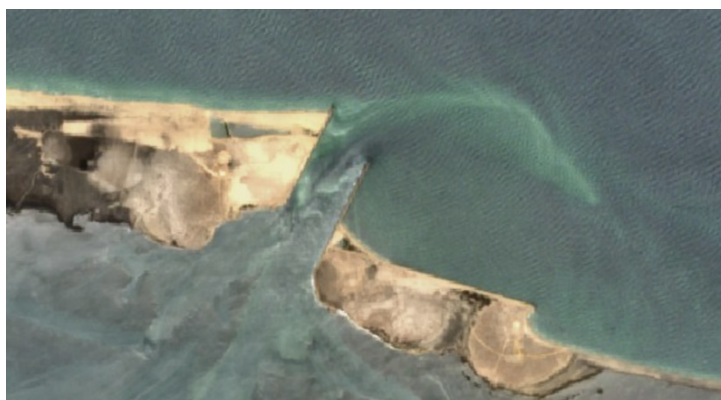


Figure 5.5: The spit at Boughaz 2 in June 2023 (Sinergise Ltd., 2023).

5.3.2 Morphological response to interventions

To draw conclusions on the morphological response to the interventions, the morphological changes for fine sand sediment under summer conditions for the Status Quo and Early Works scenarios are compared in figures 5.6 to 5.9. The aim of this comparison is to assess either reduced or increased closure of the inlets and to find any processes impeding the effects of the interventions.

Boughaz 1

In Boughaz 1, the interventions result in a larger deposition of sediment in the inner flood-tidal delta than in the Status Quo. There is a significant increase in total sedimentation in section B1 Flood Delta 1 in Table 4.3, especially during the winter season. This effect corresponds with the increased import of sediment found over Boughaz 1 after the implementation of the interventions. During both winter and summer seasons, the main channel starts filling up on the inward side of the channel, just behind the narrowest part of the inlet. The maximum sedimentation after a 2-month simulation is in the order of 1.5m, meaning the remaining depth is still substantially higher than in SQ.

During the simulation period, there is no sign of a decrease in discharge through Boughaz 1 as a result of this sedimentation in the dredged channel. In the short-term simulation period, the inlet does not close and the function of the inlet is not impeded. However, if this sedimentation process continues and reinforces

itself over an extended period, it could directly impede flow through Boughaz 1 and therefore cause the loss of function of the interventions. The net sedimentation process in the channel could also stop without decreasing flow through Boughaz 1 after finding a new equilibrium depth. In this case, the dredging depth of the channel could be reduced.

During the simulation period, there is no impediment to the function of the interventions in Boughaz 2. There is increased sedimentation in the dredged channel area on the inside of the inlet. Due to the increased cross-sectional area of the inlet, increased morphological activity does not definitively result in decreased stability. No conclusions can be made on the change in stability of the inlet in the simulation period. The rate of sedimentation in the inner flood-tidal delta is however alarming.

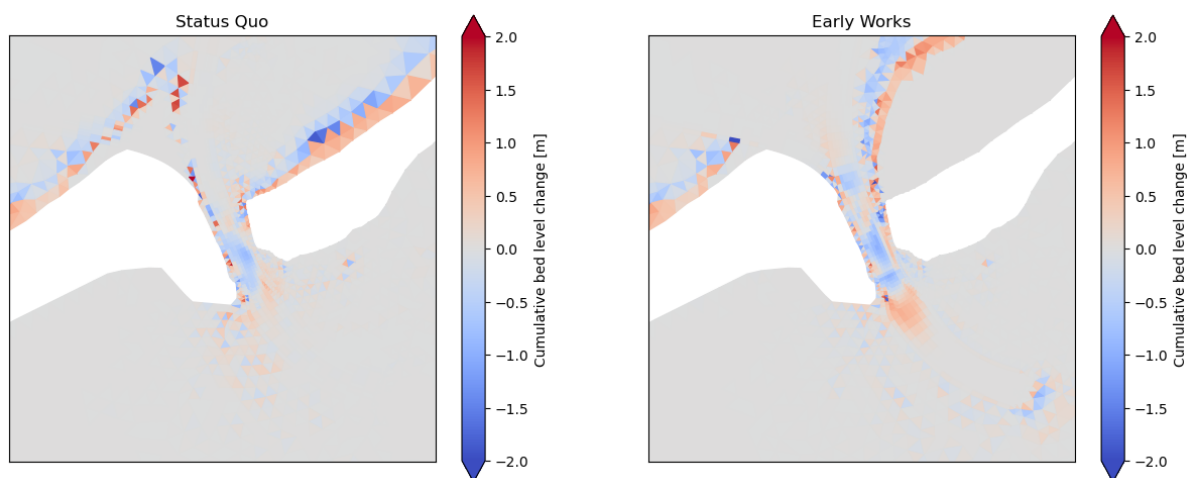


Figure 5.6: Bed level change in Boughaz 1 during 2-month summer simulation period for SQ and EW.

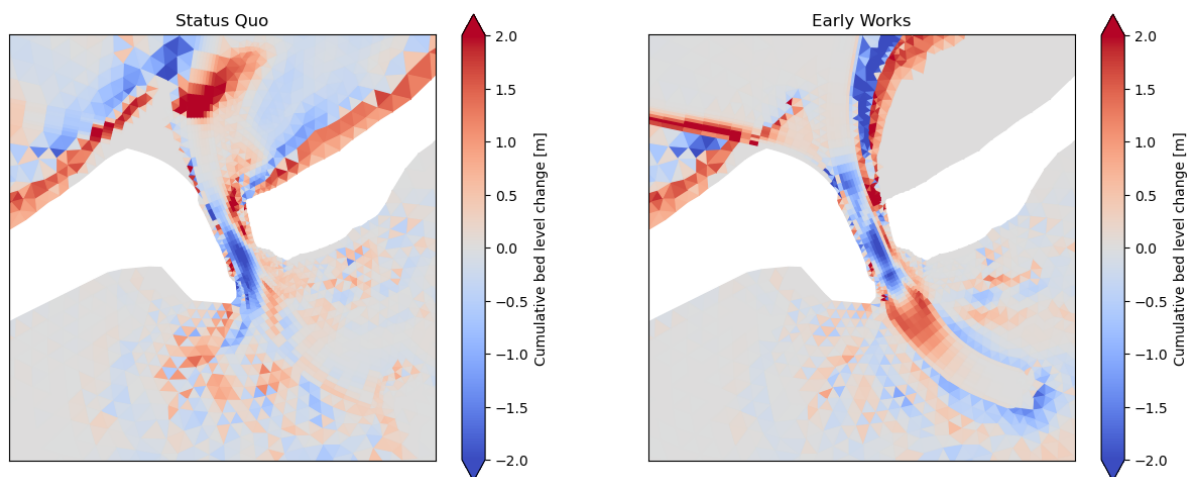


Figure 5.7: Bed level change in Boughaz 1 during 2-month winter simulation period for SQ and EW.

Boughaz 2

In summer conditions, Boughaz 2 is much more morphologically static, there is less sedimentation in the inner region of the flood-tidal delta and the updrift side of the channel after the interventions are implemented. The decrease in the inner flood delta region is supported by the values for total sedimentation per section found in Table 4.4. Even though sedimentation increases over the total flood-tidal delta after interventions, the sedimentation in the inner flood-tidal delta corresponding to B2 Flood Delta 2 decreases. As with

Boughaz 1, this is consistent with the change in import of sediment over Boughaz 2. Decreased import of sediment causes decreased sedimentation in the inner flood-tidal delta in this case. This is an indication of improved stability. In the short term, there are no indications of any hindrances to the functioning of the intervention in Boughaz 2 during summer in terms of reduced discharge. However, a slight increase in sedimentation is observed over the total flood-tidal delta, which could potentially pose long-term issues if it persists over an extended period.

In the winter season, the sedimentation in the inner flood-tidal delta of Boughaz 2 reduces between SQ and EW. This results in net erosion over the section of B2 Flood Delta 2 in Table 4.4. There is substantial deposition of fine sand sediment on the edges of the channels of the flood-tidal delta and the dredged channel. This is demonstrated by the increase in sedimentation over the total flood-tidal delta for Boughaz 2 in Table 4.4, whereas a decrease in sedimentation was found over the two smaller sections. This deposition of fine sand is presumably the effect of resuspended sediments due to wind waves flowing towards Boughaz 2. The amount of fine sand sediment transported towards Boughaz 2 from the basin increases due to the interventions, as can be seen in Figure C.8. Additionally, there is a large deposition of fine sands upwards of 3.5m on the updrift side of the dredged area on the seaward side of the inlet. Deposition in this area is expected, as a new ebb-tidal delta will form itself in the dredged area. In this simulation period, there is no indication yet what the shape of this new ebb-tidal delta will be. The potential new mode of sand bypassing would be a relevant observation, as it could indicate a change in stability of the inlet.

During the simulation period, there is no impediment to the function of the interventions in Boughaz 2. The inlet is less morphologically dynamic after interventions, which in combination with the increased cross-sectional area would indicate improved stability.

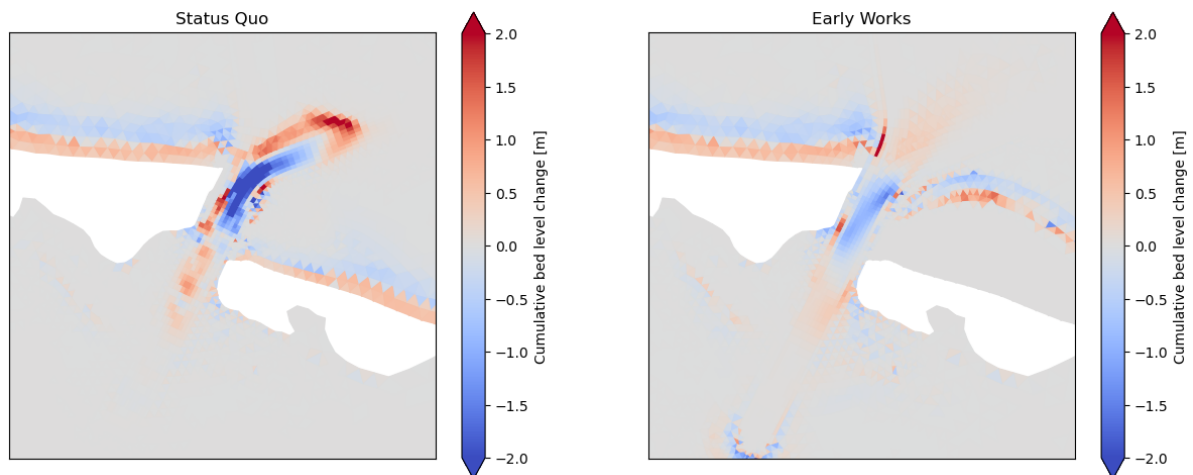


Figure 5.8: Bed level change in Boughaz 2 during 2-month summer simulation period for SQ and EW.

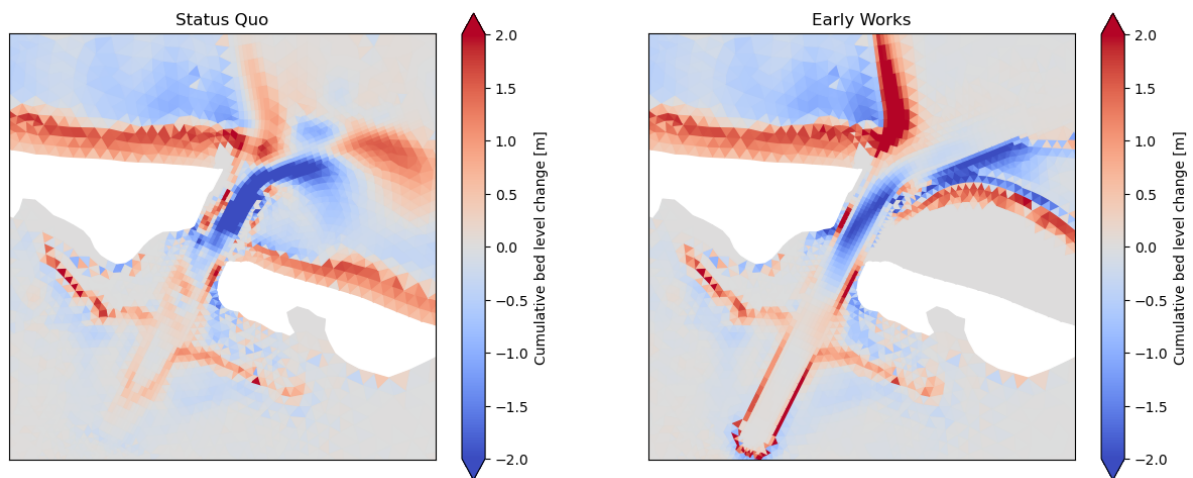


Figure 5.9: Bed level change in Boughaz 2 during 2-month winter simulation period for SQ and EW.

5.4 Considerations interpreting conclusions

The predictions made in this study are based on certain assumptions, this affects the results. The following things should be considered interpreting the conclusions of this thesis.

5.4.1 Unknown parameters

As very few measurements have been done in the area, almost all of the used parameters are estimates. Parameters such as bathymetry, friction and metocean conditions are all estimated. With some being more educated estimates than others.

The bathymetry in and outside the lake has been interpolated between lines of measurements. This means important features are possibly missing in the input bathymetry. For example, it could very well be possible that the shape found in the spit at Boughaz 2 after winter simulations was already there in reality at the moment of measuring but was not captured in the measurement campaign.

Friction in Lake Bardawil is one of the biggest unknowns. It is difficult to measure or estimate. It is not known if there is any vegetation on the bed that could increase friction. Different values for bed friction can have a significant impact on the results for the tidal range in the basin as shown in subsection C.1.4.

The metocean conditions employed for modelling in this study have been derived from other models. The tidal data is derived from a tidal model, the weather conditions are derived from a meteorological model, and the wave input is derived from a wave model. It is important to acknowledge that these derived conditions come with inherent uncertainties regarding their accuracy. Any differences between the parameters used in the model and reality will result in differences in the results. To obtain more precise conditions, it would be necessary to conduct long-term local measurements.

5.4.2 Modelling

Modelling is an approximation of reality. A result like a sediment transport is an approximation of sediment transport, based on an approximation of bed shear stress, which is based on an approximation of currents and waves. Consequently, errors are introduced at each level, ultimately leading to an accumulation of errors in a final result, such as sediment transport.

The model used in this research uses depth-averaged flow velocities. This means differences in flow velocity or differences in flow direction over the water column are neglected. This affects the hydrodynamics and possibly morphodynamics of the system. In Lake Bardawil, there are two main causes for such differences.

Firstly, wind setup causes a return flow along the bed due to differences in hydrostatic pressure. More relevantly for Lake Bardawil, the substantial difference in salinity and therefore water density between Lake Bardawil and the Mediterranean Sea could result in three-dimensional circulation flow effects in the inlets. The hypersaline nature of the lagoon would result in a circulation pattern with net outward flow along the bed of the inlet. This could mean the resulting sediment-importing nature of both inlets is exaggerated due to the depth-averaged model applied when compared to reality or a 3D model.

Another effect of depth-averaged flow modelling is a reduction in cross-shore sediment transport as the return flow of breaking waves is neglected. While there is some cross-shore transport in the model results, these mainly correct the initial shore profile. In reality, shores usually erode during storms and slowly accrete in calmer periods. Neglecting these cross-shore processes could have an influence on the validity of the longshore transport of sediment predicted.

The three-hour coupling used in the coupled model means that the wave height for each location is constant for three hours. In these three hours, the flow model stays dynamic, meaning the depth at this location could change substantially, either due to the tide or wind setup. This results in larger than realistic shear stresses in shallow locations that get even shallower during this three-hour period. This effect is most clear during winter storms, where the western side of the basin becomes shallower during three-hour periods due to wind setup. The large shear stresses don't seem to result in abnormal transport in these areas.

5.4.3 No clay/silt fractions used

The exclusion of clay and silt sediments in the morphological study introduces a limitation in comparing the results with the actual conditions. Grab samples reveal the presence of clay and silt sediments within the basin. It is expected that these sediments, particularly during winter storms, will become suspended and transported towards Boughaz 2, following a similar pattern observed for the fine sand fraction. The expectation is that very little fines will settle in the inlet, the majority will be transported through. The fines that do settle in the inlet after a storm, during tidal slack, are expected to be transported away during ebb or flood.

5.4.4 Limitation of using summer and winter periods

While the simplification of using only a summer and a winter period looks to be fairly accurate for Lake Bardawil, it is not reality. During spring, there are slightly northerly stronger winds than in the summer, which will have an effect on incoming waves and possibly on wind-induced currents. During both autumn and spring, the effect of evaporation is smaller than in the summer periods considered.

5.4.5 Assumption of a two inlet system

The Lake Bardawil system was simplified to a two inlets system for this research. In reality, there is however a third, natural inlet in the eastern part of the lake. The connection between Lake Bardawil and the Mediterranean Sea in this inlet is so small that it is assumed negligible. The connection will however have an effect on the hydrodynamics of the basin. It is also very well possible that the increased tidal range due to interventions will increase the role of the third inlet.

6 Conclusion

- The interventions in the tidal inlets at Lake Bardawil result in the growth of the tidal prism by a factor of 1.6. This is expected to result in an increase in fish migration of at least the same magnitude. Additionally, the interventions are expected to cause a reduction of salinity in the eastern basin.
- Based on Escoffier theory, the interventions result in a change from convergence to closure of both inlets in the Status Quo to convergence to a stable equilibrium for both inlets in the new situation.
- The results from the morphological model do not indicate increased stability for Boughaz 1. The increased sedimentation in the inner flood delta, while not causing impediment to the functioning of the interventions in terms of discharge in the short term, could hinder the function of the increased tidal prism of the interventions in the long term.
- For Boughaz 2, the morphological results indicate improved stability. The interventions result in a decrease in morphological activity in the inlet. Sedimentation is reduced in the areas of the updrift side of the inlet channel and the inner flood delta, which are associated with the closure of the inlet.

This research aimed to predict the short-term hydrodynamic and morphological response to dredging interventions in Lake Bardawil, a complex double-inlet coastal system. This was done using a review of literature and reference cases and a hydrodynamic and morphological modelling study.

In the review of literature and reference cases, tidal propagation in shallow micro-tidal lagoons was found to be mainly influenced by inlet cross-section, friction and, in the case of multiple inlet systems, interaction between tidal waves.

The processes governing the morphology of Lake Bardawil are divided into two categories: The processes influencing the inlets and the processes influencing the basin itself. Natural changes to the inlets are mainly influenced by currents of tidal and meteorological nature in combination with the wave-induced longshore sand transport. As the longshore transport does not change due to the planned interventions, changes to currents are most important for morphological changes to the inlets. In addition to general changes to the morphology of inlets, tidal currents, or more precisely flow velocity amplitudes in the inlets have been linked to inlet stability. From reference cases, it can be concluded that in the basin, the micro-tidal nature of the area results in insufficient magnitude of tidal currents for significant morphological change. The main driver of morphological changes in similar lagoons is found to be meteorological, driven by wind waves and in some cases wind-induced currents.

To assess the impact of the interventions on the hydrodynamic and morphological behaviour two different models are used: A hydrodynamic model in D-flow FM and a morphological model using a coupling between D-waves and D-flow FM. The hydrodynamic model is used to investigate the initial hydrodynamic response to the interventions. Initially briefly looking at the parameters that are expected to influence fish migration and water quality. But most importantly looking at processes that influence the morphology of the basin and stability of the inlets. The morphological model is used to predict local morphological changes and their effect on the inlets.

The hydrodynamic model shows that the interventions result in a growth in tidal prism by a factor of 1.6 and increased interaction between the inlets compared to the Status Quo. The growth in tidal prism is expected to result in an increase in fish migration of at least equal magnitude. The combination of a larger tidal prism and interaction between the inlets is expected to result in reduced salinity over the eastern basin improving the water quality and providing a more suitable habitat for fish.

The larger tidal prism is related to increased inlet stability through the theory by Escoffier (1940) through

the inlet velocity amplitude. The interventions change the closure curve for both inlets. In the Status Quo scenario, the closure curve for both inlets does not intersect with the curve for the equilibrium velocity, meaning the inlets will move along the curve towards closure. In the Early Works scenario, Boughaz 1 is located just below the equilibrium velocity on the right-hand side of the new Escoffier curve. The new location on the new curve for Boughaz 2 is above the equilibrium velocity, close to the right-hand side equilibrium cross-section. This means theoretically both inlets move along the curve towards a stable equilibrium, instead of closure, as it is in Status Quo conditions.

The interventions result in a slight general increase in magnitude of tidal currents over the whole basin. The new maximum tidal current velocities do not exceed critical values for the initiation of motion for sand particles outside of the direct vicinity of the inlets. Larger tidal currents due to interventions do not have an impact on the morphology of the majority of the basin.

Merely considering tidal currents provides an incomplete understanding of the dynamics in Lake Bardawil. Weather effects have a significant impact on currents within the system. Interaction between the inlets in Lake Bardawil is mainly driven by weather effects with Boughaz 1 importing water and Boughaz 2 exporting water in both summer and winter. Under summer conditions, the tidal prism of Boughaz 2 decreases by roughly 2.5% due to weather-induced interaction and evaporation in the basin. Winter storms cause substantially larger maximum flow velocities in the basin, extending beyond the vicinity of the inlets. During these storms, the flow direction is mainly governed by wind, resulting in flow going from Boughaz 1 to Boughaz 2. Locally, these velocities do exceed the threshold of motion for sand particles. The interventions cause an increase in these wind-induced currents during winter storms, resulting in increased sediment transport during winter storms.

In addition to larger flow velocities, winter storms cause larger wind waves in the basin. These wind waves cause resuspension of sediments which are then transported mainly to Boughaz 2 due to the net wind-induced flow from Boughaz 1 to Boughaz 2. As flow to Boughaz 2 increases as an effect of the interventions, sediment transport towards Boughaz 2 is expected to increase in the Early Works situation.

The coupled morphological model shows very little morphological change in the majority of the basin. Only the inlets and their direct surrounding show significant morphological changes. While no notable morphological changes are observed in the basin, there is transport of suspended fine sediments into Boughaz 2 in winter scenarios, which increases as a response to the interventions.

The behaviour of the inlets changes due to the interventions. Boughaz 1 starts importing slightly more sediment into the basin during both summer and winter. In contrast, the sediment-importing nature of Boughaz 2 reduces greatly during summer and the exporting nature of sediment increases during winter.

From observations in the coupled model for the Status Quo conditions, combined with the knowledge that both inlets are unstable in this condition, it is expected that the closure of the inlets is caused by sedimentation on the updrift side of the inlet channel and on the inner side of the inlet, in the flood-tidal delta region. The function of the interventions is not impeded within the simulation period considered, expected tidal discharge through the inlets is not reduced due to morphological changes. Conclusions on longer-term stability can not be made. The initial behaviour of the inlets can be used as an indication towards the new stability conditions. In this regard, the response to the interventions is different for each of the inlets.

The main response in Boughaz 1 is sedimentation on the inner side of the dredged channel. The deposition in the channel is larger than it is in the flood-tidal delta during Status Quo. This is consistent with the increased import of sediment found. The effect occurs during both winter and summer seasons. If this effect persists long-term and reinforces itself, it could hinder the inflow of water, possibly reducing the tidal prism. This would directly impede the function of the interventions.

Boughaz 2 behaves differently, the interventions result in a less morphologically dynamic inlet. There is less deposition of sediment in the area of the flood-tidal delta region and the updrift side of the inlet channel in

the Early Works situation compared to the Status Quo situation for both summer and winter. This effect can also be traced back to the changed sediment import/export character of Boughaz 2. The reduced deposition of sediment indicates improved stability of the inlet as a result of the interventions.

To conclude, the short-term response to the dredging interventions at the Lake Bardawil double inlet system will be as intended. The response of the system will result in an increased tidal prism and is expected to result in reduced salinity in the eastern basin. Theoretically, the interventions should cause both of the inlet cross-sections to move towards a stable situation. The simulations do not indicate any short-term impediment to the functioning of the inlets in terms of discharge. In Boughaz 1, it is inconclusive during the simulated period whether stability is improved, there is no indication of improved stability. For Boughaz 2 there is an indication of improved inlet stability due to decreased morphological activity in the flood-tidal delta and reduced sedimentation on the updrift side of the inlet channel.

7 Recommendations

More measurements

The first step to gaining more certainty in the results of the models used in this research and future models is doing more measurements. Long-term measurements for wave height, wind speed and direction and tidal range would create more certainty on model input, making for better results. In addition to measurements for input certification, measurements for validation of this and future models could be done. Measuring the tidal elevation in a few locations in the system would help with the calibration and validation of a hydrodynamic model. Additionally, measurements for estimating longshore sand transport along the coast could be done. By excavating a section of the shoreline and closely monitoring the time it takes to refill while recording wave conditions, an estimation of real-world transport can be derived. This knowledge can then be used for the calibration of the morphological model.

Long-term simulations using equivalent conditions

When there is more confidence in the model performance, long-term simulations start to become a little more realistic. In order to do this without using an unrealistic amount of computational time, equivalent wave, wind and tidal climate needs to be constructed. Due to the complex nature of the system, creating this climate will be a complex exercise. The findings of this research could help in taking a step towards simplification of this climate, as it can be concluded that sediment transport from outside of the lagoon into the inlet is much larger than sediment transport from inside the lagoon. Therefore it could be sufficient to calibrate the equivalent climate to the longshore transport.

In these long-term simulations, there are different things to focus on for each inlet. In Boughaz 1, the development of the accretion of sediment in the dredged inner channel needs to be monitored. In Boughaz 2, the eventual mode of bypassing will give an indication towards long-term inlet stability.

Research role of the third inlet

The influence of the third inlet in Lake Bardawil represents an uncertainty that needs to be addressed. To investigate the role of the third inlet, it is necessary to conduct observations and measurements. Then, using the new knowledge gained, a dedicated modelling study can be done to explore the influence of this natural inlet on the system.

Design considerations

Based on this research, a few considerations can be made regarding the inlet intervention designs. First of all, looking at figures 4.2 and 4.3, it can be seen that the tidal range reduces substantially directly behind the inlet. This suggests that further enlargement of the tidal range is feasible. It would be valuable to conduct a modelling study to investigate the potential benefits of increasing the inlet cross-sections beyond the current design. This study could explore the effects of not only increasing the depth but also widening the inlets, potentially leading to even more effective designs.

Depending on the long-term development of the sedimentation in the channel behind Boughaz 1 and the potential new equilibrium depth in the channel, the design of the channel behind Boughaz 1 could be altered. A shallower dredging depth could be sufficient. This would save costly dredging volumes.

Reduce computational time

For ease of further modelling, some adaptations can be made to the models used. Modelling the morphological models was extremely computationally intensive in the current setup. This research shows that morphological changes in the majority of the basin are very small. The small grid cell sizes used on the inside of the basin are unnecessary. It is therefore recommended in future similar modelling studies to simplify the inner basin and use a coarse grid for everything that is not close to the inlets or the outer shoreline.

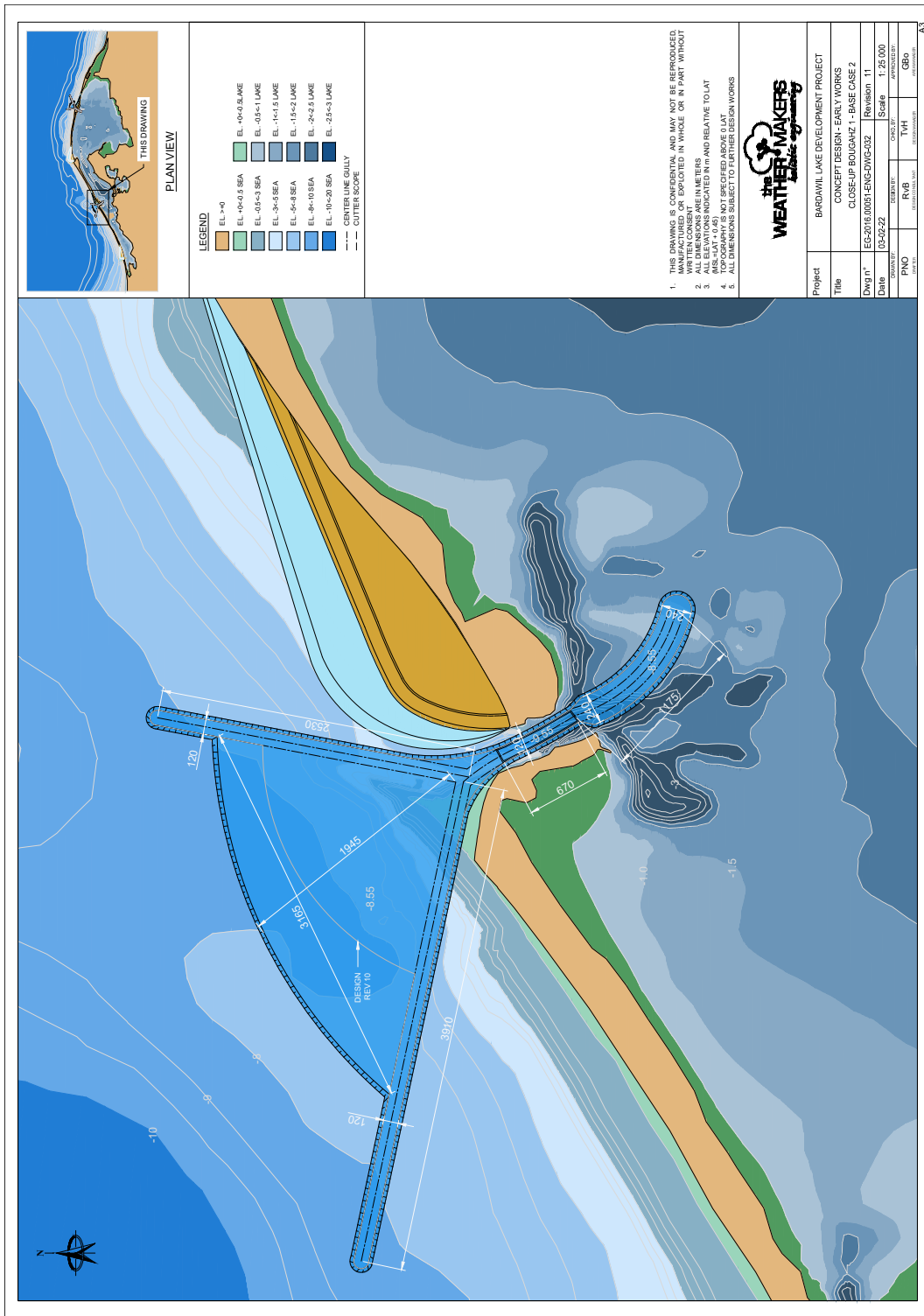
Bibliography

- Bangen, P. (2021). *The Effects of Annual Extreme Weather Conditions on the Exchange Flows between Lake Bardawil and the Mediterranean Sea* (tech. rep.).
- Bek, M., & Cowles, G. (2019). A three-dimensional circulation model of lake bardawil, egypt. *Egyptian Coastal Lakes and Wetlands: Part I: Characteristics and Hydrodynamics*, 265–283.
- Bing maps. (2023). <https://www.bing.com/maps/?cp=31.10802~33.125223&lvl=11.3&style=a>
- Bosboom, J., & Stive, M. J. (2021). *Coastal dynamics*.
- Bruun, P., Mehta, A. J. M., & Johnsson, I. G. (1978). *Stability of tidal inlets: Theory and engineering*. Elsevier Scientific Publishing.
- Cai, H. (2014). *A new analytical framework for tidal propagation in estuaries*. [s.n.]
- Carlin, J. A., Lee, G. h., Dellapenna, T. M., & Lavery, P. (2016). Sediment resuspension by wind, waves, and currents during meteorological frontal passages in a micro-tidal lagoon. *Estuarine, Coastal and Shelf Science*, 172, 24–33. <https://doi.org/10.1016/j.ecss.2016.01.029>
- Carniello, L., Defina, A., Fagherazzi, S., & D'Alpaos, L. (2005). A combined wind wave-tidal model for the Venice lagoon, Italy. *Journal of Geophysical Research: Earth Surface*, 110(4). <https://doi.org/10.1029/2004JF000232>
- Deltares. (2022). *User Manual D-Morphology* (tech. rep.).
- El-Bana, M., Khedr, A.-H., Van Hecke, P., & Bogaert, J. (2002). *Vegetation composition of a threatened hypersaline lake (Lake Bardawil), North Sinai* (tech. rep.).
- Ellah, R. A., & Hussein, M. (2009). *Physical Limnology of Bardawil Lagoon, Egypt Heat Flux of Alexandria Eastern Harbor View project The Impact of Environmental Pollutants on Some Physiological and Biological Parameters of Fishes of Qarun and Wadi El-Rayan Lakes, (STDF), 2013-2015. View project* (tech. rep.). <https://www.researchgate.net/publication/255628988>
- Escoffier, F. F. (1940). Stability of tidal inlets. *Shore and beach*, 8, 111–114.
- Euroconsult. (1995). *Bardawil Development Project* (tech. rep.).
- Frihy, O. E., Badr, A. A., Selim, M. A., & El sayed, W. R. (2002). Environmental impacts of El Arish power plant on the Mediterranean coast of Sinai, Egypt. *Environmental Geology*, 42(6), 604–611. <https://doi.org/10.1007/s00254-002-0563-6>
- García-Oliva, M., Pérez-Ruzafa, Á., Umgieser, G., McKiver, W., Ghezzi, M., De Pascalis, F., & Marcos, C. (2018). Assessing the hydrodynamic response of the Mar Menor lagoon to dredging inlets interventions through numerical modelling. *Water (Switzerland)*, 10(7). <https://doi.org/10.3390/w10070959>
- Green, M. O., & Coco, G. (2014). Review of wave-driven sediment resuspension and transport in estuaries. <https://doi.org/10.1002/2013RG000437>
- Hayes, M. O. (1980). *GENERAL MORPHOLOGY AND SEDIMENT PATTERNS IN TIDAL INLETS* (tech. rep.).
- InfoplazaWaveClimate. (2023). *Waveclimate.com*. <http://waveclimate.com/>
- Klein, M. (1986). *Morphological changes of the artificial inlets of the Bardawil lagoon* (tech. rep.).
- Linersund, J., & Mårtensson, E. (2008). *Hydrodynamic modelling and estimation of exchange rates for Bardawil Lagoon, Egypt. An investigation of governing forces and physical processes using numerical models* (tech. rep.).
- Maicu, F., Abdellaoui, B., Bajo, M., Chair, A., Hilmi, K., & Umgieser, G. (2021). Modelling the water dynamics of a tidal lagoon: The impact of human intervention in the Nador Lagoon (Morocco). *Continental Shelf Research*, 228. <https://doi.org/10.1016/j.csr.2021.104535>
- Makers, T. W. (2022). *Early works concept design* (tech. rep.).
- Mariotti, G., & Fagherazzi, S. (2013). Wind waves on a mudflat: The influence of fetch and depth on bed shear stresses. *Continental Shelf Research*, 60. <https://doi.org/10.1016/j.csr.2012.03.001>

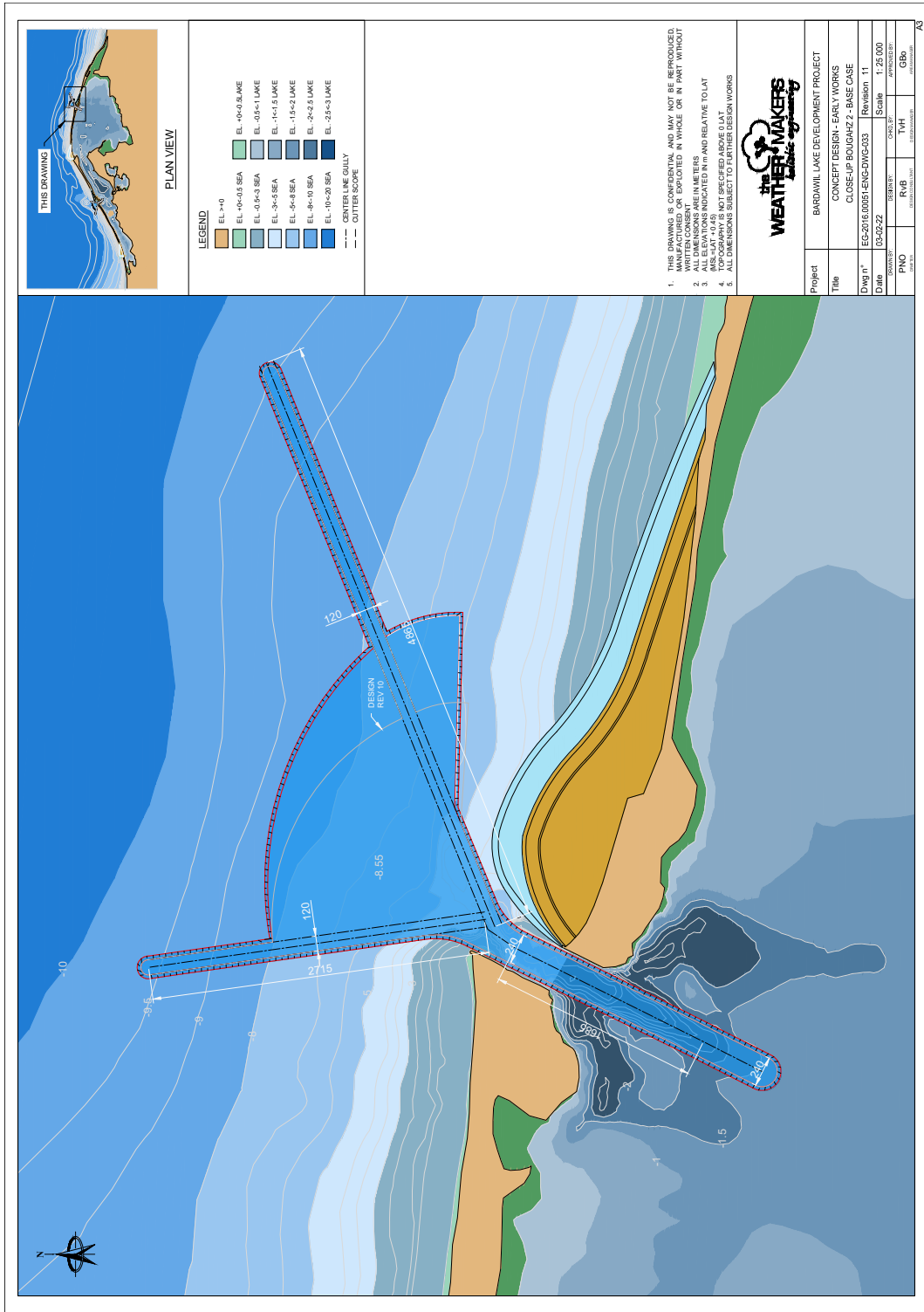
Bibliography

- Meteoblue. (2020). *Meteoblue*. <https://content.meteoblue.com/en>
- Nassar, K., Mahmud, W. E., Masria, A., Fath, H., & Nadaoka, K. (2018). Numerical simulation of shoreline responses in the vicinity of the western artificial inlet of the Bardawil Lagoon, Sinai Peninsula, Egypt. *Applied Ocean Research*, 74, 87–101. <https://doi.org/10.1016/j.apor.2018.02.015>
- O'Brien, M. P. (1969). Equilibrium flow areas of inlets on sandy coasts. *Journal of the Waterways and Harbors Division*, 95(1), 43–52.
- OpenAltimetry.org. (n.d.). *Openaltimetry*. <https://openaltimetry.org/>
- Serrano, D., Ramírez-Félix, E., & Valle-Levinson, A. (2013). Tidal hydrodynamics in a two-inlet coastal lagoon in the Gulf of California. *Continental Shelf Research*, 63, 1–12. <https://doi.org/10.1016/j.csr.2013.04.038>
- Sinergise Ltd. (2023). *Sentinel playground*. <https://apps.sentinel-hub.com/sentinel-playground>
- van de Kreeke, J., & Brouwer, R. (2017). *TIDAL INLETS*.
- Van Rijn, L. (n.d.). *Simple general formulae for sand transport in rivers, estuaries and coastal waters*. Retrieved June 6, 2023, from <https://www.leovanrijn-sediment.com/papers/Formulaesandtransport.pdf>
- van Bentem, R. (2020). Morphological response to Lake Bardawil adaptations.
- Wageningen Marine Research. (2016). *Development of Lake Bardawil* (tech. rep.).
- Walton, T. L., & Adams, W. D. (1976). Capacity of inlet outer ears to store sand. *Coastal engineering proceedings*, (15), 111–111.

A Inlet designs



Appendix A. Inlet designs



B Model conditions

B.1 Weather conditions

B.1.1 Hydrodynamic model

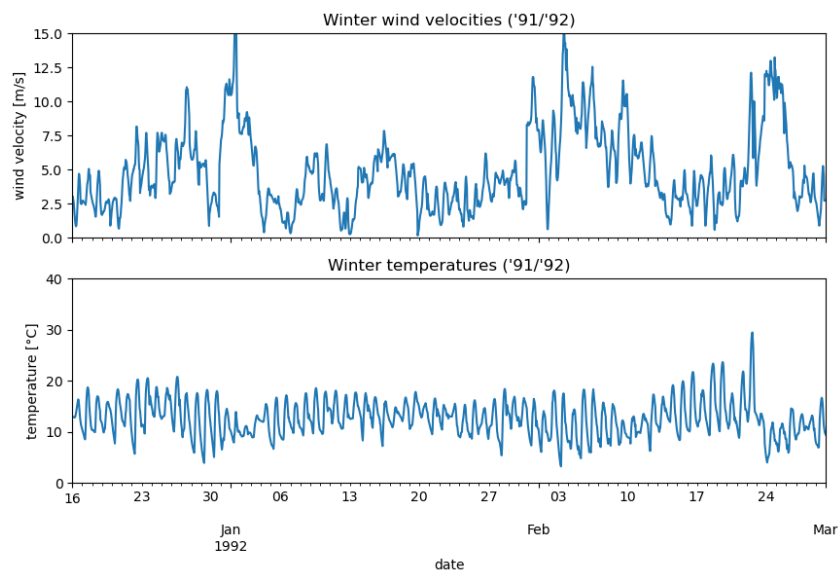


Figure B.1: Weather conditions used in the hydrodynamic model (wind velocity and temperature) for a 2.5 month period during winter in 1991-1992 (meteoblue citation needed).

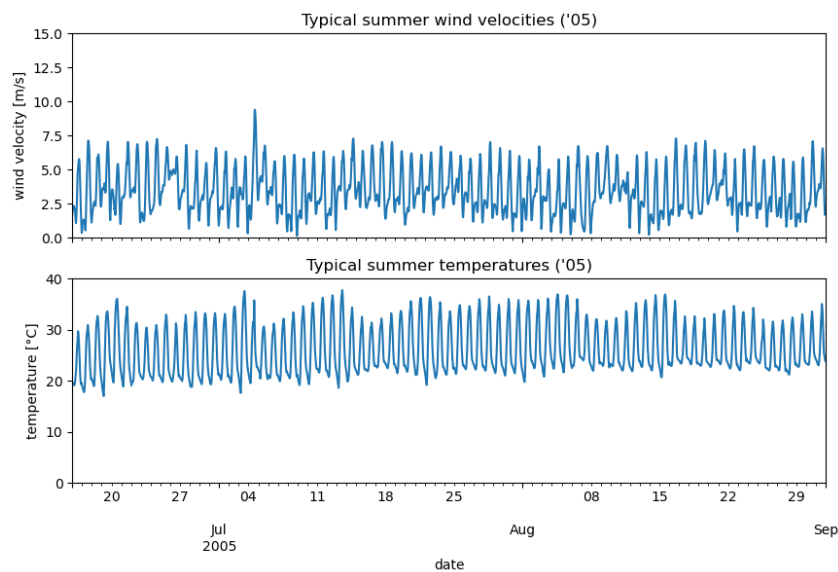


Figure B.2: Weather conditions used in the hydrodynamic model (wind velocity and temperature) for a 2.5 month period during summer in 2005 (meteoblue citation needed)

B.1.2 Morphological model

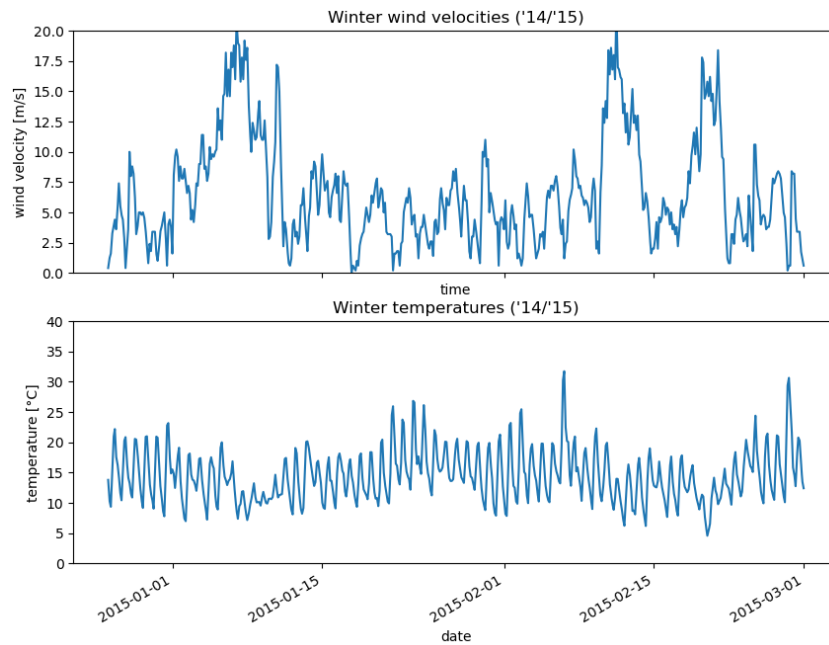


Figure B.3: Weather conditions used in the morphological model (wind velocity and temperature) for a 2 month period during winter in 1991-1992 (meteoblue citation needed) and (waveclimate)

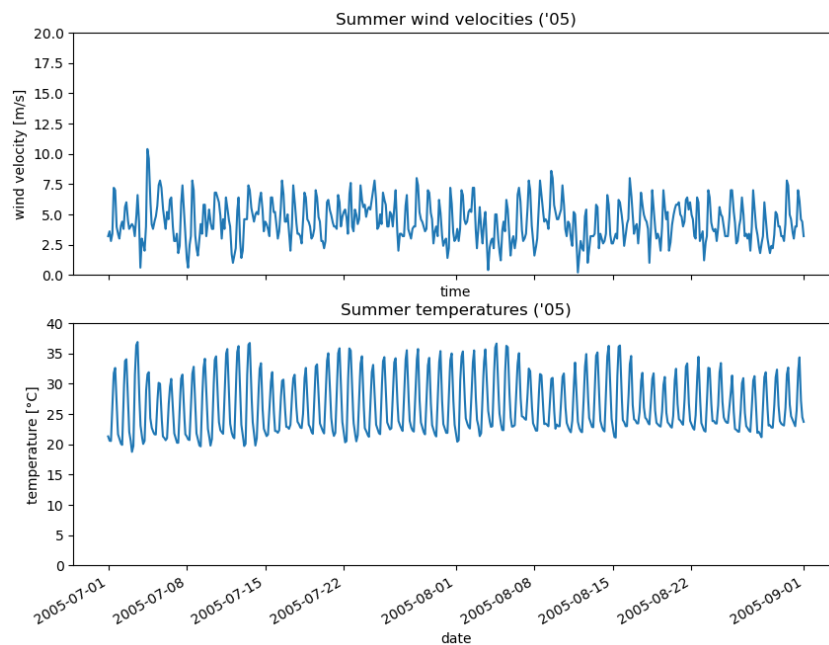


Figure B.4: Weather conditions used in the morphological model (wind velocity and temperature) for a 2.5 month period during summer in 2005(meteoblue citation needed)(waveclimate).

B.2 Validation of initial conditions

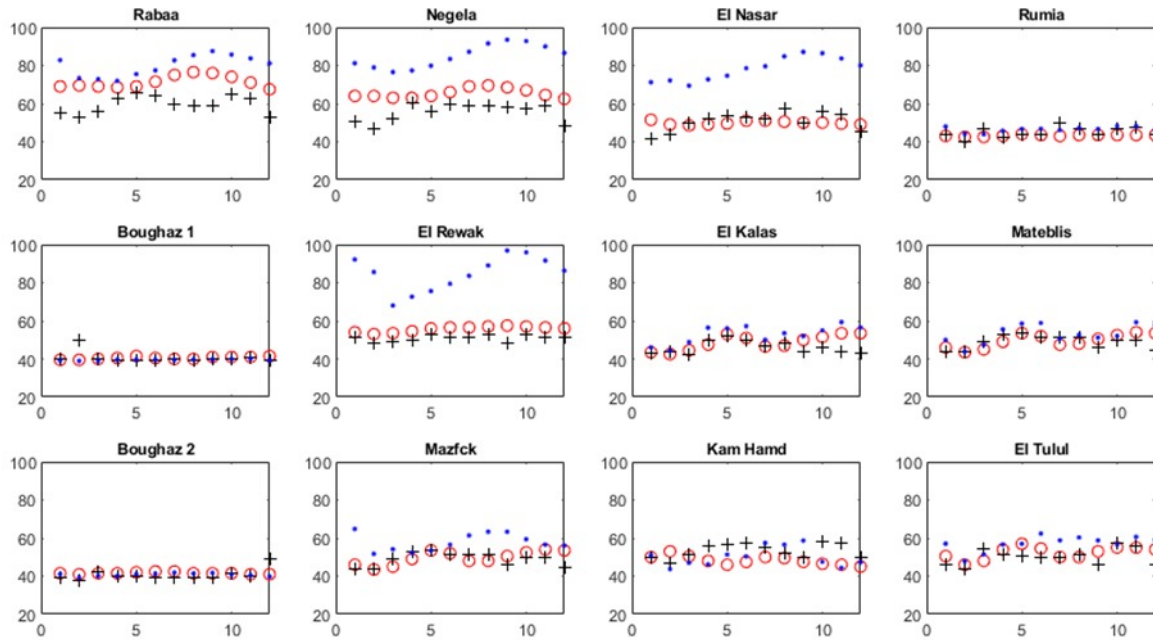


Figure B.5: Monthly averaged salinity data comparison for 12 measurement locations. Black plus: measurements taken in 1999 (Bek and Cowles, 2019); Red circle: model results of Bek and Cowles (2019); Blue dot: model results of TWM (2021).



Figure B.6: Locations for modelled and measured salinity

C Additional results

C.1 Hydrodynamic response to tidal forcing

C.1.1 Water levels in remote areas

The waterlevels over a single tidal cycle in three remote locations of Lake Bardawil are shown in Figure C.1. The tidal range is generally increased from SQ to EW. In the two semi-enclosed areas (orange and yellow) the tidal range increase is presumably hindered by the tight access channel to these remote locations. The relative increase in tidal range is larger for the green location. For the easternmost location (yellow), in addition to an increase in tidal range, the mean water level is increased.

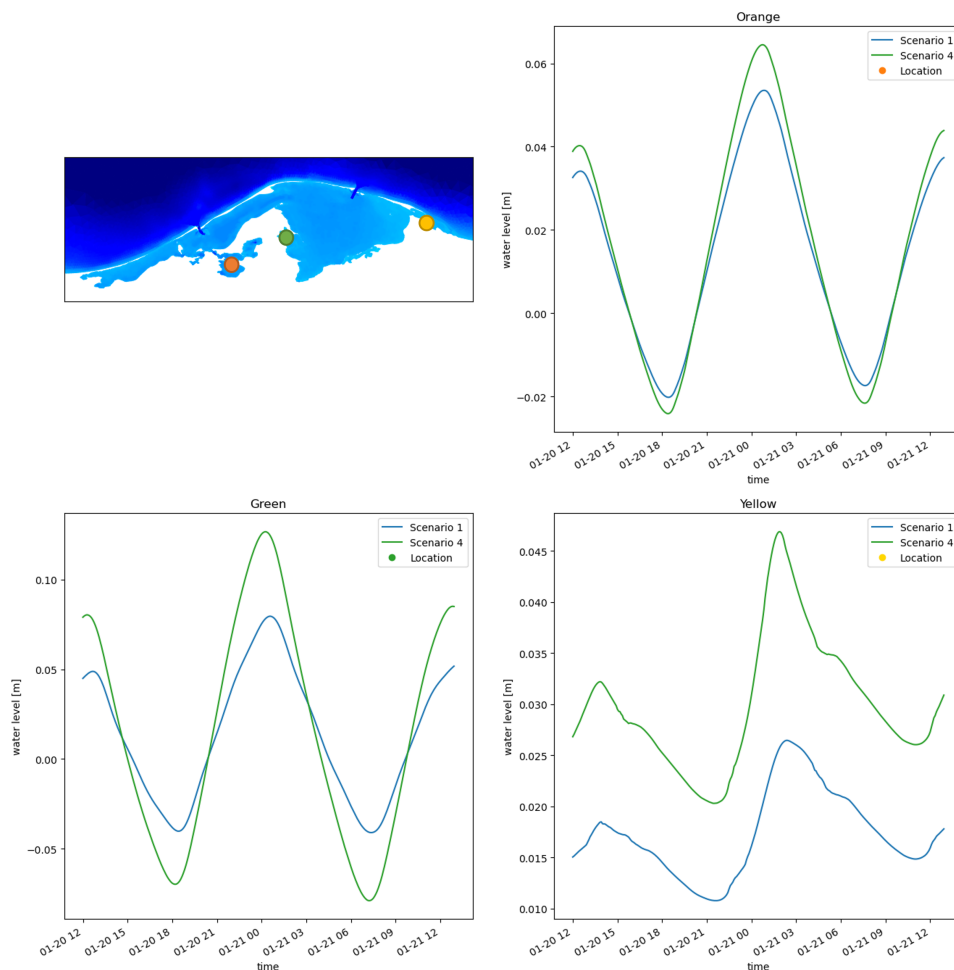


Figure C.1: Water levels over one tidal cycle in remote locations shown in the top left image. The orange location corresponds to the water levels shown in the top right graph, green corresponds to bottom left graph and yellow corresponds to the bottom right graph.

C.1.2 Velocity vectors during ebb & flood

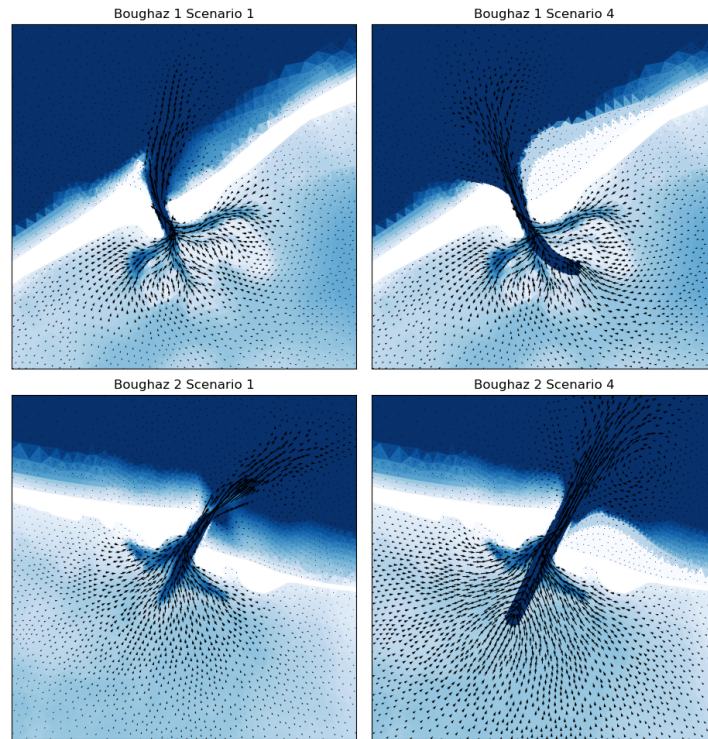


Figure C.2: Flow velocity vectors during ebb for Boughaz 1 and Boughaz 2 in SQ and EW

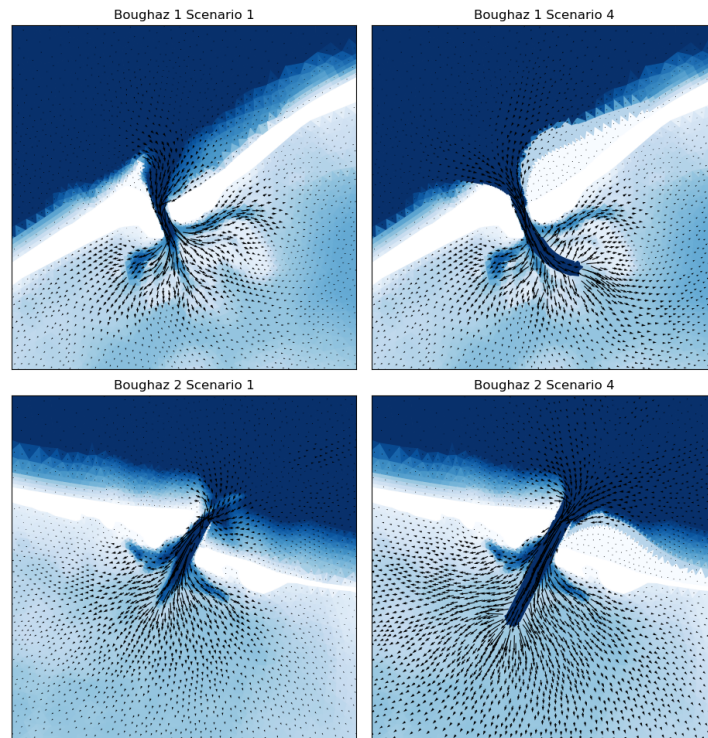


Figure C.3: Flow velocity vectors during flood for Boughaz 1 and Boughaz 2 in SQ and EW

C.1.3 Sediment transport

Import and export of sediment

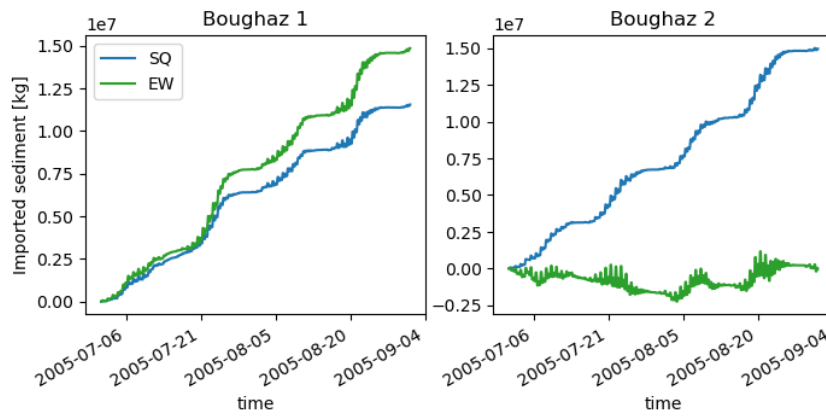


Figure C.4: Sediment import (positive) and export (negative) for SQ and EW over Boughaz 1 and Boughaz 2 during summer for the medium sediment fraction with $D_{50} = 0.7$ mm

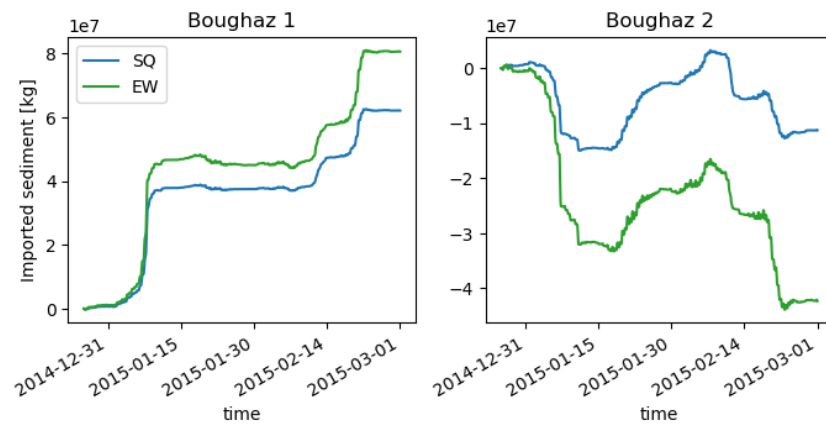


Figure C.5: Sediment import (positive) and export (negative) for SQ and EW over Boughaz 1 and Boughaz 2 during winter for the medium sediment fraction with $D_{50} = 0.7$ mm.

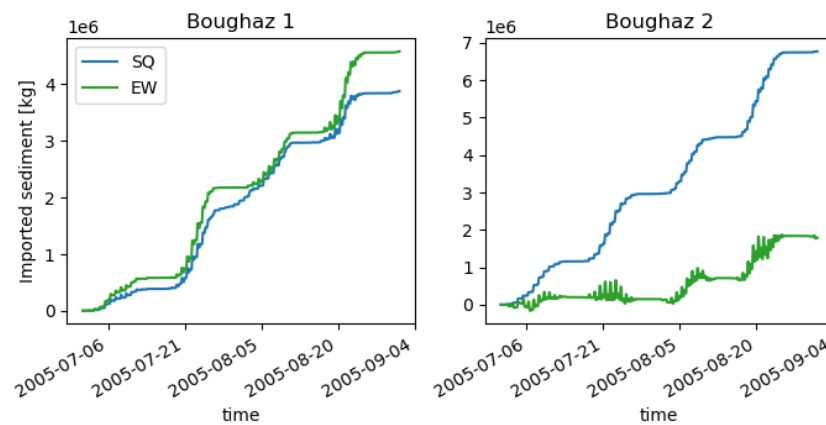


Figure C.6: Sediment import (positive) and export (negative) for SQ and EW over Boughaz 1 and Boughaz 2 during winter for the coarse sediment fraction with $D_{50} = 2$ mm.

Increased sediment transport to Boughaz 2

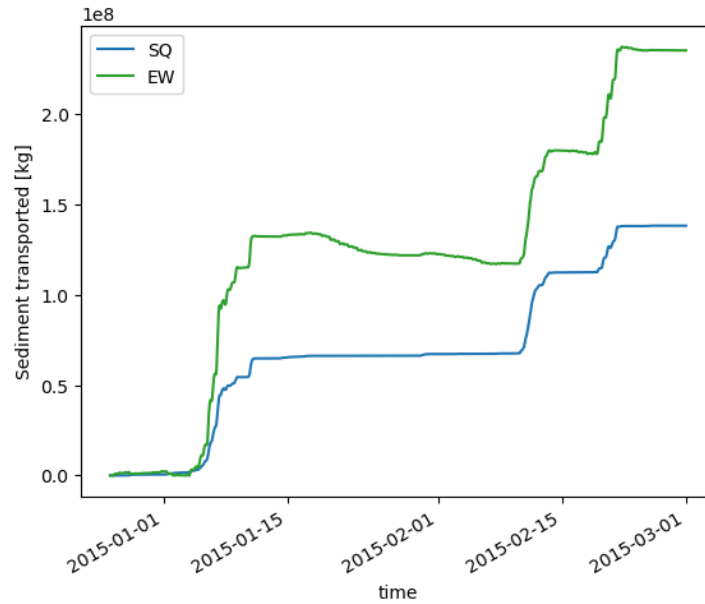


Figure C.7: Fine sediment transport from the basin into the flood-tidal delta of Boughaz 2 during winter, SQ compared to EW.

C.1.4 Sensitivity to friction

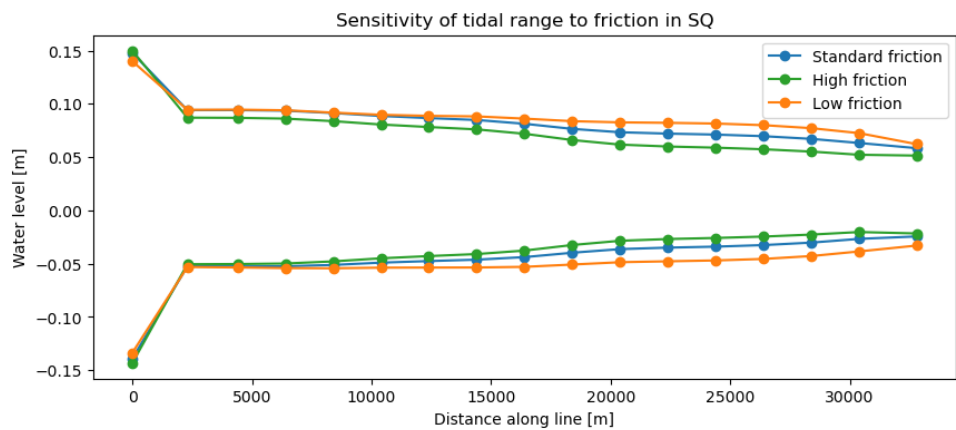


Figure C.8: Sensitivity of the maximum and minimum water level to varying values for bottom friction. Using high friction Manning values of 0.032 ($K = 67$), standard Manning values of 0.023 and low friction Manning values of 0.015 ($K = 31$).

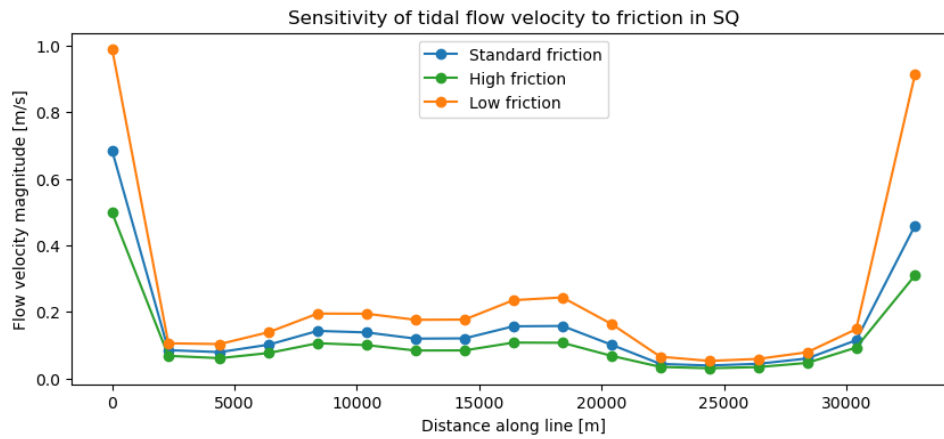


Figure C.9: Sensitivity of tidal flow velocity to varying values for bottom friction. Using high friction Manning values of 0.032 ($K = 67$), standard Manning values of 0.023 and low friction Manning values of 0.015 ($K = 31$).

C.1.5 Salinity

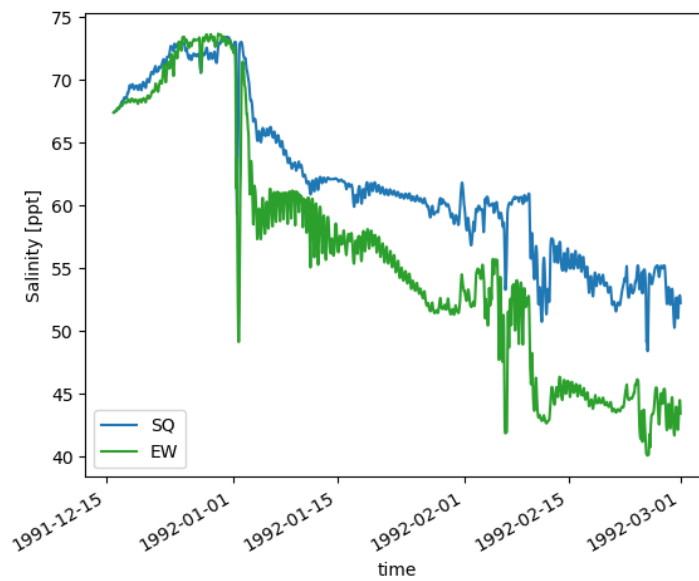


Figure C.10: Salinity values for SQ and EW in the middle of the eastern basin of Lake Bardawil over a 2.5-month winter period.

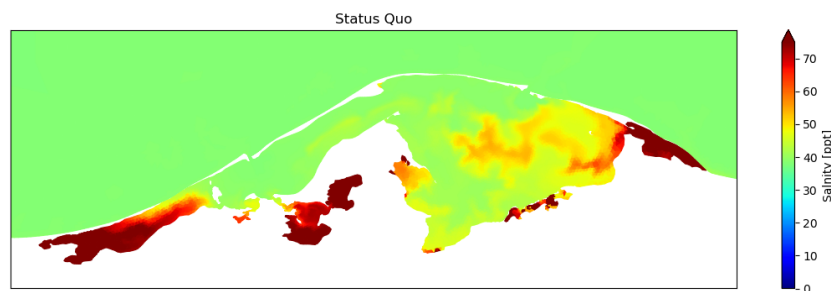


Figure C.11: Salinity in Lake Bardawil after a 2-month winter simulation in the Status Quo scenario.

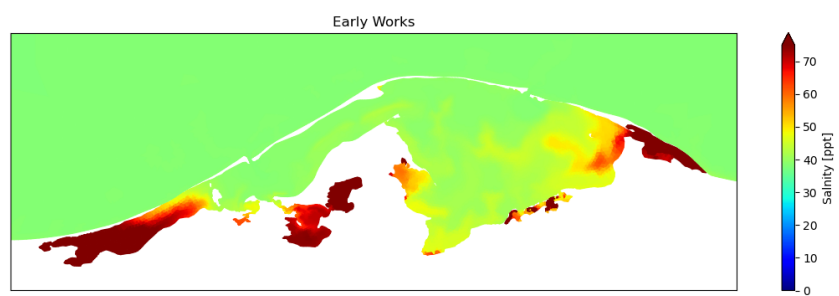


Figure C.12: Salinity in Lake Bardawil after a 2-month winter simulation in the Early Works scenario.

D Reference figures

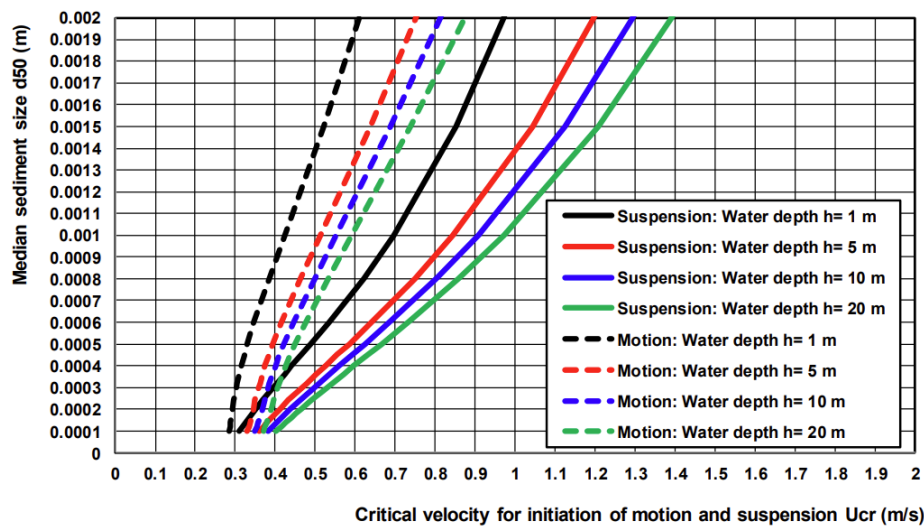


Figure D.1: Critical depth-averaged velocity for initiation of motion and suspension (Van Rijn, n.d.).

E Sediment fractions

As can be seen in Figure E.1, the situation with all three sediment fractions resembles the situation with only fine sediment the most. Using this knowledge, the assumption can be made that morphological predictions made using only medium and fine sediments can come close to predictions made using the full sediment range.

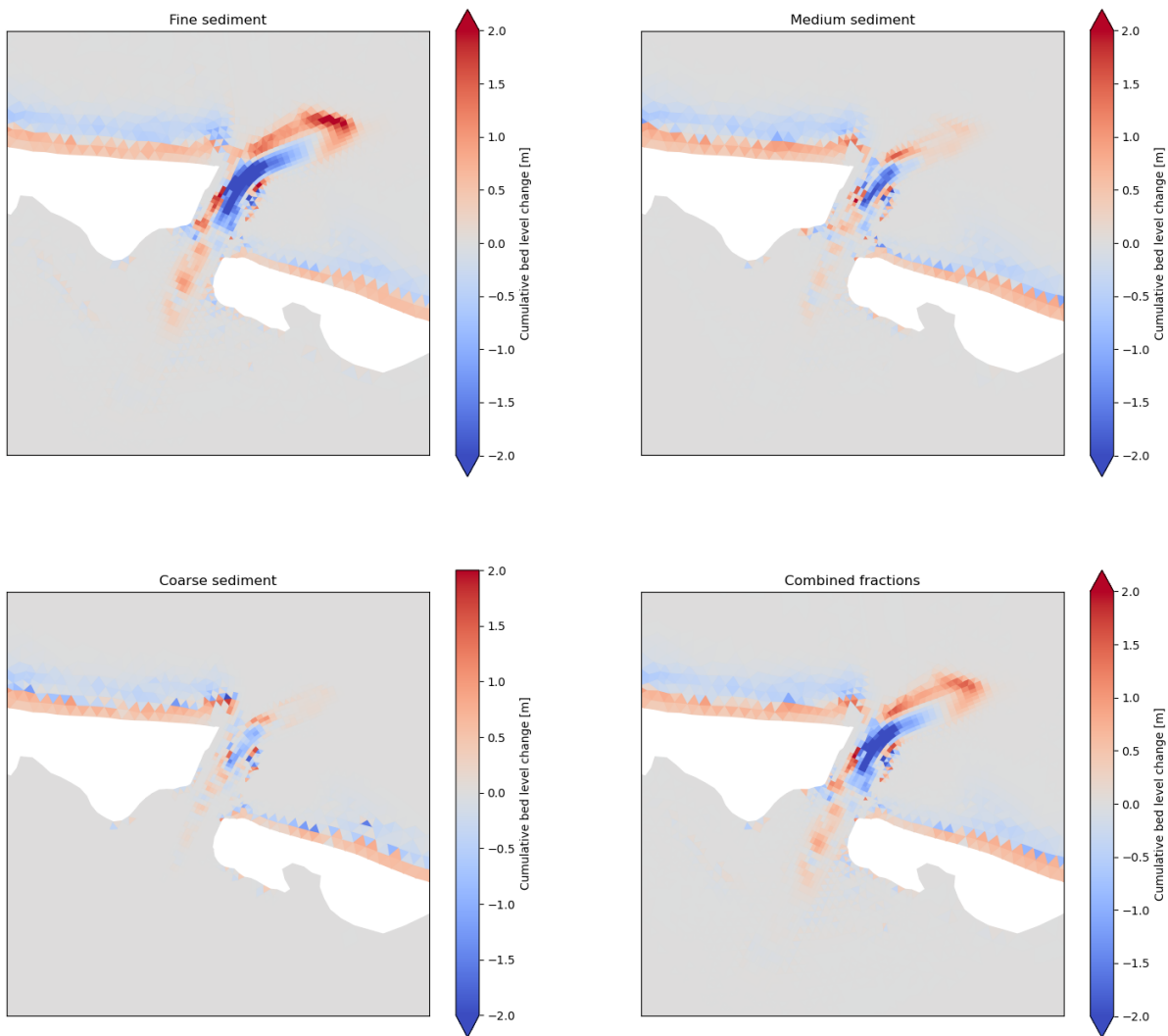


Figure E.1: Comparison of the results of summer simulations for fine sediment, medium sediment, coarse sediment and a combined simulation with fine, medium and coarse sediment included